

**Compound Specific Isotope Correlation (CSIC)
Using Gasoline Range Hydrocarbons:
A Novel Approach for Petroleum Exploration**

by

**Scott A. Harris
B.Sc., McGill University, 1996**

A Thesis Submitted in Partial Fulfillment of the
Requirements for the Degree of

MASTER OF SCIENCE

in the School of Earth and Ocean Sciences

We accept this thesis as conforming to the required standard

[Redacted Signature]

Dr. M.J. Whitticar, Supervisor (School of Earth and Ocean Sciences)

[Redacted Signature]

Dr. E. Van der Flier-Keller, Departmental Member (School of Earth and Ocean Sciences)

[Redacted Signature]

Dr. J. Harper, Departmental Member (School of Earth and Ocean Sciences)

[Redacted Signature]

Dr. P.R. West, Outside Member (Department of Environmental Studies)

[Redacted Signature]

Dr. M.G. Fowler, External Examiner (Geological Survey of Canada - Calgary)

© Scott Allan Harris, 1999

University of Victoria

All rights reserved. Thesis may not be reproduced in whole or in part, by photocopy or other means, without the permission of the author.

Supervisor: Dr. Michael J. Whiticar

ABSTRACT

Most oils and condensates contain gasoline-range hydrocarbons (C₅-C₁₀) that potentially can be used as geochemical indicators or signals. The abundance and mobility of this hydrocarbon fraction is particularly useful for reservoir and oil-oil correlation. Previous correlation techniques based on biomarkers, structural or molecular composition of oils sometimes fail because of alterations to the oils at high maturities (condensates), biodegradation or oxidation. Compound Specific Isotope Correlation (CSIC) uses the stable carbon isotope ratios of individual hydrocarbons in the gasoline range fraction as a diagnostic fingerprint that can be used to correlate oils to each other or to potential sources.

CSIC takes advantage of an improved method developed for molecular and stable isotope analysis of gasoline range hydrocarbons using Solid Phase MicroExtraction (SPME). Analytes are sampled from the headspace above oil droplets and analyzed by gas chromatography and continuous-flow isotope ratio mass spectrometry (CF-IRMS). Analytical considerations with this sampling technique include equilibration times, vapor pressure/temperature effects, and the presence of a complex matrix. Instrumentation factors such as column/split flows are also considered. The results are compared with an alternative purge and trap method. Molecular analyses prove reproducible between the two methods, however, stable carbon isotope ratios exhibit a non-systematic depletion and enrichment of 0.2 - 2.0‰ for 16 pre-selected compounds.


A sample suite of 27 oils primarily of Devonian age from the Western Canada Sedimentary Basin tests both the technology and technique of CSIC. Oils are correlated to each other using hierarchical cluster analysis of $\delta^{13}\text{C}$ signatures for 15 gasoline range compounds, taking into consideration the geologic setting where reservoirs are located. From this process, 6 groups of oils were generated and most can be attributed to a common source rock, the Upper Devonian Duvernay formation. It is unclear if Nisku formation source beds have contributed partially or completely to some of these oils.

Comparison of isotope ratios from different compound classes in the gasoline range may provide information on the origin of oils and light hydrocarbons. Straight-chain and branched alkanes display both a molecular and isotopic correlation to each other, while cyclic and aromatic compounds show more variable results. The data in this study support a steady-state or kinetic mechanism for oil generation, in contrast to previous thermodynamic models. Systematic isotopic offsets of individual compounds with similar carbon number or chemical structure also indicate some form of source control on isotopic composition of oils. LMW compounds are generally enriched in ^{13}C relative to heavier compounds. Thermochemical Sulfate Reduction (TSR) appears to result in pronounced ^{13}C enrichment for several compounds relative to unaltered samples.

Examiners:


Dr. M.J. Whiticar, Supervisor (School of Earth and Ocean Sciences)


Dr. E. Van der Flier-Keller, Departmental Member (School of Earth and Ocean Sciences)


Dr. J. Harper, Departmental Member (School of Earth and Ocean Sciences)


Dr. P.R. West, Outside Member (Department of Environmental Studies)


Dr. M.G. Fowler, External Examiner (Geological Survey of Canada - Calgary)

Table of Contents

ABSTRACT	ii
TABLE OF CONTENTS	iv
LIST OF FIGURES	vi
LIST OF TABLES	ix
LIST OF ABBREVIATIONS.....	x
ACKNOWLEDGEMENTS	xii
CHAPTER 1 – STATEMENT OF PROBLEM	1
SYNOPSIS OF THESIS.....	3
CHAPTER 2 – BACKGROUND.....	7
OIL CLASSIFICATION	7
OIL-OIL/OIL-SOURCE CORRELATION	11
CONTINUOUS FLOW-ISOTOPE RATIO MASS SPECTROMETRY (CF-IRMS)	23
ORIGIN OF GASOLINE RANGE (C ₅ TO C ₁₀) HYDROCARBONS.....	33
CHAPTER 3 – ANALYTICAL METHODOLOGY	36
METHODS	39
EXPERIMENTAL RESULTS AND DISCUSSION	44
SAMPLING	48
INSTRUMENTATION	65
CHAPTER 4-COMPOUND SPECIFIC ISOTOPE CORRELATION (CSIC):	
EXAMPLES FROM CENTRAL AND SOUTHERN ALBERTA	71
SAMPLES AND GEOLOGIC BACKGROUND	71
RESULTS.....	76

MOLECULAR VARIABILITY.....	76
STATISTICAL ANALYSIS	81
MOLECULAR CORRELATIONS	83
COMPOSITIONAL RELATIONSHIPS.....	90
STABLE CARBON ISOTOPES	94
ISOTOPIC VARIABILITY.....	94
HIERARCHICAL CLUSTER ANALYSIS	101
OIL-OIL/OIL-SOURCE CORRELATIONS	106
DISCUSSION.....	124
CHAPTER 5 – OUTLOOK AND CONCLUSIONS	132
REFERENCES	134
APPENDIX A - DEVONIAN PETROLEUM SYSTEMS (DPS) REPORT.....	145
FACIES ANALYSIS.....	145
THERMAL MATURITY	147
SOURCE ROCKS OF THE NISKU FORMATION	147

List of Figures

		Page
FIGURE 2.1	A) CLASSIFICATION DIAGRAM OF WILLIAMS (1974) B) CARBON ISOTOPE COMPOSITION RELATIONSHIP BETWEEN C15+ AROMATIC VERSUS SATURATE FRACTIONS OF SOFER (1984).	8 8
FIGURE 2.2	A) THEORETICAL MATURATION DIAGRAM OF JAMES (1983) B) COMPARISON OF CARBON ISOTOPE MATURITY MODELS OF JAMES (1983) AND THE BGR (FABER, 1987)	13 13
FIGURE 2.3A	EXAMPLE OF C7 OIL TRANSFORMATION STAR DIAGRAM OF HALPERN (1995)	16
FIGURE 2.3B	EXAMPLE OF C7 OIL CORRELATION STAR DIAGRAM OF HALPERN (1995)	17
FIGURE 2.4.	NATURAL GAS PLOT OF CHUNG ET AL. (1988)	21
FIGURE 2.5	COMPARISON OF ISOTOPE RATIOS FOR SEPARATE COMPONENTS IN OILS OF DIFFERENT ORIGIN	24
FIGURE 2.6	CARBON ISOTOPE RATIOS OF INDIVIDUAL N-ALKANES (NC) AND ISOPRENOIDS (IP) OF AN OIL-CONDENSATE PAIR FROM WELL K-4, OFFSHORE TAIWAN.	26
FIGURE 2.7	A) ISOTOPIC COMPOSITION OF INDIVIDUAL N-ALKANES FOR 4 PAIRS OF WEATHERED (W) AND UNWEATHERED (U) OILS. B) ISOTOPIC COMPOSITION OF INDIVIDUAL N-ALKANES FOR OIL COLLECTED FROM BIRDS KILLED IN A RECENT SPILL. (FROM MANSUY ET AL., 1997)	32 32
FIGURE 3.1:	A) SCHEMATIC DRAWING OF SPME SYRINGE AND FIBER ASSEMBLY B) HEADSPACE SAMPLING TECHNIQUE USING SPME.	41 41
FIGURE 3.2:	TYPICAL GASOLINE RANGE GAS CHROMATOGRAM OF CHESTER OIL	45
FIGURE 3.3:	CF-IRMS MASS 44 TRACE AND 45/44 RATIO FOR CHESTER OIL.	46
FIGURE 3.4:	A) COMPARISON OF RELATIVE GC PEAK AREAS BETWEEN P&T AND HSPME SAMPLING METHODS FOR CHESTER OIL. B) COMPARISON OF RELATIVE PEAK AREAS PRODUCED FROM GC AREA COUNTS AND CF-IRMS MASS 44 TRACE FOR CHESTER OIL USING HSPME SAMPLING.	49 49
FIGURE 3.5:	$\delta^{13}\text{C}$ RATIOS FOR ALL 16 COMPOUNDS RECORDED FROM 8 ANALYSES	51

FIGURE 3.6:	COMPARISON OF SELECTED GASOLINE RANGE HYDROCARBONS FROM NA-1 OIL BY P&T, HSPME, AND WHOLE OIL (MOBIL) EXTRACTION METHODS.	53
FIGURE 3.7:	TIME REQUIRED FOR ESTABLISHMENT OF (A) MOLECULAR AND (B) ISOTOPIC EQUILIBRIUM. ALSO SHOWN ARE CHANGES WITH TIME (C,D)	56
FIGURE 3.8:	EFFECT OF VAPOR PRESSURE/TEMPERATURE ON $\delta^{13}\text{C}$ RATIOS	61
FIGURE 3.9	COMPARISON OF CAPILLARY COLUMNS FOR SEPARATING GASOLINE RANGE COMPOUNDS.	70
FIGURE 4.1	MAP OF PROVINCE OF ALBERTA SHOWING DISTRIBUTION OF MAJOR ENVIRONMENTAL FACIES OF THE WOODBEND GROUP.	73
FIGURE 4.2	STRATIGRAPHY OF UPPER DEVONIAN WOODBEND-WINTERBURN GROUPS.	74
FIGURE 4.3	CHROMATOGRAMS FOR 14 WCSB OILS SHOWING DIVERSITY IN COMPOSITION FOR GASOLINE RANGE COMPOUNDS.	77
FIGURE 4.4	AGGOLMERATION SCHEDULE AND CORRESPONDING DENDOGRAM FOR HIERARCHICAL CLUSTER ANALYSIS OF MOLECULAR CONCENTRATIONS FOR 14 WCSB OILS.	86
FIGURE 4.5	MAP OF PROVINCE OF ALBERTA SHOWING LOCATION OF 14 WCSB OILS.	88
FIGURE 4.6	CROSS-PLOTS OF THE MOLECULAR CONCENTRATIONS FOR INDIVIDUAL COMPOUNDS ILLUSTRATING INTERDEPENDANCIES AND RELATIONSHIPS	92
FIGURE 4.7	CROSS-PLOTS OF THE MOLECULAR CONCENTRATIONS FOR INDIVIDUAL COMPOUNDS ILLUSTRATING INTERDEPENDANCIES AND RELATIONSHIPS	93
FIGURE 4.8	ISOTOPOGRAMS OF 4 WCSB OILS ILLUSTRATING THE CARBON ISOTOPE RATIO OF 15 INDIVIDUAL GASOLINE RANGE HYDROCARBONS.	97
FIGURE 4.9	COMPARISON OF THE ISOTOPOGRAMS OF 4 BASHAW OILS	99
FIGURE 4.10	ISOTOPOGRAMS FOR A) SWALWELL AND B) FENN BIG VALLEY OILS	100
FIGURE 4.11	HIERARCHICAL CLUSTER ANALYSIS DENDOGRAM USING AVERAGE LINKAGE (BETWEEN GROUPS) METHOD.	102

FIGURE 4.12A	HIERARCHICAL CLUSTER ANALYSIS DENDOGRAM USING AVERAGE LINKAGE (BETWEEN GROUPS) METHOD (RIGHT SIDE). EXPECTED GEOGRAPHIC PROXIMITY RELATIONSHIPS ALONG WITH CSIC AND INFERRED GEOLOGIC RELATIONSHIPS ARE ALSO SHOWN (LEFT SIDE).	104
FIGURE 4.12B	MAP OF PROVINCE OF ALBERTA SHOWING LOCATION OF 27 WCSB OILS.	105
FIGURE 4.13	ISOTOPOGRAMS FOR GROUP A AND B OILS	107
FIGURE 4.14	ISOTOPOGRAMS FOR GROUP C AND D OILS.	110
FIGURE 4.15	ISOTOPOGRAMS FOR GROUP E AND F OILS.	113
FIGURE 4.16	A) COMPARISON OF CARBON ISOTOPE RATIOS FOR C5-C9 N-ALKANES B) THE MAGNITUDE OF ^{13}C ENRICHMENT FOR NC5 (PENTANE) VERSUS OTHER N-ALKANES	115
FIGURE 4.17	COMPARISON OF CARBON ISOTOPE RATIOS FOR SPECIFIC COMPOUNDS BETWEEN OILS	117
FIGURE 4.18	COMPARISON OF CARBON ISOTOPE RATIOS FOR SPECIFIC COMPOUNDS BETWEEN OILS	118
FIGURE 4.19	CROSS-PLOTS OF THE ISOTOPIC RATIOS FOR INDIVIDUAL GASOLINE RANGE COMPOUNDS ILLUSTRATING INTERDEPENDANCIES AND RELATIONSHIPS	120
FIGURE 4.20	CROSS-PLOTS OF THE ISOTOPIC RATIOS FOR INDIVIDUAL GASOLINE RANGE COMPOUNDS ILLUSTRATING INTERDEPENDANCIES AND RELATIONSHIPS	122
FIGURE 4.21	CROSS-PLOTS OF THE ISOTOPIC RATIOS FOR INDIVIDUAL GASOLINE RANGE COMPOUNDS ILLUSTRATING INTERDEPENDANCIES AND RELATIONSHIPS	123
FIGURE 4.22	A) COMPARISON OF CARBON ISOTOPE RATIOS FOR C5-C9 N-ALKANES	129
	B) COMPARISON OF CARBON ISOTOPE RATIOS FOR CYCLIC ALKANES	129
	C) COMPARISON OF CARBON ISOTOPE RATIOS FOR METHYLCYCLIC ALKANES	130
	D) COMPARISON OF CARBON ISOTOPE RATIOS FOR AROMATIC COMPOUNDS	130

List of Tables

	Page
TABLE 3.1: LIST OF COMPOUNDS IDENTIFIED IN FIGURES 3.2, 3.3, 3.9	47
TABLE 3.2: CARBON ISOTOPE RATIOS FOR PURE STANDARDS AND MIXTURES	64
TABLE 3.3: CHESTER OIL INJECTOR SPLIT RATIO TEST	66
TABLE 4.1 LIST OF SELECTED WCSB OILS	72
TABLE 4.2 EXAMPLE DATA SET FRO DETERMINING SQUARED EUCLIDEAN DISTANCE	82
TABLE 4.3 PEAK AREAS NORMALIZED TO HEPTANE FOR 14 WCSB OILS	84
TABLE 4.4 CARBON ISOTOPE RATIOS OF OILS IN CSIC STUDY	95
TABLE 4.5 PEAK AREAS OF OILS IN CSIC STUDY	128

List of Common Abbreviations

b.p.	boiling point	Pr	pristane
BTEX	Benzene, Toluene, Ethylbenzene, Xylene	% Ro	percent vitrinite reflectance
°API	degrees API (American Petroleum Institute)	RT	retention time
CO ₂	carbon dioxide	SANA	saturate, aromatic, NSO, asphaltene
C _x	carbon _{number}	SBC	straight-branched chain and cyclic aliphatic hydrocarbons
CF-IRMS	continuous flow - isotope ratio mass spectrometer	SEOS	School of Earth and Ocean Sciences
CSIA	Compound Specific Isotope Analysis	SPME	Solid Phase MicroExtraction
CSIC	Compound Specific Isotope Correlation	TOC	total organic carbon
δ	delta notation	UVIC	University of Victoria
DST#	drill stem test #	WCSB	Western Canada Sedimentary Basin
FID	flame ionization detector	iC5	iso-pentane
GC	gas chromatograph	nC5	n-pentane
HMW	high molecular weight	22DMC4	2,2-dimethylbutane
HSPME	Headspace Solid Phase MicroExtraction	CYC5	cyclopentane
H ₂ O	water	23DMC4	2,3-dimethylbutane
iC _x	iso-C _{number} (branched compound)	2MC5	2-methylpentane
LMW	low molecular weight	3MC5	3-methylpentane
MS	mass spectrometer	nC6	n-hexane
n-alkane	normal alkane (straight chain)	22DMC5	2,2-dimethylpentane
NSO	Nitrogen, Sulfur, Oxygen compounds	MCYC5	methylcyclopentane
P&T	Purge and Trap	24DMC5	2,4-dimethylpentane
PAH	Polycyclic Aromatic Hydrocarbons	223TMC4	2,2,3-trimethylbutane
PDB	Peedee Belemnite	Benz	benzene
‰	per mil or parts per thousand	33DMC5	3,3-dimethylpentane
Ph	phytane	CYC6	cyclohexane
ppt	parts per trillion	2MC6	2-methylhexane
		23DMC5	2,3-dimethylpentane
		11DMCYC5	1,1-dimethylcyclopentane
		3MC6	3-methylhexane
		1c3DMCYC5	1-cis-3-dimethylcyclopentane

List of Common Abbreviations (continued)

1t3DMCYC5	1-trans-3-dimethylcyclopentane	1t2c4TMCYC5	1-trans-2-cis-4-trimethylcyclopentane
1t2DMCYC5	1-trans-2-dimethylcyclopentane	33DMC6	3,3-dimethylhexane
nC7	n-heptane	1t2c3TMCYC5	1-trans-2-cis-3-trimethylcyclopentane
1c2DMCYC5	1-cis2-dimethylcyclopentane	223TMCYC6	2,2,3-trimethylcyclohexane
MCYC6	methylcyclohexane	Tol	toluene
22DMC6	2,2-dimethylhexane + co-elute	2MC7	2-methylheptane
113TMCYC5	1,1,3-trimethylcyclopentane (minor)	3MC7	3-methylheptane
EtCYC5	ethylcyclopentane	1c4DMCYC6	1-cis-4-dimethylcyclohexane
25DMC6	2,5-dimethylhexane	nC8	n-octane
24DMC6	2,4-dimethylhexane	nC9	n-nonane
		nC10	n-decane

Acknowledgements

Very few people are given the opportunity to study in a place where they feel both challenged and unfettered (yes, I said unfettered) at the same time. I consider myself fortunate to be given that opportunity throughout my M.Sc.

I would like to thank my supervisor Dr. Michael Whitticar for encouraging me to come to Victoria and introducing me to the realm of organic and stable isotope geochemistry. In sharing your knowledge and guidance with a relative newcomer in this area, you have encouraged me to seek new goals and challenges throughout my academic endeavors. I would also like to thank you for your confidence in my abilities, especially when I was questioning my own.

This research was made possible by financial support from the National Science and Engineering Research Council, Pan Canadian Petroleum, and a bursary given to me by the University of Victoria. I would like to thank Tony Cadrin, Wayne Cox, and Martin Fowler for their guidance in this project. I would also like to thank my graduate committee of Paul West, John Harper, and Eileen Van der Flier-Keller for their comments and reviews of the thesis.

My work would not have been completed without the help of my fellow lab “dudes” in Biogeochemistry Facility here at UVIC. People like Mike Kory, Hinrich Schäfer, Ruben Veefkind, Lisa Kadonaga, Nick Grant, Melissa McQuoid, and Paul Eby, without whose friendship and assistance I would not be the man I am today (whatever that means.....). Outside of the lab, while I have made many other friends, I would like to thank Dave Sims, Joe Henton and Peter Leong for hours of good times completely unrelated to whatever I was working on.

I must give special thanks to Magnus Eek without whose unending kindness, patience, knowledge and time shared with me I could not have completed any of this. I consider myself fortunate to know you and hope that you always remember if you are ever in need of anything, you can count on me to help in any way I can. Tack så mycket my friend.

Finally, I give thanks to my Mom. For everything, but most importantly, for being there. This belongs to you as much as it does to me.

CHAPTER 1 – STATEMENT OF PROBLEM

Develop a new analytical methodology for extracting gasoline range hydrocarbons from oils using Solid Phase MicroExtraction (SPME). This method is developed for use with Compound Specific Isotope Correlation (CSIC). CSIC uses the stable carbon isotope ratios of individual hydrocarbons in the gasoline range fraction as a diagnostic fingerprint that can be used to correlate oils to each other or a common source.

Reliable methods for oil-oil and oil-source rock correlations have long been a goal in petroleum exploration. Correlations are based on the recognition of physical and chemical similarities either between individual oils or with their prospective source rocks. To classify oils into groups or families, there must be significant or diagnostic differences between them (Murphy, 1995). The properties used to distinguish between oils must also be resistant to secondary alteration processes, such as biodegradation, water-washing, or time. A successful correlation requires a distinction between genetic and non-genetic oil properties, and specific molecular characteristics (e.g. biomarkers) along with stable carbon isotopes are among the best parameters for this purpose (Curiale, 1994).

Numerous techniques have been developed to characterize or classify petroleum over the past half century, but the majority of these have focused on the bulk or molecular composition of oils (e.g. Magoon and Claypool, 1983; Moldowan et al., 1985). Early analyses of isotopic ratios in oils also concentrated on bulk/whole oil measurements or

those of the dominant distillate and C_{15+} compositional fractions (saturates, aromatics, asphaltenes) (e.g. Silverman, 1964, 1971; Kvenvolden and Squires, 1967; Stahl, 1977, 1978; Sofer, 1984a; Northam, 1985; Chung et al., 1994). However, these ratios along with other traditional bulk correlation methods relying on physical (API, color, viscosity), compositional (SANA, SBC) or elemental properties of oils are all susceptible to secondary alteration processes, whose effects alter the original oil composition.

The development of continuous-flow isotope ratio mass spectrometry (CF-IRMS) has allowed scientists to determine isotope ratios for individual components of complex mixtures such as oils (Whiticar and Snowdon, 1998). Several studies have applied this compound specific technique in developing potential oil-oil and oil-source correlations (e.g. BJORoy et al., 1991a,b, 1994; Chung et al., 1992; Wilhelms et al., 1994; Dowling et al., 1995), while others have used it to determine sources of petroleum pollution in the environment (e.g. O'Malley et al., 1996; Mansuy et al., 1997). In a majority of studies, compounds analyzed are in the C_{10} - C_{40} range, with n-alkanes, isoprenoids (e.g. pristane, phytane), and polycyclic aromatic hydrocarbons (PAH's) the most common choices. This is probably due to the high abundance of these compounds in most samples, along with the relative ease of the analysis involved.

Compound Specific Isotope Correlation (CSIC) uses the stable carbon isotope ratios of individual hydrocarbons in the gasoline range fraction (C_5 - C_{10}) as a diagnostic fingerprint that can be used to correlate oils to each other or a common source. Gasoline range hydrocarbons comprise between 20-40% of most crude oils. This makes them among the most dominant and important components in petroleum. CSIC was initially developed in work by Murphy (1995), who analyzed individual gasoline range

hydrocarbons in Canadian crude oils chosen from varying sources and differentially affected by alteration processes. The choice of sample set enabled testing to show that compound-specific, gasoline range isotope ratios could be used as an independent parameter to characterize and correlate oils and source rocks. Cycloalkanes and the branched alkanes seemed to yield the most reliable isotope data, while straight-chain alkanes (especially nC₅ and nC₈) and aromatics produced more variable ratios (up to 1 ‰ in some cases). Thermal maturation did not appear to result in a significant isotope effect, and the isotope ratios were resistant to secondary alteration processes such as biodegradation (generally less than 1 ‰ variation; experimental error ranged from ± 0.3 to 0.5 ‰).

Synopsis of Thesis

In the past 30 years, the use of gasoline range compounds in petroleum exploration/geochemistry has seen significant changes. **Chapter 2 (Background)** serves as a brief summary of their use in classifying oils, along with applications to oil-oil and oil-source correlation methods. We have also learned a considerable amount about petroleum formation and composition from these previously ignored sources of information. In addition to the gasoline range compounds, Chapter 2 also includes reviews of some studies utilizing analysis of stable isotope ratios of dominant hydrocarbon fractions (e.g. saturates, aromatics), as they offer insight on previous methods of oil classification and correlation. There is also a section on past work with continuous-flow isotope ratio mass spectrometry (CF-IRMS), and its potential benefits to petroleum geochemistry. A brief discussion on the origin of light hydrocarbons summarizes recent advancements in this highly controversial field of study.

Gasoline range hydrocarbons have analytical constraints associated with their measurement (**Chapter 3 - Analytical Methodology**). They are liquids at room temperature (25 °C), but occupy a very volatile region of phase stability. Many of these compounds, especially those in the C₅-C₆ range, have high vapor pressures and low boiling points and tend to the gas phase at room temperatures (e.g. nC₅; b.p. 36 °C). Care must be taken to minimize sample transfer and subsequent evaporation during handling of oil samples.

The rationale in selecting the gasoline-range fraction for stable isotope analysis includes: (1) it is frequently a dominant hydrocarbon fraction of oils; (2) availability of different compound classes (n-, iso-, cyclo-alkanes and aromatics); and (3) good analytical separation of individual compounds for CF-IRMS (Murphy, 1995; Whiticar and Snowdon, 1998). Traditional methods of oil analysis focussed on the C₁₅₊ fractions and involved diluting the oil with a low b.p. solvent such as n-hexane, and injecting the sample directly into a gas chromatograph (GC). An unfortunate result of this technique is that the solvent peak obscures those of other compounds that may be of interest in the gasoline range. To avoid this, solventless extraction techniques such as purge and trap (P&T) have been used for extracting gasoline range analytes from oil samples.

Murphy (1995), Whiticar and Snowdon (1998) utilized a modified P&T system for extracting gasoline range hydrocarbons from the headspace above oil. While the P&T method is efficient in extracting the desired analytes, it is also time consuming, laborious, and suffers from evaporative losses. Controlling the amounts (nmoles) of individual components in the sample introduced to the CF-IRMS is a further concern.

To circumvent the problems of P&T, I experiment with Solid Phase MicroExtraction for introducing gasoline range analytes into GC or CF-IRMS. Chapter 3 discusses the numerous analytical and instrumental parameters that must be tested in conjunction with the development of this new method. SPME involves exposing a fused silica fiber coated with a liquid polymeric phase to a sample by either directly immersing the fiber in an aqueous phase or to the headspace above it (Zhang and Pawliszyn, 1993a,b). The fiber is conveniently held within a syringe mechanism, and the composition of coating is dependant upon the type of compounds being analyzed. Numerous studies have been performed using SPME (e.g. Arthur and Pawliszyn, 1990; Arthur et al., 1992a,b; Louch et al., 1992; Potter and Pawliszyn, 1994; Dias and Freeman, 1997), but most have involved directly immersing the fiber into an aqueous phase to extract organic analytes. In a large percentage of previous experiments using hydrocarbons, a relatively limited number of compounds (usually BTEX) were analyzed. Fewer studies (e.g. Zhang and Pawliszyn, 1993a,b, 1994; MacGillivray et al., 1994; Steffen and Pawliszyn, 1996; Boyd-Boland et al., 1996) have dealt with headspace sampling using SPME, and its ability to analyze complex mixtures such as soils, sludges, flavor volatiles and pesticides.

The current study presents one of the most complex matrices for SPME analysis to date. I demonstrate that SPME can be used as a simple, fast, reliable and inexpensive method for gasoline range hydrocarbon analysis. To be effective, SPME must produce a reproducible, representative result of the gasoline range for any given oil. The development of the SPME method is summarized as follows:

- Determination of molecular signatures of gasoline range fraction for selected oils by helium stripping/capillary gas chromatography. The gasoline range compounds were first analyzed according to the P&T procedure of Murphy (1995)

- Testing and development of the Solid Phase MicroExtraction technique for sampling gasoline range fraction of oils. This involves examination of potential molecular and isotopic effects associated with the sampling method.
- Determination of molecular signatures of gasoline range fractions of oils by SPME and comparison to results previously obtained by procedure of Murphy (1995)
- Determination of isotopic signatures for the oils using SPME and CF-IRMS. Comparison to procedure of Murphy (1995) where applicable.

The current study (**Chapter 4 – CSIC: Examples from Central and Southern Alberta**) also builds upon the work of Whiticar and Snowdon (1998) who performed a CSIC study on oils ranging from Devonian to Cretaceous age of the Western Canada Sedimentary Basin (WCSB). Several compound classes (n-, iso-, cyclo alkanes and aromatics) were examined, and in many instances isotope ratios of non-straight chain hydrocarbons were more diagnostic than the n-alkanes for correlation purposes. Statistical analysis using a hierarchical cluster method was used to correlate oils from similar/same sources, and the clear isotopic relationships suggested a steady-state kinetic relationship for the generation of oil and gas.

Samples in this study were chosen as part of a project with PanCanadian Petroleum (Calgary, Alta.) to attempt a more direct application of the CSIC technique. Oils from central and southern Alberta that have all been attributed to a common source (Upper Devonian Duvernay formation) were analyzed to determine if the isotopic signatures of gasoline range compounds could be used to distinguish those from same or similar source rocks. If successful, CSIC has the potential to become a powerful new tool in petroleum geochemistry.

CHAPTER 2 – BACKGROUND

Oil Classification

Williams (1974) split over 100 oils from the Williston Basin into three major groups using a ternary diagram based on percentage of straight, branched and cyclic hydrocarbons in C₄-C₇ range (Figure 2.1a). This was combined with other methods including optical rotation, C₁₅₊ gas chromatography, and stable carbon isotopes on bulk oils to further support the classification.

Koons et al. (1974) used CYC5/n-alkane ratios in the C₄-C₇ range along with biomarker data and stable carbon isotopes to classify oils in the Lower Cretaceous Tuscaloosa Formation. Stable isotope analysis was only performed on the saturate (aliphatic) and aromatic fractions. The isotopic composition of the saturate fraction was used as a maturity indicator, assuming ¹³C enrichment as maturation increases. One explanation for this effect was related to a slow cracking of high molecular weight (HMW) saturates releasing light hydrocarbons enriched in ¹²C, with the residual saturates enriched in ¹³C. Another explanation involved nonhydrocarbons, enriched in ¹³C that are transformed into saturated hydrocarbons by disproportionation reactions involving hydrogen exchange but little carbon-carbon bond breakage.

Sofer (1984a) used the relationship between the isotope ratios of aromatic and saturate hydrocarbons for distinguishing between marine and terrestrial sourced oils (Figure 2.1b). He statistically evaluated the difference through a parameter called a 'canonical variable' which correctly classified approximately 90 % of marine and non-marine oils. The common explanation for the difference in isotopic composition between

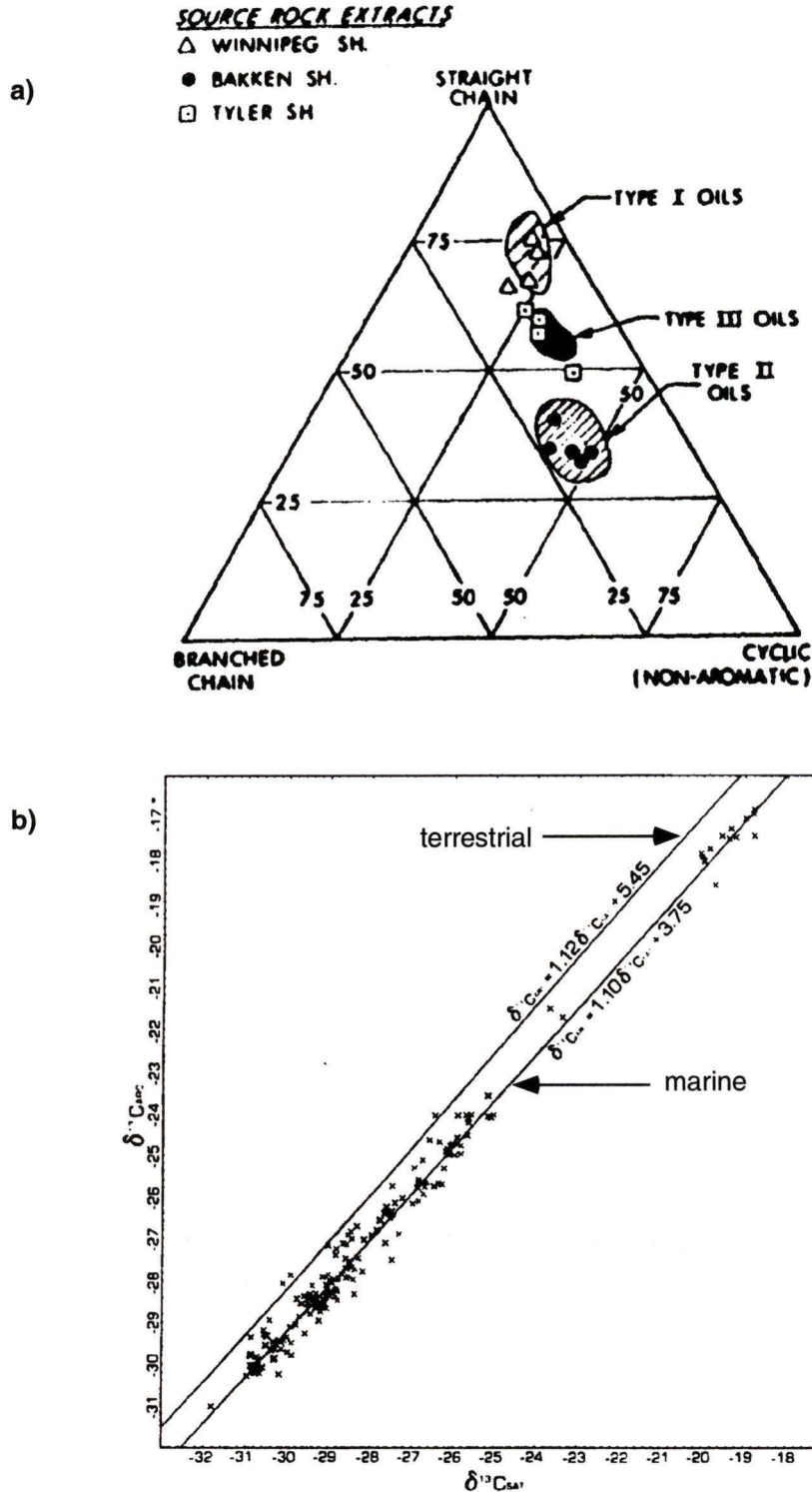


Figure 2.1 a) Classification diagram of Williams (1974) showing oil families and corresponding source rock extracts for the Williston Basin based on percentage of straight-chain, branched and cyclic hydrocarbons in the C_4 - C_7 range.
b) Carbon isotope composition relationship between C_{15+} aromatic versus saturate fractions of non-waxy or marine oils of Sofer (1984). Relationship between saturates and aromatics for terrestrial or waxy oils is also shown.

marine and terrigenous oils was the source of CO₂. However, Sofer (1984a) found this highly oversimplified, as photosynthetic pathways were not considered and lacustrine phytoplankton were grouped with land plants, when he felt they should be grouped with marine phytoplankton. Little or no consideration was given to CO₂ availability (bicarbonate) in marine systems, along with species or temperature variations in determining phytoplankton isotopic composition. Therefore, Sofer (1984a) concluded that similar isotopic composition can be observed in different depositional environments, and single oil component fractions are not unique to a specific depositional environment. He added that stable carbon isotopes could be used (in select cases) to correlate biodegraded oils to their sources, and thermal maturity or isotopic variation in source rocks can only cause a 2‰ variation within an oil family. He also inferred from his experimental results that stable carbon isotopes could substitute for n-alkane distribution as a source indicator. In later work, Sofer et al. (1985) used stable carbon isotopes and statistical analysis on the C₁₅₊ saturates, aromatics, terpane and sterane biomarkers to identify genetically different groups of oils.

Snowdon and Osadetz (1988) reported that gasoline range compounds were poor familial affinity indicators for various types of oils from the Williston Basin. However, certain ratios were good indicators of biodegradation (iC₅/nC₅, 3MC₅/nC₆, nC₁₇/Pr, nC₁₈/Ph) and water washing (CYC₆/Ben, 3MC₅/Ben, MCYC₆/Tol), but dependant upon source rock composition and thermal maturity. In extreme cases, water washing was indicated by a low concentration of gasoline range fractions relative to HMW fractions. The general persistence of significant light hydrocarbon components in some biodegraded oils was unexplained, with compositions missing heavier n-alkanes and

acyclic isoprenoids representing a departure both from expected biodegradation sequences and other studies (Thompson, 1983). Similar conflicts had been attributed to new oil influx into biodegraded pools (Philip, 1983, Seifert et al, 1984), but this was not the case in the Williston basin.

Osadetz et al.(1992, 1994) identified several oil families and their source rocks in the Williston Basin based on biomarker and gasoline range hydrocarbon composition. Type I source rocks in Middle and Upper Ordovician formations generated oils predominantly in Ordovician and Silurian reservoirs characterized by distinctive gasoline range chromatograms and C_{15+} saturate chromatograms associated with Upper Ordovician Yeoman Fm. shales (Williams, 1974). Biomarker analysis showed low C_{23} tricyclic/ C_{30} pentacyclic terpane (C_{23}/C_{30}) ratios and C_{34} hopane predominance. Type II organic matter in the Middle Devonian Winnipegosis Fm. was designated the source for oils in middle Devonian strata, characterized by high Pr/Ph and C_{23}/C_{30} ratios lacking n-alkanes in saturate gas chromatograms. Gasoline range chromatograms indicated similar maturities and long migration pathways for many Type II oils (Thompson, 1983). Snowdon and Osadetz (1988) also reviewed gasoline range chromatograms for Type II oils to determine if oil family classifications could be revised based on Williams (1974) criteria. Some oils were enriched in n-alkanes like Type I oils but most had similar gasoline range chromatograms which classified them as Type II. Stable isotope ratio variations did not complement biomarker compositional distinctions, and gasoline range thermal maturity indicators showed generally poor correlation or sensitivity to other maturity dependant compositional ratios. Oils classified as low maturity by gasoline range parameters showed bulk and saturate fractions indicating higher maturity regardless

of biodegradation. Such contradictory results were in accordance with similar values for other oil studies in the Williston Basin (Thompson, 1983, Osadetz et al., 1992).

Oil-Oil/Oil-Source Correlation

Erdman and Morris (1974) used ratios of the physical/chemical properties of compounds in the C_1 - C_{10} range, along with carbon isotope ratios of individual C_1 - C_5 components to formulate gas-oil correlations. Fractional distillation was used to separate the desired hydrocarbon fractions from the bulk oil, and concentrations of individual components were then determined by packed-column and capillary gas-solid or gas-liquid chromatography. By selecting a set of ratios based on concentrations of individual components with similar boiling points (e.g. 22DMC5/MCYC5) in one oil (R) and dividing them by the same set of ratios for another oil (R'), the similarity between oils would be readily apparent (R/R' of 1 denotes identical match). They found that many factors beside source rock affect the absolute concentrations of C_1 - C_{10} components in petroleum, including reservoir conditions, possible migration, and sampling procedures. The results of the ratio technique were easy to analyze and interpret, however, it was not applicable to oil-spill identification as the most volatile constituents (C_1 - C_5) are lost before sampling can occur. Erdman and Morris (1974) used the unique variability of C_1 - C_5 carbon isotope data to distinguish reservoir horizons and correlate gas pools in areas where the ratio technique was not applicable.

James (1983) calculated separations of carbon isotopes between n-alkanes of natural gas and related them to source rock maturity by use of a single, continuous diagram

(Figure 2.2a). He proposed a strong relationship between isotope ratios of C₁-C₅ compounds and maturity. He stated that the isotopic composition of these compounds reflects source, level of maturity, and extent to which kerogen structure influences gas composition. Source control was strongest for gases from highly structured types of kerogen. With increasing molecular weight, carbon isotope ratios of gases approach that of the source, with isobutane matching the source. As maturity increases, components may get heavier relative to source, and suffer from thermal degradation making correlation difficult. Propane was most susceptible to maturity effects. In a later study, James (1990) measured the carbon isotope composition of wet gas components (propane, isobutane, butane) and used them for correlating reservoired gases. Samples from the Rimbey-Meadowbrook reef trend (RMT) (central Alberta) were all of high maturity, with similar isotopic composition for all three wet gas components with two exceptions due to thermal degradation. This implied that all had a common source (Duvernay Formation). When plotted on the maturity diagram of James (1983), gases were generated at LOM (Level of Organic Maturation) 11-13, and this agrees with maturity of Duvernay strata on either side of the RMT and biomarker data. Based on the similar isotopic composition of wet gases, James (1990) proposed that Devonian gases may have migrated to Lower Cretaceous reservoirs at eastern portion of reef trend, and distinct signatures help distinguish Devonian from Cretaceous and Mississippian (Simonette) reservoirs. Bacterial alteration could change wet gas component isotopic compositions (propane and butane most likely) (James and Burns, 1984), but, the isotopic composition of wet gas components could be used to recognize bacterial influence, mixing of sources, and thermal maturity.

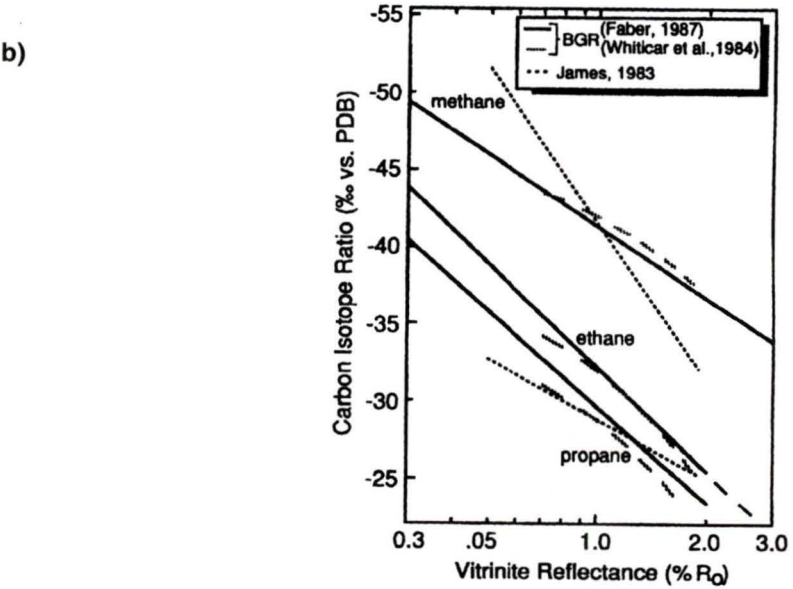
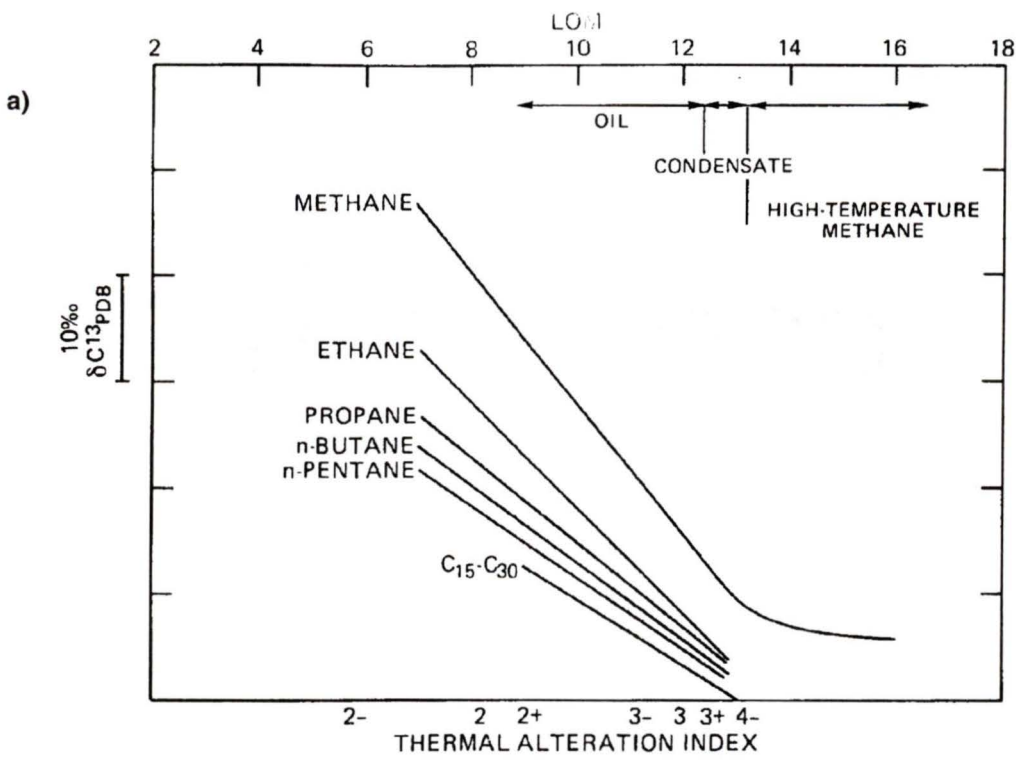


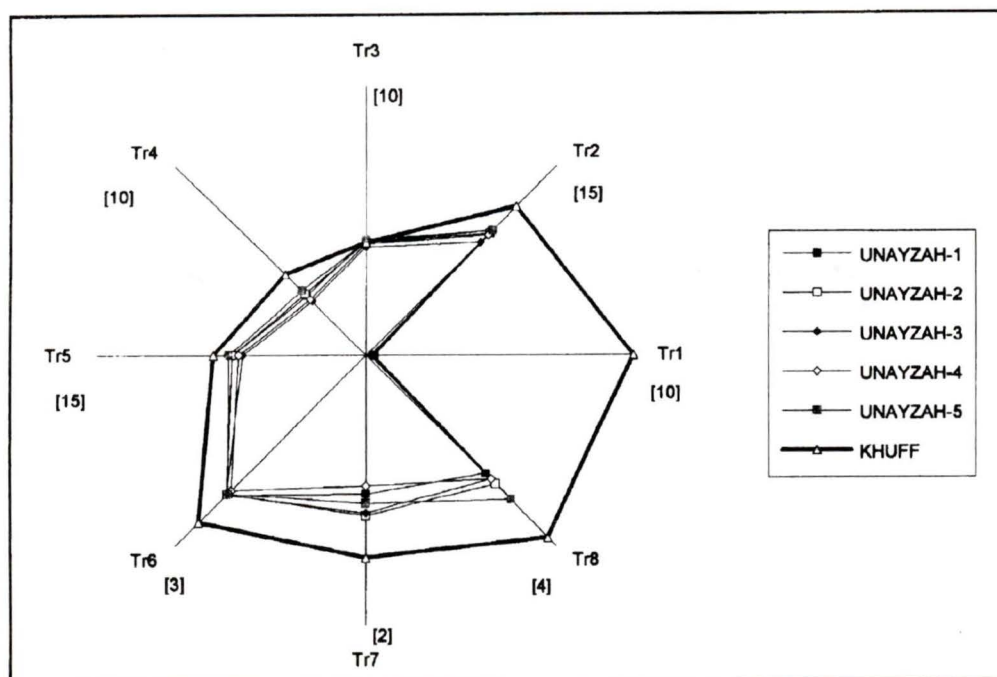
Figure 2.2 a) Theoretical maturation diagram of James (1983) showing calculated separations between gas components plotted against source rock Level of Organic Maturation (LOM).
b) Comparison of carbon isotope maturity models of James (1983) and the BGR (Faber, 1987). (From Whiticar, 1994)

Peters et al. (1989) is an excellent correlation study using stable isotopes in conjunction with biomarkers to determine the origin of oils in the Beatrice field (North Sea). In assigning the oils to a Devonian or Jurassic source, stable isotope analysis of bulk oils and source rock bitumens was performed with the knowledge that typically bitumens are 0-1.5‰ enriched in ^{13}C compared to related oils. All potential source rocks fell outside this range for Beatrice oil, and biomarker ratios provided a mixed signal with characteristics of both sources. Peters et al. (1989) calculated a standard mixing ratio using the $\delta^{13}\text{C}$ ratios and results indicated a 60% Devonian, 40% Jurassic mixed source.

Whiticar (1994) reviewed how stable carbon isotope ratios of natural gas and other wet gas components could be used to correlate light hydrocarbons to their sources. This was done by modeling theoretical relationships between source rock maturity and $\delta^{13}\text{C}$ ratios of the light hydrocarbons generated. Previous models by Galimov (1974) and James (1983) used equilibrium isotope effects (EIE) (thermodynamically controlled processes) to explain the distribution of carbon isotopes in light hydrocarbons. Whiticar (1994) notes that the more accepted view of isotope redistribution involves kinetic isotope effects (KIEs), whereby light hydrocarbons formed by the saturation of an alkyl group cleaved from a kerogen molecule will be depleted in the heavier isotope (^{13}C) relative to the remaining kerogen. Thus, light hydrocarbons will consistently have lower $\delta^{13}\text{C}$ ratios than the precursor organic matter. The magnitude of KIEs related to formation of hydrocarbon gases by bacteria are frequently even larger than those of strictly thermogenic origin. Therefore, when attempting to model the isotopic composition of light hydrocarbons as a function of source rock maturity (e.g. Stahl and Koch, 1974; Faber, 1987; James, 1983; Whiticar et al, 1984), Whiticar (1994) suggests that

inconsistency observed between theoretical models (Fig 2.2b) may be due to “calibration difficulties”, that is, determining the correct or apparent KIEs responsible in different kerogen types with various thermal histories.

Halpern (1995) used two types of star diagrams (multivariate plots in polar coordinates) to assess chemical differences among oils based on analysis of C_7 hydrocarbons. The first co-ordinate system was based on eight ratios (Tr1-Tr8) of C_7 compounds used to characterize variations in oils caused by secondary alteration (water-washing, biodegradation, evaporation) (Figure 2.3a). The second diagram consisted of five ratios (C1-C5) using compounds resistant to secondary alteration and thus useful for correlating oils (Figure 2.3b). Halpern (1995) applied the star diagrams to both exploration and production concerns such as reservoir connectivity, casing leakage, and evaluation of oil quality.



The Parameters Used and Their Order for the C_7 Oil Transformation Star Diagram

Position On Star Diagram	Parameter Name	Ratio	Boiling Point (°C)
1	Tr1	Toluene/1,1-dimethylcyclopentane	110.6/87.8
2	Tr2	n-C7/1,1-dimethylcyclopentane	98.4/87.8
3	Tr3	3MH/1,1-dimethylcyclopentane	91.8/87.8
4	Tr4	2MH/1,1-dimethylcyclopentane	90.0/87.8
5	Tr5	P2/1,1-dimethylcyclopentane*	91/87.8
6	Tr6**	1-cis-2-dimethylcyclopentane/1,1-dimethylcyclopentane	99.5/87.8
7	Tr7	1-trans-3-dimethylcyclopentane/1,1-dimethylcyclopentane	90.8/87.8
8	Tr8	P2/P3†	91/85

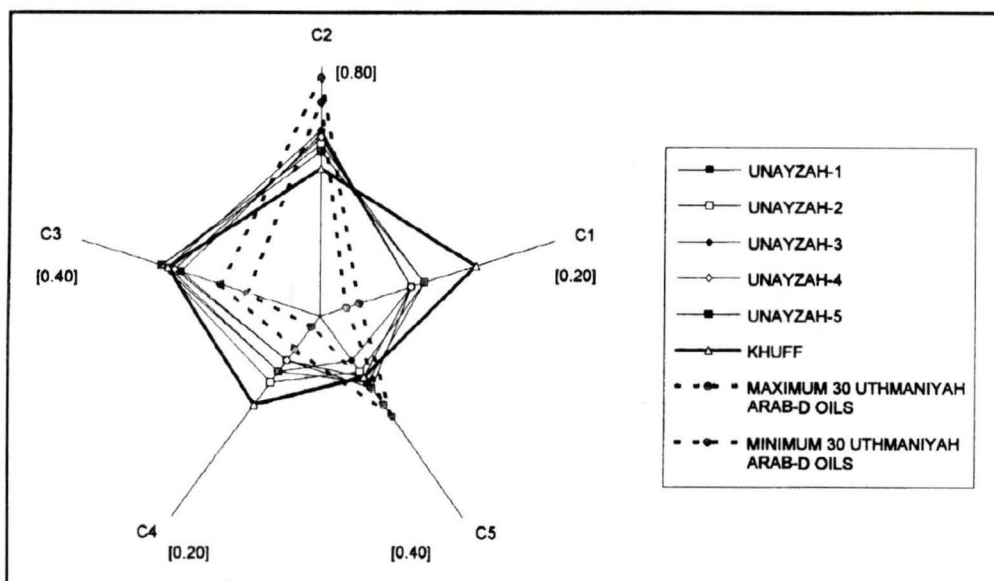
*P2 = 2-methylhexane + 3-methylhexane.

**The large boiling point difference in the compounds comprising Tr6 make it useful as a light-end loss (evaporation) parameter

†P3 = 2,2-dimethylpentane + 2,3-dimethylpentane + 2,4-dimethylpentane + 3,3-dimethylpentane + 3-ethylpentane.

††Some values are approximate.

Figure 2.3a Example of C_7 oil transformation star diagram of Halpern (1995) for oil and condensate samples from different fields. Numbers in brackets are the endpoint values of the individual radii.



The Parameters Used and their Order for the C₇ Oil Correlation Star Diagram

Position On Star Diagram	Parameter Name	Ratio	Boiling Point (°C)
1	C1	2,2-dimethylpentane/P3**	79.2/85
2	C2	2,3-dimethylpentane/P3	89.8/85
3	C3	2,4-dimethylpentane/P3	80.5/85
4	C4	3,3-dimethylpentane/P3	86.1/85
5	C5*	3-ethylpentane/P3	93.5/85

*The large boiling point difference in the compounds comprising C₅ make it useful as a light-end loss (evaporation) parameter

**P3 = 2,2-dimethylpentane + 2,3-dimethylpentane + 2,4-dimethylpentane + 3,3-dimethylpentane + 3-ethylpentane.

†Some values are approximate.

Figure 2.3b Example of C₇ oil correlation star diagram of Halpern (1995) for oil and condensate samples from different fields. Numbers in brackets are the endpoint values of the individual radii.

Petroleum Generation

Leythaeuser et al. (1979a,b) examined light hydrocarbons (C₂-C₇) in sediment samples from several sedimentary basins throughout Northwest Europe, and found that iso-/n-alkane ratios for butanes, pentanes and heptanes were primarily controlled by kerogen quality. Source beds with a larger component of marine organic matter (Type II - high H content) generated higher total concentrations of light hydrocarbons with low iso-/n-alkane ratios, while kerogens with a significant terrestrial component (Type III - lower H content) yielded higher ratios in lower total concentration. It was also noted that for C₆-C₇ hydrocarbons the ratio of aromatics to cycloalkanes was significantly higher for terrestrial vs. marine dominated source beds. Diffusion of light hydrocarbons through shales was also proposed as a contributing process for primary hydrocarbon migration.

Thompson (1983) looked at light hydrocarbon composition with increasing levels of catagenesis to determine the conditions necessary for petroleum generation. Using two temperature dependant indices, he was able to estimate catagenic grade, type of source kerogen (aromatic vs. aliphatic rich), and possible biodegradation for a large suite of oils. Thompson (1983) also developed a concept based on the principle of geographic homogeneity where primary (n-alkane dominant) oils are homogenous in gasoline range composition over wide areas, while napthenic, biodegraded oils exhibit wider variability. Based on this assumption, a boundary can be placed in terms of gasoline range properties between oils generated in sediments of minimum maturity versus those that are biodegraded.

Hunt (1984) studied generation and migration of light hydrocarbons (C₁-C₁₄) in near-

surface and subsurface sediments. He discussed three types of reactions primarily responsible for light hydrocarbon generation: (1) biological – microbial fermentation and degradation of terpenoids and other HMW compounds; (2) low temperature (<50°C) –to produce branched-chain hydrocarbons; (3) high temperature – cracking reactions producing mostly straight-chain hydrocarbons. Hydrocarbons with tertiary carbon atoms form earlier than structures with quaternary carbons due to the higher stability of the intermediate tertiary carbonium ion/free radical. Hunt (1984) proposed that hydrocarbon generation zones in drill wells can be identified by the distribution pattern of light hydrocarbons in the sediments. Migration of light hydrocarbons occurred through diffusion in fine grained sediments and a more traditional oil-gas phase for larger pore openings.

In studies focusing on the generation of light hydrocarbons, Thompson (1987, 1988) proposed evaporative fractionation for observed changes in the molecular composition of related gas-condensate reservoirs. Evaporative fractionation involves several phenomena whereby gas is separated from oil in the subsurface, and LMW compounds are preferentially fractionated into the vapor phase. The ability of a compound to enter the vapor phase depends on its fugacity, molecular weight, isomeric structure, hydrocarbon class, and composition of mixture (i.e. if other hydrocarbons present). Aromatic compounds behave anomalously, as all except benzene are polar structures which induce polarity in other molecules and form transitory structures of high molecular weight, limiting escape from the liquid phase. Residual oils bear evidence of the fractionation, with conspicuous overall loss of light hydrocarbons, and an overall increase in the content of light aromatic and naphthenic hydrocarbons relative to paraffins. Gas (bearing

oil in solution) can be conducted along faults to form independent gas-condensate accumulations elsewhere.

Chung et al. (1988) examined the generation of gaseous hydrocarbons via irreversible thermal cracking of isotopically homogenous parent molecules. They developed an equation that relates the carbon isotope ratio of individual gaseous molecules as a function of the inverse carbon number of the molecule. Other equation variables included the stable isotope ratio of the terminal carbon attached to the gas molecule prior to cracking, and the ratios of other carbon atoms in the gas molecule. From this equation a “natural gas plot” was developed that can be used in gas-gas and oil-gas correlations (Figure 2.4). The relative success of the equation in predicting isotope ratios for gaseous hydrocarbons generated in laboratory heating experiments of crude oils and source rocks suggested that the ratios of individual hydrocarbons are controlled by kinetic isotope effects during carbon-carbon bond breakage as opposed to equilibrium isotope effects.

Clayton (1991) examined how $\delta^{13}\text{C}$ ratios of oils are affected by thermal alteration and phase effects inherent with the formation of condensates. He discussed two types of isotope effects associated with petroleum generation. Individual compounds are subject to kinetic isotope effects, whose magnitude is dictated by the molecular weight of the products and reactants involved. Reactions involving compounds with six or more carbon atoms would show negligible fractionation, as the effect of ^{13}C atoms on reaction rates for HMW compounds is minimal. The second isotope effect involved bulk oil fractions with variable $\delta^{13}\text{C}$ ratios dependant on the relative proportions of isotopically dissimilar compounds within each fraction. The example given involved removal of ^{12}C n-alkanes from the saturate fraction during biodegradation producing a net shift in ^{13}C .

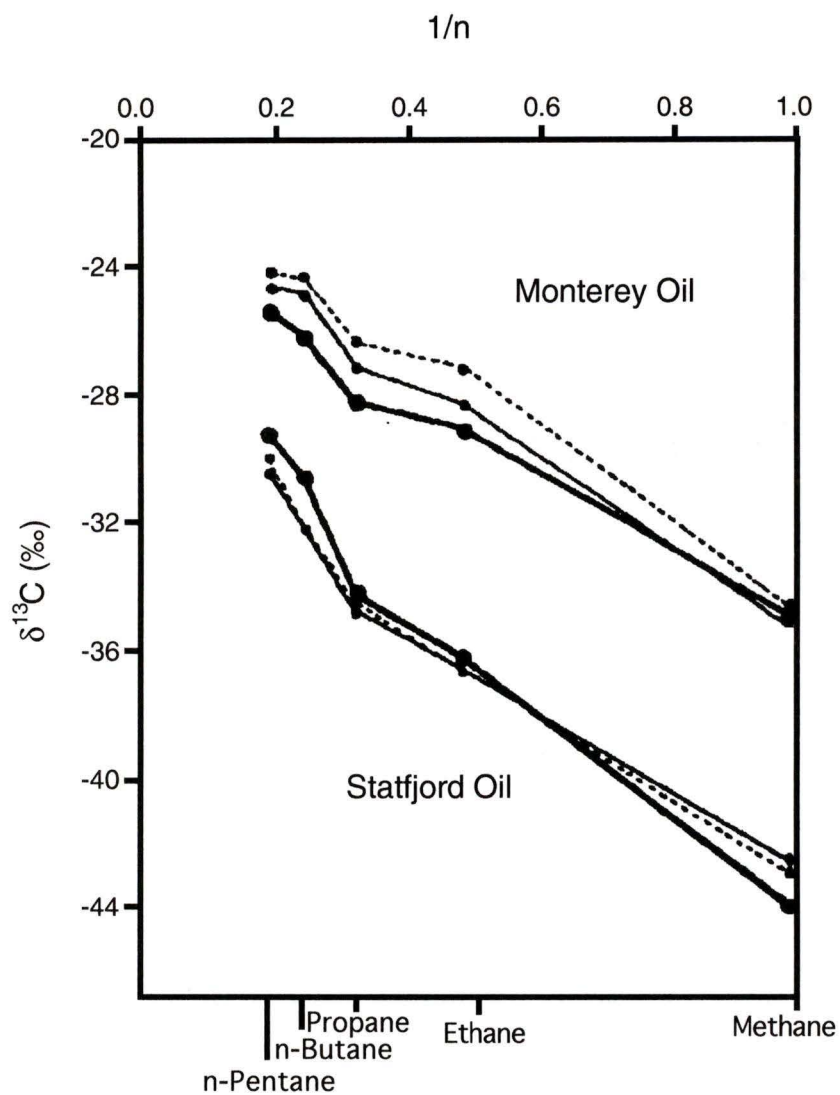


Figure 2.4. Natural Gas Plot of Chung et al. (1988) for C_1 - C_5 hydrocarbons generated from laboratory heating experiments of two North Sea oils. Plot shows carbon isotope ratio of compound as a function of the inverse carbon number of the molecule ($1/n$). The main benefit of the diagram is that differences in isotopic composition between oils are readily apparent.

Clayton (1991) added that during oil generation, the kerogen becomes enriched in ^{13}C (ca. 1‰) due to release of ^{12}C rich oil and gas. Kinetic isotope effects become more important during subsequent oil to gas/condensate cracking, as the increase in the $\delta^{13}\text{C}$ ratio of the remaining oil could be modeled by a Rayleigh distillation process. A clear trend showed low maturity oils producing a gas/condensate lighter than the oil phase, and the reverse for higher maturity oils. This was because low molecular weight (LMW) compounds would become enriched in ^{13}C faster than HMW compounds, and the magnitude of this effect would increase systematically with the maturity of the oil.

Chung et al. (1992) reviewed the $\delta^{13}\text{C}$ values for a wide variety of marine crude oils, and discussed numerous causes of the variations between samples. Factors, such as marine vs. terrestrial carbon source, variable marine photosynthetic fractionation of carbon isotopes during primary production of organic carbon as a function of atmospheric CO_2 , depositional environments, and secular $\delta^{13}\text{C}$ variation of marine bicarbonate must all be considered. They add that $\delta^{13}\text{C}$ values are useful not only for oil-source correlations, but also for determining possible age and depositional environment of source rocks. In later work, Chung et al. (1994) specifically examined $\delta^{13}\text{C}$ of volatile hydrocarbon fractions ($<C_9$) and found them to be diagnostic for all three purposes. These compounds were isotopically lighter than the C_9 - C_{17} fraction for carbonate (marine) oils, with the opposite observed for deltaic (terrestrial) oils. This effect was explained by earlier expulsion of marine oils derived from isotopically homogenous (algal-bacterial) kerogens in rich source rocks. It was consistent with the kinetic isotope effect associated with petroleum formation, where ^{13}C is initially distributed randomly in marine organic matter, and subsequent hydrocarbon generation results in a ^{13}C enrichment confined to

the residual kerogen (up to 2‰). As a result, the petroleum is depleted in ^{13}C , the degree of depletion inversely proportional to molecular size (Chung et al., 1988). For deltaic oils, Chung et al. (1994) propose secondary cracking in a lean source rock prior to expulsion, along with the presence of isotopically heavier materials (vitrinitic or wood components) in a more heterogeneous kerogen producing an inverse effect.

Continuous Flow-Isotope Ratio Mass Spectrometry (CF-IRMS)

Bjørøy et al. (1990) were among the first groups to document the use of GC-C-IRMS (Gas Chromatography – Combustion – Isotope Ratio Mass Spectrometry) for compound specific isotope analysis of oils and condensates. They reported that there is minor variation in $\delta^{13}\text{C}$ ratios of n-alkanes and isoprenoids from whole oils versus the saturate fraction. Building on this, Bjørøy et al. (1991a) examined the individual stable carbon isotopes of n-alkanes and isoprenoids in the C_6 to C_{32} range in several oils from variable sources (terrestrial, marine, lacustrine) and locations (North Sea, Southern and Eastern US). The $\delta^{13}\text{C}$ ratios for n-alkanes showed greatest enrichment in ^{13}C for terrestrial sources, followed by marine and lacustrine samples. In terrestrial oils, as carbon number increased, n-alkane ratios became progressively depleted in ^{13}C while lacustrine and marine oils showed little variation (Figure 2.5). There was a more complex variation in $\delta^{13}\text{C}$ ratios for isoprenoids between oils, and Bjørøy et al. (1991a) concluded that their isotopic composition is more dependant on both depositional environment and type of source rock. The authors also concluded that individual carbon isotopes may be a useful tool in oil classification and correlation.

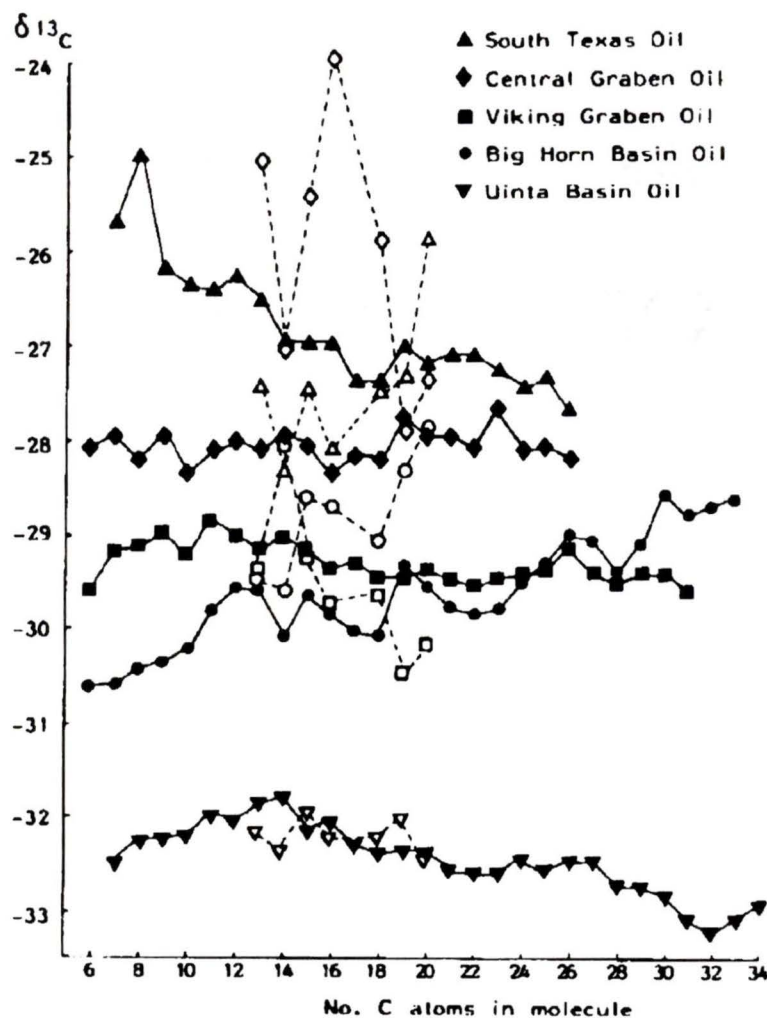


Figure 2.5 Comparison of isotope ratios for separate components in oils of different origin. Filled symbols, n-alkanes, open symbols, isoprenoids. Type of source rocks for oils are South Texas - Terrestrial, Uinta Basin - Lacustrine, Central Graben, Viking Graben and Big Horn Basin - Marine. (From Bjoroy et al., 1991a)

Bjørøy et al. (1991b) looked at possible trends in isotopic composition of n-alkanes, isoprenoids and hopanoids with increasing maturity for typical oil and gas source rocks. They pyrolyzed several different source rocks and measured the change in isotopic composition of individual hydrocarbons in the C₁₀₊ range. Variation for n-alkanes and isoprenoids was minor, with only a 1-3‰ enrichment in ¹³C for select compounds. They attributed the apparent ¹²C depletion with increasing maturity to preferential cracking of ¹²C-¹²C bonds and not to the dominant bond types in the kerogen. Bjørøy et al. (1993) then documented that the isotopic composition of n-alkanes in oils between nC₅ and nC₃₅ would be dependant on source rock type and that samples from the same source would produce similar isotopic signatures, in concurrence with work by Sofer et al. (1991) on C₁₃₊ hydrocarbons. In some cases, a monotonic increase or consistency in the isotope ratio reported by these authors may be diagnostic for a particular source rock or oil (Whiticar and Snowdon, 1998).

Dzou and Hughes (1993) examined the isotopic effects of evaporative fractionation of Thompson (1987, 1988) on individual compounds in the saturate fraction of oils and related condensates. The expected result would be that the residual oil is isotopically enriched in ¹³C (on average) than the condensate. However, in some samples the opposite was observed, an example being the K-4 oil-condensate pair taken from offshore Taiwan (Figure 2.6). Dzou and Hughes (1993) explained the enrichment in ¹³C for the saturate ratio of the condensate by analyzing the isotope ratios for individual compounds in the saturate fraction. Compound ratios became progressively lighter with increasing n-alkane carbon number, and suggested that the overall saturate ratio of the condensate is heavier due to its depletion in these isotopically light higher carbon number compounds

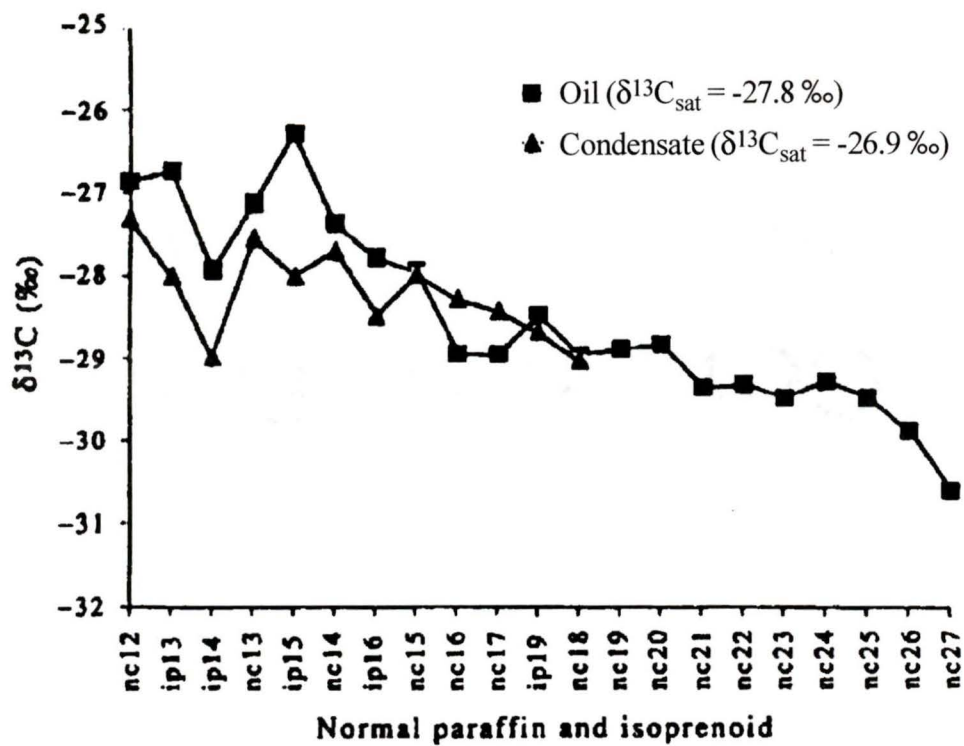


Figure 2.6 Carbon isotope ratios of individual n-alkanes (nc) and isoprenoids (ip) of an oil-condensate pair from well K-4, offshore Taiwan. (From Dzou and Hughes, 1993)

(C₂₀₊). A comparison of compounds <C₂₀ between a related oil and condensate showed that the condensate is depleted in ¹³C as expected. Thus, the benefit of a compound specific approach vs. bulk isotopic measurements was clearly shown.

Clayton and Bjorøy (1994) determined $\delta^{13}\text{C}$ values for individual hydrocarbons (C₆-C₃₀) in several compound classes (cyclic, branched, straight-chain alkanes; isoprenoids; aromatics) of North Sea oils to determine the effect of increasing maturity on the isotopic composition of 4 different samples. Maturity accounted for 50 to 90% of the observed isotopic variation for individual compounds, with $\delta^{13}\text{C}$ ratios of most compounds becoming enriched in ¹³C with increasing maturity (2 to 3‰) for the majority of oils. Compounds which deviated from this pattern (e.g. pristane, phytane, aromatics) have more source control on their $\delta^{13}\text{C}$ values. Branched alkanes exhibited anomalous behavior, with a pronounced difference in the $\delta^{13}\text{C}$ ratio of 2MC6 attributed to a different biological precursor compared to the other branched alkanes. Four cyclic compounds also showed significant variation in $\delta^{13}\text{C}$ ratios, with MCYC5 shifted almost 2‰ versus EtCYC5, and MCYC6 consistently 1‰ offset from CYC6 for all samples analyzed. This suggested that even for structurally similar compounds, the isotopic signature from differing biological sources was preserved through maturity variations. This was also the case for monoaromatic compounds, where toluene was consistently enriched in ¹³C versus benzene or xylene. Clayton and Bjorøy (1994) developed an approximation of isotopic variation resulting from maturity using Pr/Ph as a source indicator and aromatic molecular ratios to determine maturity. However, this was an iterative process with several assumptions complimentary to their sample set.

Bjorøy et al. (1994) examined potential isotopic fractionation of individual

hydrocarbons in the C₄ to C₂₀ range for North Sea oils and condensates subjected to prolonged storage and evaporation. The experiments showed that after evaporation the remaining condensate may be enriched in ¹³C by 0.5‰, independent of the type of hydrocarbon. This was a small change when compared to the natural isotope variation of different compounds (especially cyclic and branched alkanes). They concluded that the C₅-C₂₀ range could be used with confidence for oil/condensate correlation, and isotopic effects associated with storage and evaporation are not significant. Bjorøy et al. (1994) also examined whether natural fractionation could occur in a reservoir (i.e. where a condensate occurs higher up in a structure after fractionation from an oil), with results indicating that related oils and condensates exhibit characteristic and consistent variations in δ¹³C of individual compounds. They concluded that CF-IRMS data can be used with confidence as a correlation tool, and source or maturity effects on the isotopic composition of n-alkanes are greatest in C₁-C₂₀ range. The contribution of n-alkane isotope values (¹³C depleted) to whole oil values were compensated for by branched/cyclic alkanes and aromatics (normally isotopically heavier) (Galimov, 1974; Sofer, 1984a). Maturity variations had a larger effect on the isotopic composition of n-alkanes, and the overall isotopic signature of less mature oils was influenced more by source characteristics along with polar fractions (i.e. aromatics).

Wilhelms et al. (1994) used CF-IRMS to compare individual n-alkanes and isoprenoid alkanes in crude oils and asphaltene pyrolysates. The principal conclusion was that CF-IRMS fingerprints of individual molecules produces characteristic isotopic variations beyond the scale of reproducibility for the technique (4‰). Similar fingerprints for asphaltene pyrolysate n-alkanes and crude oil n-alkanes from marine oils suggested a

common precursor for the parent alkyl structures of both classes of compounds, and that asphaltenes can be used as a proxy for source rock analyses. However, this similarity was not observed in deltaic land-plant derived oils. In order to assess source rock characteristics (maturity, depositional environment, generation potential) Wilhelms et al. (1994) suggest using other parameters such as biomarkers and asphaltenes.

Murphy (1995) provides a summary of numerous oil-oil, oil-source correlation techniques and problems inherent with them. Traditionally, bulk oil and major oil fractions are measured, but the resulting isotope ratios or molecular parameters are averages of many compounds and often of limited diagnostic value. These techniques also suffer from maturation or secondary alteration processes such as biodegradation and water-washing, making correlation difficult due to changes in molecular/isotopic composition. For example, microbes preferentially attack straight-chain alkanes over the branched alkanes or cycloalkanes (Bailey et al., 1973). Researchers have moved towards more compound specific analyses yielding information on molecular and isotopic composition of individual compounds.

Dowling et al. (1995) developed bitumen-oil-source correlations based on the $\delta^{13}\text{C}$ ratios of individual hydrocarbons (n-alkanes, Pr, Ph). Differences between samples were attributed to primary source variations, with weathering and biodegradation as minor causes. The CF-IRMS analyses suffered from co-elution of some peaks observed in the mass 45/44 trace, producing mixed $\delta^{13}\text{C}$ ratios for several compounds (e.g. n-C₂₈, Pr). However, using the $\delta^{13}\text{C}$ data from other individual compounds, Dowling et al. (1995) were able to correlate bitumens from the Australian coastline to oils of Central Sumatra.

O'Malley et al. (1996) examined $\delta^{13}\text{C}$ ratios along with the molecular abundances of

individual PAH's in sediments of St. Johns Harbour (Newfoundland), to determine the primary sources of input for these toxic compounds. They sampled potential sources such as soot from domestic fireplaces and chimneys, furnaces, car mufflers, and direct petroleum sources including crankcase oils and waste oil sump of garages in the St. Johns area. Mass balance calculations using a two component Langmuir mixing model showed that between 50-80% of PAH input to harbour sediments was of combustion origin, most likely from vehicle emissions carried in surface runoff from the city. Direct petroleum pollution from spent oil products accounted for the remainder. This study concluded that compound specific isotope analysis had great potential in determining source inputs to sedimentary environments.

Dempster et al. (1997) compared isotope ratios of pure BTEX compounds versus BTEX extracted in pentane before injection into a CF-IRMS system. An error of 0.5‰ was added to values for samples run on different split (analytical) settings, however the pentane extraction method itself was found to be non-fractionating. Unique $\delta^{13}\text{C}$ values were observed for pure BTEX compounds from 3 separate manufacturers, and CF-IRMS could be used to fingerprint the individual compounds and trace them to a specific manufacturer.

Mansuy et al. (1997) analyzed oil samples by CF-IRMS to determine the effects of artificial and natural weathering processes on the isotopic composition of individual n-alkanes ($\text{C}_{10}\text{-C}_{30}$) and whether these effects compromise the correlation of this oil to a non-degraded counterpart. They also tried to establish the use of CF-IRMS as a complimentary correlation technique to GC and GC/MS. Artificially weathered samples showed evaporative loss of most compounds $<\text{C}_{15}$, but, the isotopic composition showed

good correlation ($\pm 0.3\%$ standard deviation) with the unweathered sample (Figure 2.7a). Oils that were biodegraded over periods between 2 months to 4 years, showed slight enrichment in ^{13}C , but the overall standard deviation was only 0.4% from undegraded samples. This was attributed more to analytical error rather than biodegradation effects. In cases of severely biodegraded oils, most n-alkanes are removed and Mansuy et al. (1997) applied asphaltene pyrolysis and subsequent CF-IRMS analysis to resulting aliphatic, aromatic, and NSO fractions. These also correlated well between the biodegraded and unaltered oil (0.5% std. deviation). Environmental applications of the method involved correlating individual components in light fuel oil from fugitive spills in conjunction with tests by the U.S. Coast Guard, and examination of crude oils extracted from feathers of birds killed in a recent oil spill. In both cases, CF-IRMS analysis of n-alkanes was able to correlate the weathered oil to a definitive source (Figure 2.7b).

Odden et al. (1998) provide a brief summary of previous methods for light hydrocarbon extraction (e.g. Durand and Espitalie, 1972; Philippi, 1975; Jonathan et al., 1975; Leythaeuser et al., 1979a,b;) and origin of gasoline range hydrocarbons. Odden et al. (1998) was also among the first studies to use $\delta^{13}\text{C}$ ratios of individual gasoline range compounds to effectively correlate oils to source rocks from offshore Mid-Norway. They analyzed light hydrocarbons ($\text{C}_4\text{-C}_{13}$) from source rocks by thermal-extraction GC, (IRMS) and compared them with CF-IRMS analysis of light hydrocarbons from oils and condensates in the region. Source rocks were crushed immediately prior to analysis to minimize evaporation effects. The isotope correlation technique could not only be used to distinguish the source of oils, but also to classify oils based on the molecular and isotopic compositions of $\text{C}_6\text{-C}_8$ fractions. Data from samples were plotted on ternary diagrams of

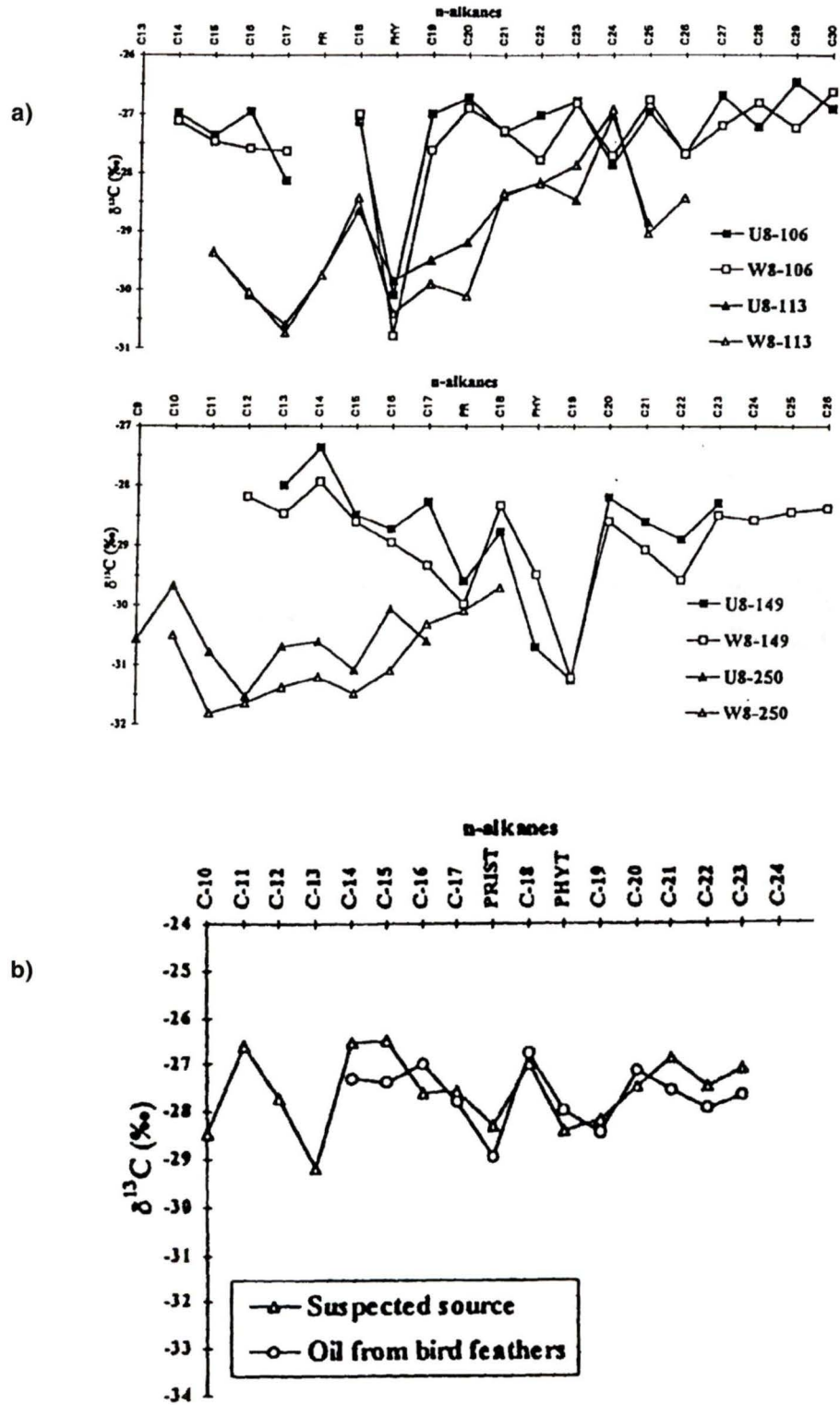


Figure 2.7 a) Isotopic composition of individual n-alkanes for 4 pairs of weathered (W) and unweathered (U) oils.
 b) Isotopic composition of individual n-alkanes (also Pristane and Phytane) for oil collected from birds killed in a recent spill. Comparing the $\delta^{13}\text{C}$ ratios to a suspected source gives a reliable match. (From Mansuy et al., 1997)

Dai Jinxing (1992) and ten Haven (1996) to distinguish between marine and terrestrial source rocks. The proportion of benzene and toluene in source rocks containing land plant derived organic matter was higher than in marine organic matter enriched in cyclopentanes. Multivariate statistical analysis showed that source facies was more important than maturity as an indicator of light hydrocarbon composition. Odden et al. (1998) then compared samples using ratios/indices of Thompson (1987) and Mango (1990b) to determine if samples had undergone evaporative fractionation or phase alterations, with mixed results. The greatest uncertainty in the study was if the light hydrocarbons analyzed in the source rock samples were representative of the petroleum generated/expelled.

Origin of Gasoline Range (C₅ to C₁₀) Hydrocarbons

Much study has focussed on the origin of light hydrocarbons. It is commonly believed that gasoline range hydrocarbons are formed through the thermal breakdown of kerogen and other HMW hydrocarbons. However, there has been disagreement over the exact mechanisms involved in the generation process. Murphy (1995) provides a summary of work by Hunt, (1980), Philippi (1975, 1977, 1981), Thompson (1979, 1983, 1987, 1988) and Mango (1987, 1990a,b, 1991, 1994), contrasting different viewpoints on this complex topic. An update on recent work by Mango (1996, 1997) and ten Haven (1996) is summarized below.

Mango (1987, 1990a,b, 1991, and 1994) proposed a steady state catalytic process, where the relative rates of product formation are constant, as an explanation for the

generation of isoheptanes and cycloalkanes. Pairwise products (e.g., 2MC₆ and 3MC₆) are formed sequentially which act as reactants to produce another pair of compounds (e.g., 23DMC₅ and 24DMC₅). These two sets of products are formed by thermal cracking, but the reactants are continually regenerated and the products continually formed which acts as the catalytic process at steady-state. Mango (1992, 1996) then proposed that transition metals (Ni, V, Ti, Co) activated in the lipophilic domains of kerogen, could also act as catalytic agents converting normal paraffins (and olefins) into light hydrocarbons and natural gas. In later work, Mango (1997a) also presented results showing petroleum decomposition into natural gas in the presence of transition metal catalysts. Although the correct theory for gasoline range hydrocarbon generation is still uncertain, Mango provides abundant supporting evidence for his theory.

Ten Haven (1996) found exceptions to the invariance ratios of Mango (1990b), and suggested that while they are excellent for homologous oil sets, they must be used in concert with more traditional correlation techniques (e.g. stable isotopes or biomarkers). The invariance ratios are useful for condensate-oil and condensate-condensate correlations, but they cannot discriminate oil/condensates from each other, unless from a common source. For characterizing (fingerprinting) individual oils, the parameters are useless as they cannot be related to a specific kerogen and/or a depositional environment.

Mango (1997b) provides a review of the opposing theories on the origin of light hydrocarbons, along with early literature on the composition, distribution (in sediments), and application of these compounds to maturity and oil correlation studies. He reiterated that while thermal cracking enjoys widespread support, the composition of light hydrocarbons and the stability of their HMW precursors are inconsistent with such a

mode of origin. If cracking of HMW compounds is the source for light hydrocarbons in oils, primary structures (compounds with structure similar to their precursor) should dominate its composition. This is not the case for the majority of oils, where primary structures are proportional to their corresponding isomers at all concentrations. Mango (1997b) restates his theory of transition metal catalysis, adding that these elements are present in organic sediments at sufficient concentrations to promote light hydrocarbon generation. Van Duin and Larter (1997) support Mango's hypothesis in presenting reaction schemes for the formation of C₇ heptane isomers from heptene precursors by a kinetically controlled reaction mechanism.

CHAPTER 3 – ANALYTICAL METHODOLOGY

Extraction of analytes by SPME has been well documented in the literature. Analytes partition from a sample onto the fiber and are thermally desorbed in the injection port of a gas chromatograph. SPME is an equilibrium method, and equilibrium is established between the liquid, headspace and fiber when the concentration of the analyte in all three phases can be considered constant (Steffen and Pawliszyn, 1996). Equilibrium is defined as when the concentration of analyte is homogenous within each phase and concentration differences between two adjoining phases has satisfied the partition coefficient between phases (equilibration time = mass adsorbed by fiber coating is 90% of final total mass) (Zhang and Pawliszyn, 1993a). For our experiments, we use a simpler definition of Dias and Freeman (1997) where equilibrium is achieved when the amount of analyte extracted remains constant regardless of increasing exposure time between fiber and sample. Equilibration times are dependant on partition coefficients between the liquid-headspace and headspace-fiber. The limiting mass transfer step is from the liquid to the headspace, and the extraction profile has the characteristic shape of a sharp rise and then shallowing out. The rate of each segment of the profile is dependant on the convective and diffusive transport of analytes in the sample matrix or a product of slow desorption kinetics (Zhang and Pawliszyn, 1993a).

Zhang and Pawliszyn (1993a) was one of the first studies that detailed the equilibrium and kinetics of headspace SPME (HSPME), and compared it with direct SPME sampling of an aqueous phase for BTEX and several polycyclic aromatic hydrocarbons (PAH). They showed that detection limits of headspace sampling were approximately twice that

of aqueous sampling, and the headspace technique resulted in decreased sampling times and increased extraction efficiency for all compounds. This was a significant improvement over traditional sampling methods such as liquid-liquid extraction, solid-phase extraction (SPE), and P&T. Using HSPME, matrix effects are reduced and interferences involved with a liquid sample are eliminated (Steffen and Pawliszyn, 1996). Zhang and Pawliszyn (1993a) presented a simple one-dimensional kinetic model to study the diffusion processes involved with HSPME. The chemical potential difference of analytes among the three phases (coating, headspace, liquid) present is the driving force moving analytes from the aqueous matrix into the fiber. The limiting step in the process is considered to be the diffusion rate of analytes for the different phases. A low diffusion rate is observed between the liquid and headspace, while diffusion of the analytes from the headspace to fiber is four orders of magnitude higher. Approximately 50% less analyte is adsorbed with headspace sampling versus immersing the fiber in an aqueous solution. HSPME was found to be ideally suited to organic compounds with high volatility, hydrophobicity, and could be used for sampling compounds as large as three-ring PAHs. The technique could also isolate less volatile analytes if the desired sensitivity could be achieved prior to attaining equilibrium. Zhang and Pawliszyn (1993a) also noted that the time required for both volatile and less volatile analytes to equilibrate with the fiber coating could be minimized by agitating the aqueous phase, reducing the headspace volume (Louch et al., 1992) or heating the sample (Zhang and Pawliszyn, 1993b).

Zhang and Pawliszyn (1993b) used HSPME to isolate BTEX compounds from water, sand, clay and sludge samples. Extraction profiles (time vs. mass adsorbed) at 50°C for

all compounds showed that different amounts of each analyte were adsorbed by the coating based primarily on the partition coefficients of each compound (equilibration times are rapid, ca. 1 min.), not choice of substrate. When the matrix adsorbs the analyte strongly, or the volatility of the analyte is low, the concentration of analyte in the headspace is low, and the amount adsorbed on the coating is minimal, leading to poor sensitivity. Gasoline range analytes with high volatility avoid such obstacles, and we need only allow enough time for analytes to equilibrate with the three phases present.

One of the few studies to use SPME for stable isotope analysis was performed by Dias and Freeman (1997) on a combination of hydrocarbons and organic acids (toluene, hexanol, methylcyclohexane, acetic, propionic, and valeric acids). Nonpolar compounds extracted with a nonpolar phase were slightly enriched in ^{13}C (0.5‰) versus organic acids extracted by a polar phase that showed a depletion in ^{13}C (1.5‰) with respect to the remaining liquid. Direct immersion of the fiber into an aqueous solution was used for extracting the analytes, and isotope ratios were measured with instrumentation similar to that in this study.

In our experiments, the high concentrations (and sheer number) of analytes present in each oil results in an enormous amount of sample being adsorbed on the fiber. The mass of a single compound (m_i) introduced to the GC from the SPME fiber is determined using the open split ratio (R_{os}) of the IRMS, molecular weight of the compound (M_i), and the number of carbons in the molecule (C). Typically, the quantity of a single analyte adsorbed (e.g. n-C₇) out of 100-200 total analytes is (after Dias and Freeman, 1997):

$$m_i = (n_s/C)M_iR_{os}$$

$$m_i = 2.13 \mu\text{g n-C}_7 (\sim 21 \text{ nmol})$$

n_s = number of moles of CO₂ at the source and is determined by

$$n_s = A/(SWqN_A)$$

$$n_s = 1.754 \times 10^{-9} \text{ moles CO}_2$$

where A is the mass 44 response (\cong peak area (Vs)), W is the resistance of the amplifier circuit ($3 \times 10^8 \Omega$), q is the charge of an electron ($1.609 \times 10^{-19} \text{ C}$), N_A is Avogadro's number ($6.023 \times 10^{23} \text{ atoms/mol}$), and S is the sensitivity of the IRMS (5.0×10^{-4} ions/molecule). The open split ratio is determined by injecting a known concentration of a standard compound into the GC and mass 44 response (A) is recorded from which n_s can be calculated.

Methods

Two oils collected from wells in Alberta, Canada (Chester, NA1) are used as standards in the experiments reported. These oils have a representative composition of gasoline range hydrocarbons in most light and medium crude oils. Oils are stored in a refrigerator (3°C) to lower vapor pressures and minimize evaporation of volatile hydrocarbons. For experiments involving pure standards, reagent grade solvents were acquired from several laboratories.

Purge and Trap - Deactivated alumina (80-200 mesh) is used as a substrate onto which oil droplets are coated. Approximately 1 ml of the alumina is placed in a vial. A drop of oil is transferred to the alumina by a clean wire. The alumina/oil mixture is stirred/mixed

to distribute oil on the substrate. Several grains are transferred to a smaller vial for application to the gas chromatograph (GC).

The smaller vial containing grains is connected to a 6 port valve (see Fig. 2 of Whiticar and Snowdon, 1998). The vial is sealed with a cap lined with a Teflon septa. Purge helium flows into the small vial through a needle. From the vial, the helium plus hydrocarbons flow through a needle (and tubing) to the valve and into the trap. Sample is purged with helium for 8 minutes while liquid nitrogen is used to trap the volatiles. The liquid nitrogen is removed as the 6 port valve is switched to the on column position, and the sample flows into the GC for analysis. To prevent peak tailing, the trap is immersed in hot water immediately upon removal of the liquid nitrogen. For further details on this technique, refer to Murphy (1995) or Whiticar and Snowdon (1998).

SPME – The fiber mechanism and polydimethylsiloxane (PDMS) coating is selected based on its performance for analysis of non-polar volatile compounds, i.e. hydrocarbons (Louch et al., 1992; Zhang and Pawliszyn, 1993a) (Figure 3.1a). PDMS is hydrophobic and offers a compositional similarity to capillary columns used in GC analysis. PDMS is thermally stable up to 300°C, and its melting point of -50°C is significantly below the temperatures encountered in sampling and desorption. Therefore, no phase transitions are related with this material, and all fibers are preconditioned before use.

Oils are sampled by pasteur pipette and a droplet is placed in a clean 1/2 dram vial (pre-fired at 450°C to remove contaminants). The amended vial is capped and sealed with a teflon lined septa. Replicate analyses use a new droplet/vial to preclude any depletion of gasoline range compounds. At least 1 hr is allowed to establish liquid-vapor

Solid Phase MicroExtraction (SPME)

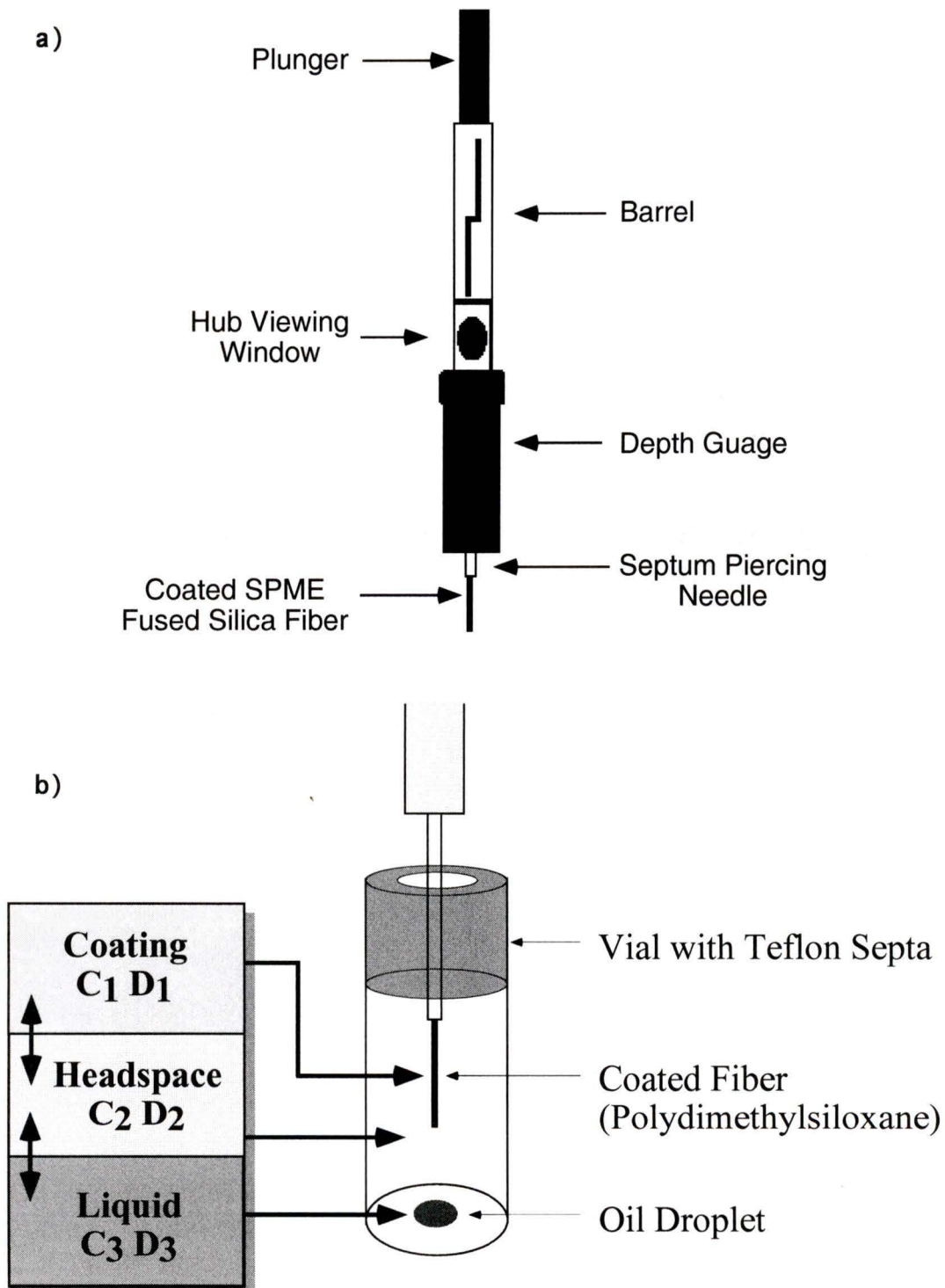


Figure 3.1 a) Schematic drawing of SPME syringe and fiber assembly. b) Headspace sampling technique using SPME. Analytes equilibrate between the three phases (coating, headspace, liquid) based upon their concentration (C) and diffusion (D) coefficients.

equilibrium in the vial. Compounds in the C₅-C₁₀ range have sufficient vapor pressures at room temperature to enter the vapor phase. This results in an efficient separation of the gasoline fraction from the bulk oil. It should be noted that hydrocarbons as large as C₂₀ are present in the headspace in trace amounts.. The most volatile compounds in the C₁-C₄ range are not present in measurable quantities resulting from rapid evaporation and are often lost before the lab receives an oil for analysis.

A heavy gauge needle pierces the septa to allow the SPME fiber to pass through unharmed. The fiber is extended into the headspace, but does not come in direct contact with the oil at any time (Figure 3.1b). The fiber is exposed ca. 15 minutes, allowing analytes sufficient time to establish equilibrium between the three phases (liquid, headspace, coating). It is important to maintain a constant temperature during adsorption since large fluctuations in temperature may affect mass transfer rates and equilibration times (Boyd-Boland et al., 1996). Once equilibrium is reached, the fiber is retracted and immediately transferred to the GC split/splitless injector. The fiber is extended in the injection port (260°C), where analytes are thermally desorbed and swept onto the column. This technique prevents a substantial amount of oxygen or moisture from entering and degrading the GC column. A special glass inlet designed for SPME is also employed in the injector. This inlet has a smaller (0.75 mm) inner diameter than conventional inlets (2 mm) that results in a faster, more thorough/concentrated heating of the fiber, and thus a more rapid desorption of analytes. The inlet also serves to focus the sample, improving peak shape (minimizing tailing) and resolution.

For molecular analysis by P&T and SPME, a stand-alone GC is used equipped with a flame ionization detector (FID). The gasoline range components are separated on a J&W

60m x 0.32 mm DB-1 fused silica capillary column with a 1 μ m film thickness.

Compounds are separated using a temperature program of 35°C for 1min, ramp 2°C/min to 90°C, hold for 5 min., ramp to 280°C at 20°C/min, hold at 280°C for 7 min. to burn off any higher molecular weight (HMW) compounds lingering in the column. The total time for sample analysis is approximately 1 hr.

Stable carbon isotope analysis is done using the advantages of a CF-IRMS system. The GC utilizes the same column and temperature program as for molecular analysis in CF-IRMS. Following partitioning of the C₅-C₉ compounds on the GC column, they are directed with the carrier gas (helium) into a microcombustion oven consisting of an alumino-silicate capillary tube with internal Cu/Pt wires heated to 850°C. All compounds greater than C₉ are backflushed off the GC column. Hydrocarbons are oxidized into CO₂ and H₂O, and the H₂O is removed by a Nafion water trap before the CO₂/He enter the IRMS source. The ¹³C/¹²C ratio of CO₂ evolved from each specific compound is determined sequentially by conventional CF-IRMS measurement and data reduction. Results are reported in conventional δ -notation relative to the PDB standard and expressed in units of per mil or parts per thousand (‰).

$$\delta^{13}\text{C} = \left[\frac{(^{13}\text{C}/^{12}\text{C})_{\text{sample}} - (^{13}\text{C}/^{12}\text{C})_{\text{standard}}}{(^{13}\text{C}/^{12}\text{C})_{\text{standard}}} \right] \times 1000$$

where: $\delta^{13}\text{C}$ = deviation in parts per thousand (‰) of a sample as compared to a standard
¹³C/¹²C = isotope ratio of ¹³C to ¹²C in the sample or standard

Experimental Results and Discussion

Our main sources of data are from examination of gas chromatograms and $\delta^{13}\text{C}$ ratios of selected gasoline range hydrocarbons from analysis of the standard oils used throughout our experiments (Figure 3.2). Approximately 40 compounds can be resolved using these methods, comprising all the typical components of the gasoline range (Table 3.1). However, the number of compounds that produce a reliable/diagnostic molecular or isotopic signature is significantly lower. This is due to numerous factors such as several compounds with similar physical properties, or simply the low concentration of many analytes in the oil due to different sources or other genetic characteristics.

The CF-IRMS system also places certain constraints upon gasoline range analyses. The dynamic range of the system is limited (approx. 0.5 – 7 V, mass 44 amu) and compounds must produce a signal within this range for a precise/reproducible measurement (Figure 3.3). Compounds eluting in minute quantities (<0.5 V) are below the resolution of the detectors, while those eluting in higher quantities (>7 V) will saturate the amplifiers. Good baseline separation is also a pre-requisite, as any co-elution of compounds as doublets and triplets results in their mass 45/44 signatures blending together producing obscure and often meaningless values. Therefore, we only record results from 16 specific compounds ranging between C₅-C₉ based on their high resolution and abundance in the majority of samples analyzed (denoted by * in Table 3.1).

As we require some form of reference to establish the validity of the results, we compare data using HSPME with experiments on the same oils analyzed by the modified P&T technique (Murphy, 1995). When possible, we also compare our results to those

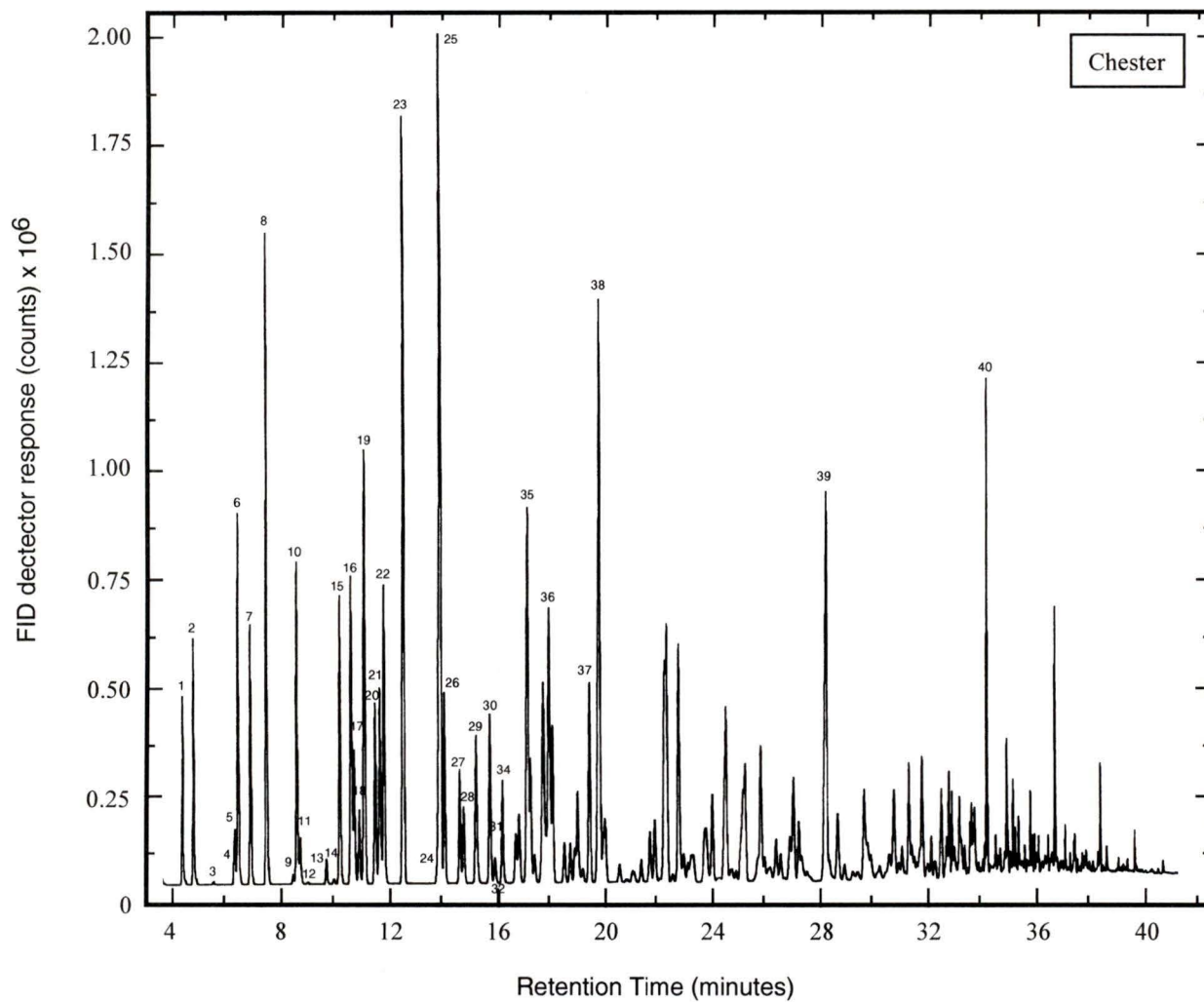


Figure 3.2 Typical gasoline range gas chromatogram of Chester oil produced by HSPME sampling. Peak identifications are listed in Table 3.1

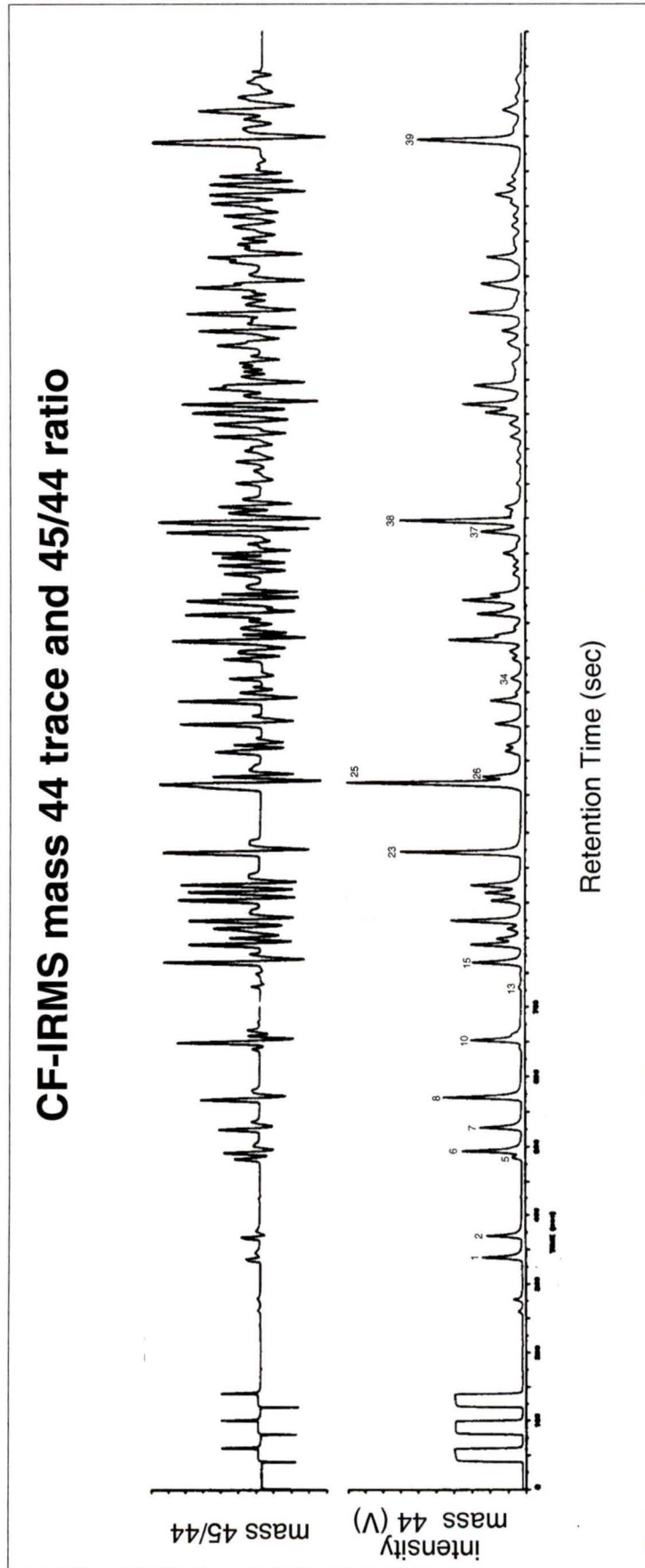


Figure 3.3

CF-IRMS Mass 44 and 45/44 trace for Chester Oil. The 16 Compounds chosen for stable isotope data are identified as listed in Table 3.1. Note that scaling for both mass 44 trace and 45/44 ratio is greatly compressed both horizontally and vertically.

Table 3.1 – List of compounds identified in Figures 3.2, 3.3 and 3.9.

cpd#	abbr.	chemical name
1*	iC5	i-pentane
2*	nC5	n-pentane
3	22DMC4	2,2-dimethylbutane
4	CYC5	cyclopentane
5*	23DMC4	2,3-dimethylbutane
6*	2MC5	2-methylpentane
7*	3MC5	3-methylpentane
8*	nC6	n-hexane
9	22DMC5	2,2-dimethylpentane
10*	MCYC5	methylcyclopentane
11	24DMC5	2,4-dimethylpentane
12	223TMC4	2,2,3-trimethylbutane
13*	Benz	benzene
14	33DMC5	3,3-dimethylpentane
15*	CYC6	cyclohexane
16	2MC6	2-methylhexane
17	23DMC5	2,3-dimethylpentane
18	11DMCYC5	1,1-dimethylcyclopentane
19	3MC6	3-methylhexane
20	1c3DMCYC5	1-cis-3-dimethylcyclopentane
21	1t3DMCYC5	1-trans-3-dimethylcyclopentane
22	1t2DMCYC5	1-trans-2-dimethylcyclopentane
23*	nC7	n-heptane
24	22DMC6	2,2-dimethylhexane + co-elute
	113TMCYC5	1,1,3 trimethylcyclopentane (minor)
25*	MCYC6	methylcyclohexane
26*	1c2DMCYC5	1-cis-2-dimethylcyclopentane
27	EtCYC5	ethylcyclopentane
28	25DMC6	2,5-dimethylhexane
29	24DMC6	2,4-dimethylhexane
30	1t2c4TMCYC5	1-trans-2-cis-4-trimethylcyclopentane
31	33DMC6	3,3-dimethylhexane
32	1t2c3TMCYC5	1-trans-2-cis-3-trimethylcyclopentane
33	223TMCYC6	2,2,3-trimethylcyclohexane (minor)
34*	Tol	toluene
35	2MC7	2-methylheptane
36	3MC7	3-methylheptane
37*	1c4DMCYC6	1-cis-4-dimethylcyclohexane
38*	nC8	n-octane
39*	nC9	n-nonane
40	nC10	n-decane

of Mobil Oil, Houston, TX. As a broad classification of all the variables examined, we divide them into two categories: (1) Factors/variables pertaining directly to properties/characteristics of the HSPME fiber (Sampling) and (2) concerns related to the effect of changing settings on analytical instruments (Instrumentation).

Sampling

Diagnostic Reproducibility - A primary objective of this HSPME technique is to establish that the molecular and stable isotope data produced is representative of the sample. The method must also be robust, with high resolution, sensitivity and reproducibility.

The standard is first analyzed by GC using both P&T and HSPME to characterize gasoline range analytes. Peak areas of the 16 selected compounds from the resulting chromatograms are normalized to the area of a common peak (n-C₇). Results from the two methods are plotted against each other (Figure 3.4a), and peak areas show good correlation for >90% of compounds ($r^2 = 0.953$). This indicates that HSPME yields a representative molecular analysis. An enhanced recovery (as indicated by larger peak areas) of the most volatile constituents (C₅-C₆) is observed with HSPME due to decreased sample transfer and dilution inherent with this method versus P&T. MacGillivray et al. (1994) also compared a P&T extraction method to HSPME for BTEX compounds in water and found sensitivity between methods nearly identical (0.99 correlation) with enhanced recovery of the most volatile analytes using HSPME. Comparison of the gas chromatograms with the mass 44 trace produced by CF-IRMS analysis with HSPME also shows excellent correlation ($r^2 = 0.981$) (Figure 3.4b).

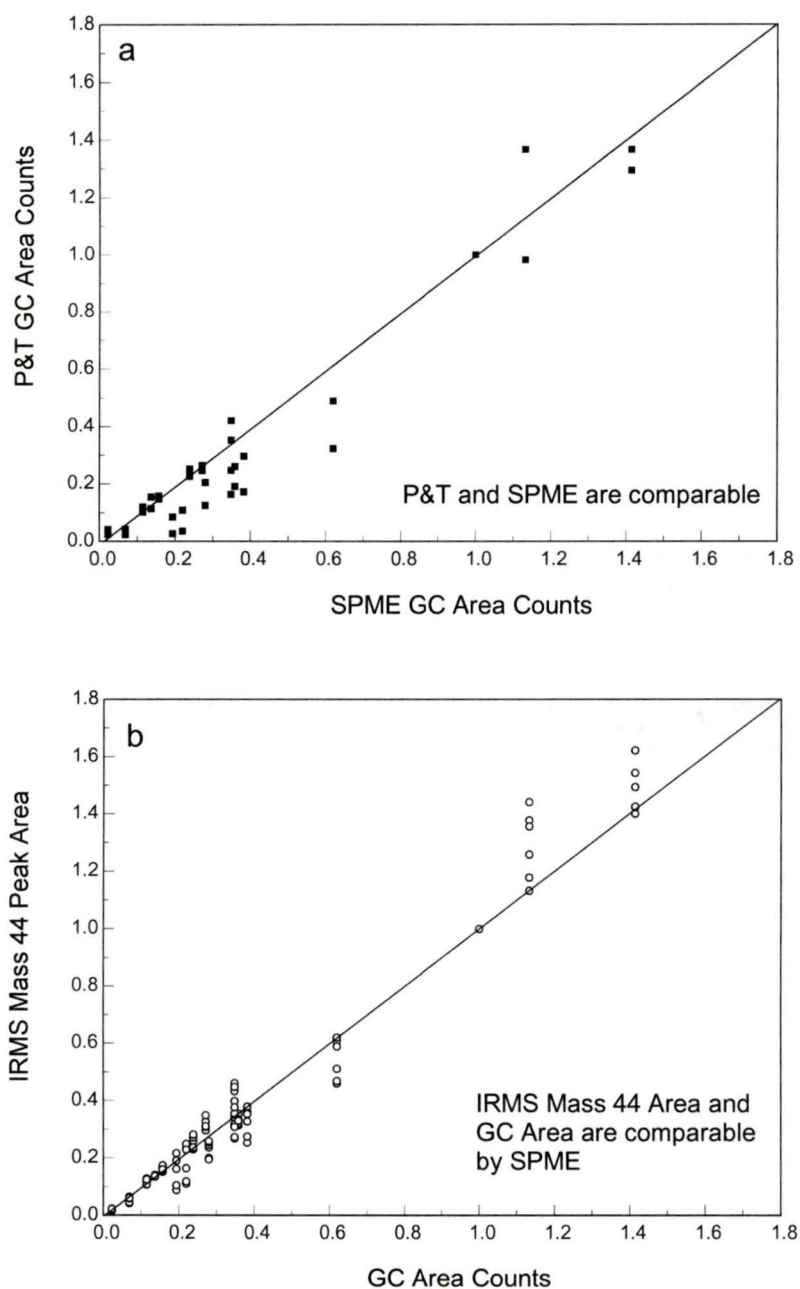


Figure 3.4 a) Comparison of relative GC peak areas between P&T and HSPME sampling methods for Chester oil. b) Comparison of peak areas produced from GC area counts and CF-IRMS mass 44 trace for Chester oil using HSPME sampling. Note: all peak areas normalized to heptane.

Reproducibility of stable isotope ratios for specific gasoline range compounds by HSPME is tested by repeated analyses using CF-IRMS. Ratios for 12 of the 16 compounds show a reproducibility of $\pm 0.2 - 0.5\%$ standard deviation, and peak resolution is also excellent for these 12 compounds as all elute in measurable quantities and do not suffer significantly from co-elution effects.

Interpreting results for the other 4 analytes (Benzene, MCYC5, 1c2DMCYC5, 1c4DMCYC6) involves caution resulting from either co-elution with other compounds or low concentrations (e.g. Benzene) present in the standard. The standard deviation ($\geq \pm 0.5\%$) in $\delta^{13}\text{C}$ ratios for these 4 compounds significantly exceeds those for the other 12 analytes (Figure 3.5). MCYC5 co-elutes with 22DMC5 and 24DMC5, and their isotopic signatures overlap and produce a ratio that varies significantly (standard deviation $\pm 1.0\%$). However, in some samples where 22DMC5 and 24DMC5 elute in small quantities, the $\delta^{13}\text{C}$ ratio for MCYC5 shows minimal standard deviation ($\pm 0.2\%$). 1c2DMCYC5 and 1c4DMCYC6 both co-elute with larger peaks (MCYC6 and n-C₈ respectively). The standard deviation of the larger peaks remains at $\pm 0.2-0.3\%$, because the baseline separation of the two smaller peaks is sufficient to process CF-IRMS data. However, due to small concentrations of 1c2DMCYC5 and 1c4DMCYC6 in most oils, integration errors resulting from low signal responses (< 0.5 mA) have a pronounced effect on their $\delta^{13}\text{C}$ ratios. This data is often unreliable.

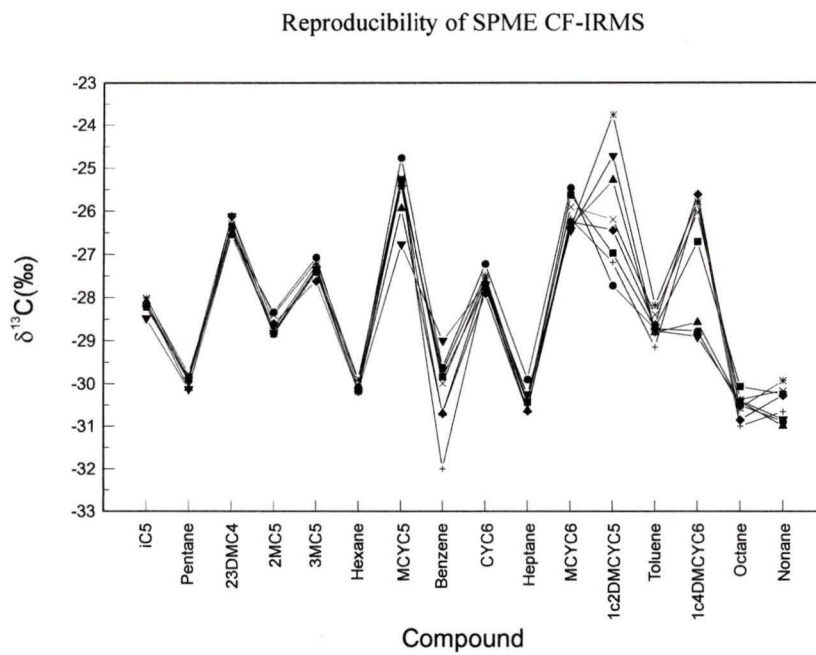


Figure 3.5 Stable carbon isotope ratios for all 16 gasoline range compounds from multiple analyses of the Chester oil. Poor reproducibility is evident for MCYC5, Benzene, 1c2DMCYC5 and 1c4DMCYC6.

Methodologies – Comparison of $\delta^{13}\text{C}$ ratios between HSPME, P&T, and Mobil Oil analysis of the NA-1 standard is performed by CF-IRMS. Mobil Oil uses a single injection of 1 μl of whole oil with a 100:1 split to introduce sample into the GC. A non-systematic enrichment and depletion in ^{13}C ranging between 0.2 to 2.0‰ is observed comparing ratios for 11 compounds extracted by HSPME versus the other methods (Figure 3.6). For $\text{C}_5\text{-C}_6$ compounds, P&T produces the heaviest ratios followed by the whole oil method and HSPME. This order changes in the C_{7+} range, with P&T producing the lightest ratios followed by HSPME and whole oil methods.

In analyzing the discrepancy between methods, we consider the possibility that some form of isotopic fractionation is occurring as analytes are adsorbed on the fiber. This is based on work by Ricci et al. (1994), who showed that CF-IRMS chromatographic resolution is often great enough that the isotope ratio of individual compounds is not homogenous as they elute off the GC column. The beginning of an eluting compound is enriched in ^{13}C , while the end is depleted as indicated by the mass 45/44 trace (Figure 3.3). Ricci et al. (1994) attribute this to isotope effects associated with chromatography derived from small differences in vibrational energy shifts associated with condensation of isotopically distinct species. The condensation or interaction of an organic molecule with a liquid phase (GC column) results in a decrease in vibrational energy (Dias and Freeman, 1997). Energy shifts are greater for molecules with the lighter isotope (Bigeleisen, 1961). Therefore, analytes containing the heavy isotope have shorter elution times. If we apply this idea to interactions between headspace analytes and the SPME fiber, this could result in a small isotope effect.

Analytes enriched in ^{13}C would have lower free mean velocities in headspace than

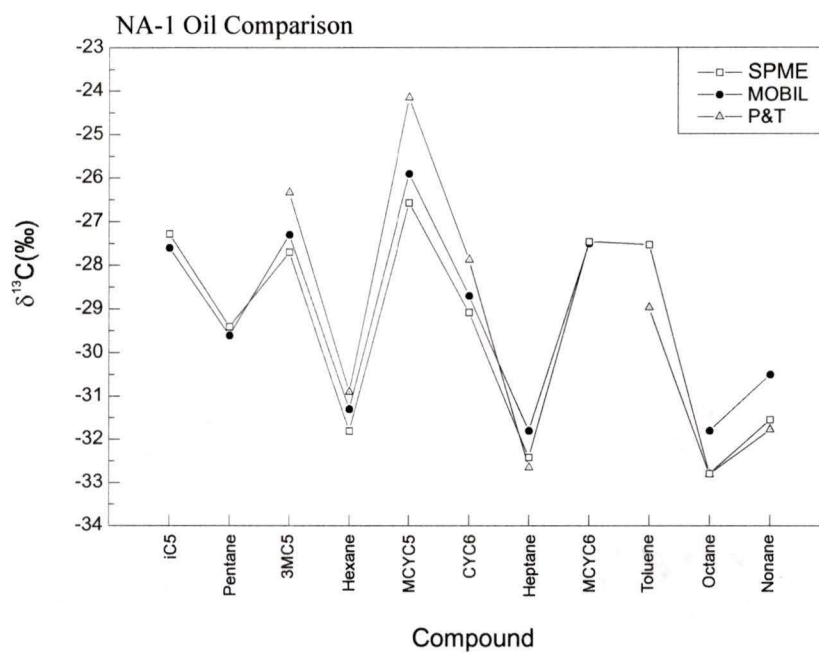


Figure 3.6 Comparison of selected gasoline range hydrocarbons from NA-1 oil by P&T, HSPME, and whole oil (Mobil) extraction methods.

their ^{12}C counterparts. This would result in a lower collision frequency between ^{13}C analytes and the fiber. Prior to attaining equilibrium, this could also lead to an isotope partitioning separate from, but in addition to, that expected based on the vapor pressures of the analytes. The overall effect would result in a slight ^{13}C depletion for analytes adsorbed on the fiber.

However, this effect should be negligible in our experiments since we allow the fiber to equilibrate in the headspace. In addition, this effect does not explain the ^{13}C enrichment observed for C_{7+} compounds analyzed by HSPME versus P&T. Dias and Freeman (1997) noted that once their fiber-water system reached equilibrium, isotopic fractionation of analytes did not vary as a function of equilibrium time, but rather due to interaction of the organic compounds with the coating of the fiber (specifically mass-dependant energy shifts upon adsorption of each analyte into the coating). Dias and Freeman (1997) proposed a method to quantify the magnitude of isotopic fractionation for extraction of an analyte with an SPME fiber. An accepted isotopic composition for each analyte was determined using closed tube combustion methods (e.g. Sofer, 1984b). Dias and Freeman (1997) compared these ratios with $\delta^{13}\text{C}$ values determined by SPME extraction, and designated the difference between them as the fractionation factor. We are pursuing this closed tube combustion technique to determine potential fractionation factors for headspace sampling.

The effect of prolonged storage of the standard oil over a period of several years resulting in possible evaporation/fractionation is also considered. The Chester standard has been analyzed regularly over the past 4 years, and no compositional change has been observed resulting from evaporation of any gasoline range analytes. Bjoroy et al. (1994)

also observed no fractionation effect with storage for light hydrocarbons, and Carpentier et al. (1996) reported similar results on a condensate sample that was analyzed by GC immediately upon arrival and then stored for several days (at room temperature) before being reanalyzed. Evaporation was observed for all compounds $<C_{10}$ (most prevalent in the C_4 - C_7 fraction), and while the condensate was depleted in ^{13}C for the C_9 - C_{14} fraction, little or no fractionation was observed in the C_6 - C_8 range.

Equilibration Times - To examine the time required before isotopic and molecular equilibrium is reached as analytes are adsorbed on the fiber, the SPME fiber is exposed to the headspace above oil droplets for periods of 30 seconds to 1 hour. All samples are analyzed by CF-IRMS at a set injector split flow to maintain high resolution and control the amount of sample applied on the column. Peak areas, amplitudes, and $\delta^{13}C$ ratios are monitored, and equilibrium is established when all three variables remain constant regardless of increasing exposure time (Dias and Freeman, 1997).

For short adsorption times of 30 seconds to 5 minutes, molecular equilibrium is not attained as determined by examination of peak areas (once again normalized to n- C_7) plotted as a function of increasing exposure time (Figure 3.7a). Compounds in the C_8+ range do not have adequate time to equilibrate with/adsorb onto the fiber due to their higher partition coefficients. Comparison of these areas with those from exposure times of 15 minutes or greater shows that after 15 minutes peak areas are constant and molecular equilibrium is reached.

In relation to the time required for establishment of isotopic equilibrium, $\delta^{13}C$ ratios for all compounds from 5+ minute exposures are consistent with those of 15+ minutes

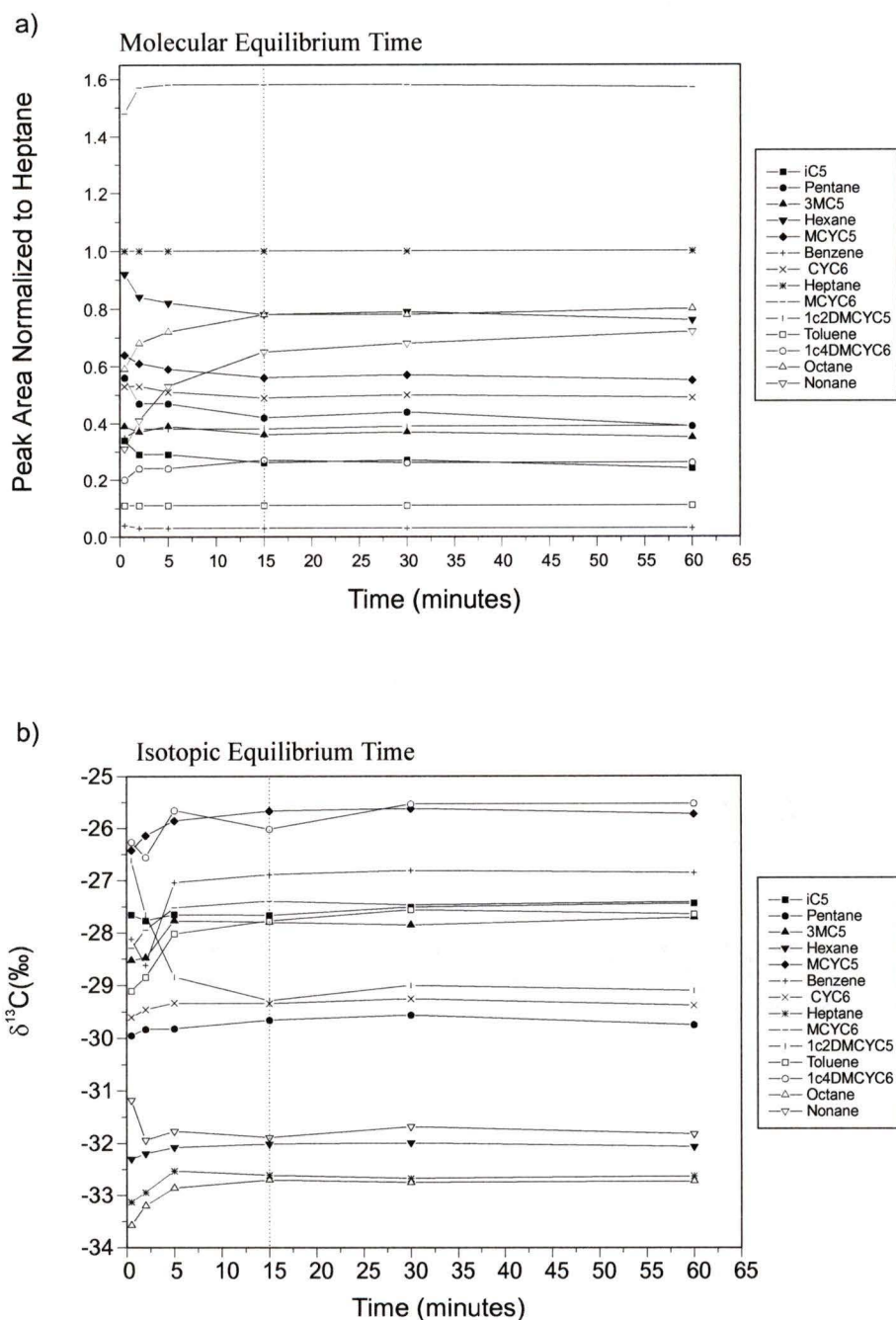


Figure 3.7 Time required for establishment of a) molecular and b) isotopic equilibrium between SPME fiber and headspace analytes. The dashed line indicates minimum adsorption time (15 min.) adopted for use in all experiments.

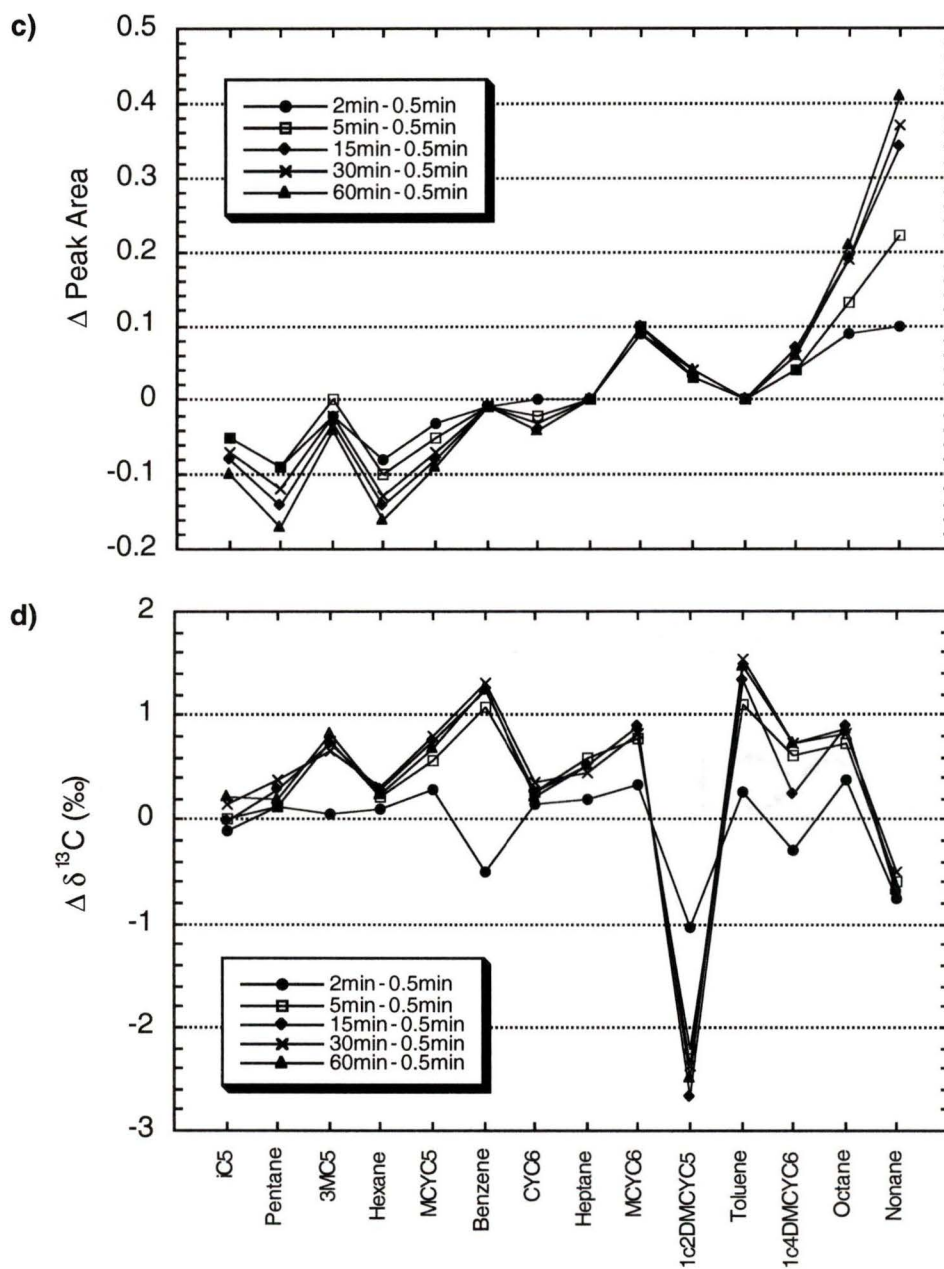


Figure 3.7 Change in relative peak area (c) and isotope ratios (d) (continued) for gasoline range analytes with increasing adsorption time.

(Figure 3.7b). Since molecular equilibrium is not attained until after 15+ minutes, it was decided that although an exposure time of 5 minutes is suitable for obtaining a representative sample (both on a molecular and isotopic level), an exposure time of 15 minutes assures constant peak amplitude/area and $\delta^{13}\text{C}$ ratios. This is comparable to other HSPME studies with BTEX compounds where exposure times of 1-10 minutes were used, e.g. Zhang and Pawliszyn, (1993a). It is also an improvement over the 30 minute adsorption time required by SPME analysis of aqueous solutions containing MCYC6 alone, e.g. Dias and Freeman, (1997).

Our extraction profiles fit the characteristic shape of other SPME studies, with a sharp rise for most compounds followed by a gradual shallowing out. This shape is inverted for the more volatile analytes ($\text{C}_5\text{-C}_6$) with respect to attaining molecular equilibrium, due to higher liquid/headspace partition coefficients which initially saturate the fiber coating at low exposure times before other HMW analytes can properly equilibrate with the fiber. This can be shown by monitoring the change in peak area with increasing adsorption time (Figure 3.7c). Octane and nonane show increasing adsorption with time up to 15 min, while other analytes display little or no change. Regardless of molecular weight, after 5 minutes exposure time all $\delta^{13}\text{C}$ ratios appear to remain invariant (Figure 3.7d).

Experiments focusing on desorption times are performed by GC. After desorbing analytes for times ranging from 30 seconds to 10 minutes, identical chromatograms produced show that as the fiber is exposed to the injector inlet, desorption of all analytes is practically instantaneous and complete. This is dependant on the fiber being extruded into the optimal/hottest section of the injector, determined by simple tests observing the amount of analytes desorbed at different injector positions. If the fiber is too high in the

injector, less sample is desorbed and peak resolution suffers (tailing caused by a temperature gradient within the injector) (Arthur et al., 1992b). To ensure complete desorption of all analytes, the fiber is left extruded in the injector for most of the sample run time (20-40 minutes). Potter and Pawliszyn (1994) noted that a PDMS coating may carryover significant quantities of semivolatile compounds (e.g. PAH's) to the next analysis if the fiber is not left to desorb for longer than 1 min (attributed to chemisorption of analyte molecules on the silica surface).

Sample Concentration - To control the amount of sample adsorbed on the fiber, 1/4, 1/2 and whole fiber lengths are exposed to the headspace for preset adsorption times (15-30 min). In experiments where only a fraction of the fiber is exposed, the remainder is kept within the septum-piercing needle to avoid direct exposure to the headspace.

When partial amounts of the fiber are exposed, no isotope effect is observed (ca. $\pm 0.2\%$ standard deviation for all compounds) and the sample appears to migrate up the fiber. This is shown by variable area and amplitude of all peaks for a set length of fiber with constant adsorption time. Longer adsorption times result in more sample adsorbed on the fiber, and this is no doubt because the remainder of the fiber within the septum piercing needle is adsorbing sample, despite not being directly exposed to the headspace. For all fiber lengths, the molecular pattern is consistent, but a injector split flow is required to control the amount of sample reaching the IRMS. (see Instrumentation section for effects of injector split flow).

Experiments with a cut fiber (5mm length) were tried to analyze samples by splitless injection, but, proved unsuccessful because all peaks produced were subject to tailing

despite controlling the amount of sample. This results in shifts in $\delta^{13}\text{C}$ measurements of all compounds towards heavier values, and produces incorrect results.

Temperature/Vapor Pressure – Among other possible causes of the $\delta^{13}\text{C}$ variations between HSPME and P&T sampling, the nature of the liquid-vapor equilibrium for gasoline range analytes between methods is a potential but unlikely candidate. In P&T sampling, the diluted oil is purged in helium to extract all compounds at their respective vapor pressures to enter the headspace (gas) phase. Therefore, an equilibrium between the oil and headspace is not attained. In HSPME, equilibrium is established and the heavier isotope should theoretically partition into the denser (liquid) phase. When the fiber is exposed in the headspace (depleted in ^{13}C), a lighter ratio would be sampled for all compounds present. In P&T extractions, this effect is minimized by purging the headspace, allowing for compounds with both heavy and light isotopes to be collected, the quantity of each dependant only on the vapor pressure of analyte to enter the vapor phase. *A priori* we would predict the magnitude of this fractionation to be small, but, any partitioning/fractionation of analytes with the fiber coating must be confirmed by experimentation.

We monitored the effects of raising or lowering the temperature of the vial (oil) during sampling, thereby increasing/decreasing the vapor pressures of the analytes. The droplet is allowed to equilibrate in a waterbath (42°C) and an icebath (0°C). The adsorption time is 15 minutes, and regardless of temperature, $\delta^{13}\text{C}$ ratios of most compounds exhibit a $\pm 0.3\%$ standard deviation (Figure 3.8). Samples from the

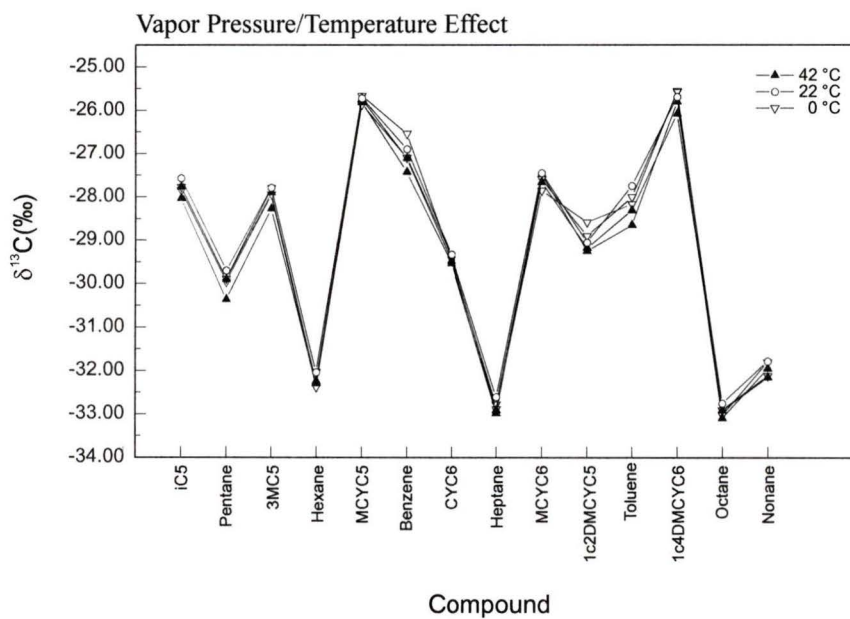


Figure 3.8 Effect of vapor pressure/temperature on $\delta^{13}\text{C}$ ratios for gasoline range analytes from NA-1 oil. Temperatures were monitored and remained constant throughout sampling.

waterbath have reduced peak areas and amplitudes for all compounds compared to the icebath.

The observed decrease in the amount of analytes adsorbed at higher temperatures is either a characteristic of the fiber, or related to increased vapor pressures. MacGillivray et al. (1994) stated that adsorption of analytes on the fiber is an exothermic process (Arthur et al., 1992a), and therefore would be favored at lower temperature. They observed that increased adsorption at lower temperature has a greater effect than the increase of analytes in the vapor phase produced at higher temperatures. While a larger number/quantity of compounds is released to the headspace, the coating/headspace coefficient decreases, and the optimum temperature for extraction is dependant on the interaction of the analytes between the three phases (Zhang et al., 1994). With respect to oil analysis, raising the temperature of the liquid releases an increased number of C₁₀⁺ compounds to the vapor phase, and their equilibration/adsorption on the fiber also results in a reduced amount of gasoline range compounds adsorbed. Agitation of the sample would also force less volatile, high molecular weight (HMW) compounds into the headspace, producing a similar effect. These HMW compounds tend to have a greater affinity for the fiber and may lead to their preferential adsorption over low molecular weight (LMW) compounds. When compounds with small Henry's coefficients are analyzed, agitation will minimize sampling times provided that the octanol-water coefficient (K_{OW}) is low. (Zhang and Pawliszyn, 1993a).

Matrix Effects – The interaction of the organic solute with other organic compounds in solution will alter its partition coefficients (Dias and Freeman, 1997). Previous studies

with complex mixtures noted that the liquid matrix itself may be a rate limiting step in adsorbing analytes on the fiber as it affects transport of analytes through the liquid phase (Steffen and Pawliszyn, 1996; Boyd-Boland et al., 1996). There are two main types of matrix interference: (1) Non-target compounds present in the sample and (2) strong adsorption properties of the matrix (Zhang and Pawliszyn, 1993b). We questioned whether as matrix complexity increases, is it possible that competition for adsorption sites on the fiber occurs on an isotopic level (^{12}C vs. ^{13}C)?

Matrix effects were tested with mixtures comprised of three, five, and seven different compounds, and found not to produce any evidence of competition for adsorption sites on the fiber (Table 3.2). The first mixture composed of n-C5, n-C6 and Benzene represents a simple matrix with only two compound classes. The $\delta^{13}\text{C}$ ratios for all compounds are within $\pm 0.3\text{‰}$ to those from HSPME analysis of the individual analytes. The addition of Toluene and n-C8 in the second mixture added to the number of compounds in the matrix, but not compound classes. The two mixtures are highly comparable to each other, with only a $\pm 0.2\text{‰}$ change in $\delta^{13}\text{C}$ ratios relative to pure compounds. The third mixture incorporated 223TMC5 and MCYC6 to not only increase the number of analytes present, but also the diversity of compound classes in the matrix. This also had no effect on $\delta^{13}\text{C}$ ratios for any of the preceding analytes, and it was decided that the large number of compounds present in the gasoline range does not result in any matrix interference or competition/bias for adsorption sites on the fiber. Similar effects investigated by Boyd-Boland et al. (1996) showed that increasing the number of analytes in an aqueous matrix from 20 to 60 does not significantly affect the adsorption/equilibration times of analytes with the fiber.

Table 3.2 - Carbon isotope ratios for pure standards and mixtures

Pure Standards	Pentane	Hexane	Benzene	223TMC5	MCYC6	Toluene	Octane
Run 1	-29.32	-30.41	-27.23	-27.87	-29.25	-28.09	-32.24
Run 2	-28.97	-30.50	-27.65	-27.81	-29.29	-27.79	-32.06
Run 3	-29.54	-30.74	-27.24	-28.02	-29.61	-27.42	-32.31
Run 4		-30.81				-27.46	
Average (‰)	-29.28	-30.62	-27.37	-27.90	-29.38	-27.69	-32.20
Std Deviation (‰)	0.29	0.19	0.24	0.11	0.20	0.31	0.13
Mixture 1							
Run 1	-29.21	-30.31	-26.52				
Run 2	-29.02	-30.51	-27.05				
Run 3	-29.23	-30.58	-27.12				
Run 4	-29.51	-30.58	-27.44				
Average (‰)	-29.24	-30.50	-27.03				
Std Deviation (‰)	0.20	0.13	0.38				
Mixture 2							
Run 1	-29.31	-30.52	-27.46			-28.00	-32.07
Run 2	-29.19	-30.53	-27.21			-27.90	-31.51
Run 3	-29.20	-30.50	-27.21			-27.89	-32.28
Run 4	-29.27	-30.37	-27.08			-27.78	-31.97
Average (‰)	-29.24	-30.48	-27.24			-27.89	-31.96
Std Deviation (‰)	0.06	0.07	0.16			0.09	0.33
Mixture 3							
Run 1	-29.37	-30.58	-27.09	-28.11	-29.51	-27.71	-31.99
Run 2	-29.64	-30.86	-27.45	-28.36	-29.43	-28.32	-32.45
Run 3	-29.57	-30.56	-27.00	-28.07	-29.59	-28.07	-32.41
Run 4	-29.75	-30.74	-27.56	-28.40	-29.89	-28.20	-32.66
Average (‰)	-29.58	-30.69	-27.28	-28.24	-29.61	-28.08	-32.38
Std Deviation (‰)	0.16	0.14	0.27	0.17	0.20	0.26	0.28

Instrumentation

Oven Combustion/Column Pressures – The Chester standard is analyzed by HSPME extraction at column pressures of 16, 18, 20, and 22 psi (flow rates 1.8 – 3.0 ml/min), to determine if the higher flow rates lead to incomplete combustion to CO₂ for any or all of the analytes. Lower column pressures resulted in more complete combustion observed in a systematic increase of $\delta^{13}\text{C}$ ratios for all compounds with decreasing flow rates. Below 16 psi (flow rate 1.8 ml/min) no further increase was seen, and as such this flow rate is adopted for all experiments detailed in this thesis. At higher flow rates, the residence time of analytes in the oven is insufficient for complete combustion to occur.

Injector Split Flows – To control the amount of sample introduced to the CF-IRMS system, we utilize a constant split injector ratio. Previous studies (Baylis et al., 1994) note that split flow can cause isotopic fractionation in light gases. To quantify this effect, a standard oil is analyzed with various split ratios (3.5:1, 7:1, 15:1) to observe the effect on $\delta^{13}\text{C}$ ratios of any analytes.

Peak areas and amplitudes decrease in direct proportion to the magnitude of increase in the injector split ratio (split ratio doubled, peak areas decrease by one-half), without significant isotopic fractionation (Table 3.3). Not all of the 16 analytes are available for comparison, as low initial split ratios resulted in the most abundant compounds (n-C7, MCYC6, n-C8, n-C9) saturating the amplifiers of the IRMS. MCYC6 oversaturates amplifiers for 2 of the 3 split settings, and is excluded from the

Table 3.3 - Chester Oil - Injector Split Ratio Test

Split Ratio	3.5:1	3.5:1	7:1	7:1	15:1	15:1								
Peak Name	Run A (%)	Run B (%)	Run C (%)	Run D (%)	Run E (%)	Run F (%)	Average A,B	Stdev A,B	Average C, D	Stdev C,D	Average E,F	Stdev E,F	Average (A-F)	Stdev(A-F)
iC5	-28.26	-28.30	-28.40	-28.11	-27.76	-28.04	-28.28	0.03	-28.26	0.21	-27.90	0.20	-28.15	0.23
Pentane	-29.93	-30.15	-30.20	-29.90	-29.53	-29.87	-30.04	0.16	-30.05	0.21	-29.70	0.24	-29.93	0.24
23DMC4 or CY	-27.04	-27.63	-27.62	-27.72	-27.73	-27.03	-27.34	0.42	-27.67	0.07	-27.38	0.49	-27.46	0.33
2MC5	-28.88	-28.91	-29.01	-28.93	-28.88	-28.95	-28.90	0.02	-28.97	0.06	-28.92	0.05	-28.93	0.05
3MC5	-27.48	-27.51	-28.18	-27.47	-27.82	-28.35	-27.50	0.02	-27.83	0.50	-28.09	0.37	-27.80	0.39
Hexane	-30.48	-30.20	-30.84	-30.69	-30.68	-30.82	-30.34	0.20	-30.77	0.11	-30.75	0.10	-30.62	0.24
MCYC5	-25.18	-25.58	-25.71	-25.68	-25.23	-25.70	-25.38	0.28	-25.70	0.02	-25.47	0.33	-25.51	0.24
Benzene	-30.86	-30.32	-31.31	-31.21	-31.95	-30.52	-30.59	0.38	-31.26	0.07	-31.24	1.01	-31.03	0.59
CYC6	-28.13	-28.45	-28.63	-28.57	-28.24	-28.83	-28.29	0.23	-28.60	0.04	-28.54	0.42	-28.48	0.26
Heptane	-	-	-30.77	-30.79	-31.04	-31.15	-	-	-30.78	0.01	-31.10	0.08	-30.94	0.19
MCYC6	-	-	-	-	-	-	-	-	-	-	-	-	-	-
1c2DMCYC5	-	-	-	-	-	-	-	-	-	-	-	-	-	-
Toluene	-27.89	-27.51	-29.47	-27.58	-29.31	-28.98	-27.70	0.27	-28.53	1.34	-29.15	0.23	-28.46	0.90
1c4DMCYC6	-	-	-26.12	-25.87	-25.28	-25.61	-	-	-26.00	0.18	-25.45	0.23	-25.72	0.36
Octane	-	-	-30.92	-30.70	-31.01	-31.23	-	-	-30.81	0.16	-31.12	0.16	-30.97	0.22
Nonane	-	-	-30.57	-30.74	-30.38	-30.62	-	-	-30.66	0.12	-30.50	0.17	-30.58	0.15
Peak Name	Peak Amp	Peak Amp	Peak Amp	Peak Amp	Peak Amp	Peak Amp	Average A,B	Stdev A,B	Average C, D	Stdev C,D	Average E,F	Stdev E,F		
iC5	2.79	2.56	1.53	1.61	0.68	0.69	2.68	0.16	1.57	0.06	0.69	0.01		
Pentane	2.77	2.55	1.50	1.63	0.68	0.69	2.66	0.16	1.57	0.09	0.69	0.01		
23DMC4 or CY	0.81	0.74	0.43	0.47	0.22	0.22	0.78	0.05	0.45	0.03	0.22	0.00		
2MC5	5.40	5.05	2.89	3.23	1.44	1.45	5.23	0.25	3.06	0.24	1.45	0.01		
3MC5	3.77	3.56	2.01	2.26	1.00	1.01	3.67	0.15	2.14	0.18	1.01	0.01		
Hexane	7.58	7.18	4.09	4.65	2.09	2.09	7.38	0.28	4.37	0.40	2.09	0.00		
MCYC5	4.77	4.48	2.51	2.83	1.33	1.32	4.63	0.21	2.67	0.23	1.33	0.01		
Benzene	0.23	0.24	0.13	0.14	0.07	0.07	0.24	0.01	0.14	0.01	0.07	0.00		
CYC6	4.65	4.44	2.50	2.84	1.33	1.34	4.55	0.15	2.67	0.24	1.34	0.01		
Heptane	-	-	6.45	7.50	3.62	3.55	-	-	6.98	0.74	3.59	0.05		
MCYC6	-	-	-	-	-	-	-	-	-	-	-	-		
1c2DMCYC5	-	-	-	-	-	-	-	-	-	-	-	-		
Toluene	1.29	1.25	0.66	0.79	0.37	0.38	1.27	0.03	0.73	0.09	0.37	0.01		
1c4DMCYC6	-	-	2.13	2.56	1.24	1.21	-	-	2.35	0.30	1.23	0.02		
Octane	-	-	6.40	7.66	3.91	3.85	-	-	7.03	0.89	3.88	0.04		
Nonane	-	-	5.21	6.30	3.23	3.21	-	-	5.76	0.77	3.22	0.01		
Peak Name	Peak Area	Peak Area	Peak Area	Peak Area	Peak Area	Peak Area	Average A,B	Stdev A,B	Average C, D	Stdev C,D	Average E,F	Stdev E,F		
iC5	11.17	9.62	5.81	6.19	2.67	2.83	10.40	1.10	6.00	0.27	2.75	0.11		
Pentane	10.90	9.50	5.68	6.22	2.59	2.68	10.20	0.99	5.95	0.38	2.64	0.06		
23DMC4 or CY	4.08	3.66	2.12	2.33	1.09	1.10	3.87	0.30	2.23	0.15	1.10	0.01		
2MC5	23.32	21.25	12.15	13.69	6.24	6.35	22.29	1.46	12.92	1.09	6.30	0.08		
3MC5	17.21	15.84	8.43	10.15	4.37	4.40	16.53	0.97	9.29	1.22	4.39	0.02		
Hexane	31.85	29.93	16.65	19.03	8.76	8.82	30.89	1.36	17.84	1.68	8.79	0.04		
MCYC5	20.60	19.02	10.71	12.12	5.69	5.68	19.81	1.12	11.42	1.00	5.69	0.01		
Benzene	1.09	1.02	0.58	0.66	0.31	0.31	1.06	0.05	0.62	0.06	0.31	0.00		
CYC6	22.87	21.54	12.04	13.68	6.53	6.50	22.21	0.94	12.86	1.16	6.52	0.02		
Heptane	-	-	31.39	36.75	17.26	17.18	-	-	34.07	3.79	17.22	0.06		
MCYC6	-	-	-	-	-	-	-	-	-	-	-	-		
1c2DMCYC5	-	-	-	-	-	-	-	-	-	-	-	-		
Toluene	7.39	7.15	3.64	4.62	2.01	1.98	7.27	0.17	4.13	0.69	2.00	0.02		
1c4DMCYC6	-	-	11.60	14.27	6.77	6.64	-	-	12.94	1.89	6.71	0.09		
Octane	-	-	34.93	42.41	20.34	20.09	-	-	38.67	5.29	20.22	0.18		
Nonane	-	-	37.54	46.53	22.26	22.18	-	-	42.04	6.36	22.22	0.06		

analysis all together. The standard oil is run twice at each split ratio to establish reproducibility. Peak areas and amplitudes have standard deviations of $\pm 10\%$, and $\delta^{13}\text{C}$ ratios for the 6 analyses are comparable with results from previous experiments with the same oil ($\pm 0.3\%$). Compounds which exhibit higher deviations are due to low concentrations at high split ratios (signal outside dynamic range of IRMS). This data is included for the purpose of peak area comparisons. If the split flow does result in any isotope effects, it is not within detection limits.

In analysis of a suite of oils for a CSIC study, some samples such as heavy crudes or those that have undergone extensive secondary alteration (e.g. biodegradation, water-washing) often have minimal amounts of gasoline range hydrocarbons remaining for analysis. With P&T, longer sampling (and total analysis) times are required to extract such low concentrations, and sometimes analysis is not practical by this method. Using split injection with HSPME, resolution is possible on the ppt level, allowing for a more routine sampling of such special cases. In oils where one compound (e.g. MCYC6, Tol) is present in extremely high concentrations relative to others, multiple analysis using variable split flows can control all peak sizes to form a merged data set with precise measurements.

It is possible that our choice of injector model may be unsuitable for this type of analysis. Louch et al. (1992) observed that at the start of desorption, the analyte is desorbed first from the layer of fiber coating in contact with the flowing gas and then from deeper in the coating. If extended to isotopes, could this relate to the heavier isotope being held somehow within the more dense fiber phase? The reason for postulating such an effect is related to examination of the mass 45/44 trace from CF-

IRMS for all samples analyzed by HSPME. A small increase in the 45/44 ratio is observed just after the majority of a compound elutes off the GC column, and the $\delta^{13}\text{C}$ measurement may exclude this small but significant detail (Figure 3.3).

GC Column – In an effort to obtain isotopic measurements for a greater number of gasoline range compounds, we attempted to improve the efficiency, selectivity, and resolution of the chromatography in the analysis by experimenting with a new GC column designed specifically for petrochemical applications. The stationary phase of the column remains DB-1 (non-polar), however, column length is increased to 100m, with inner diameter and film thickness reduced to 0.25 mm and 0.5 μm respectively. This raises the theoretical plate count of the column to over 400,000, nearly double the value of the previous column used in our experiments. The higher plate count means that column efficiency and selectivity are substantially increased, minimizing potential co-elution effects between compounds.

Gas chromatograms from analysis of the Chester standard using the new column illustrate the improved column resolution (Figure 3.9). Co-elution of MCYC5 with 22DMC5 and 24DMC5 has been eliminated, as all three peaks are clearly resolved and we are able to measure an isotopic ratio for each compound. However, in samples where 22DMC5 and 24DMC5 elute in small quantities, their $\delta^{13}\text{C}$ ratios are still of little value. Both 1c2DMCYC5 and 1c4DMCYC6 are separated off the shoulders of MCYC6 and n-C8, allowing more precise measurements for all 4 peaks. The improved resolution has also resulted in measurement of ratios for compounds that previously co-eluted as doublet or triplet peaks. An example of this is 11DMCYC5, 3MC6, 1c3DMCYC5, three

compounds that were part of an unresolvable group of peaks eluting after CYC6. A similar improvement is seen for EtCYC5, 25DMC6, 24DMC6. New peaks that can also be used for isotopic measurements include 2MC7, 3MC7 and 223TMCYC6.

Overall, the 100 m column appears to be superior to its 60 m predecessor for gasoline range analyses. Our results also suggest that the 60 m column may be starting to degrade due to extensive use. A comparison of chromatograms from current analyses versus those of Murphy (1995) shows a decrease in column efficiency and selectivity for some peaks, probably as a result of deterioration of the stationary phase in the column. This is simply a result of hundreds of oil analyses performed with this column over the past 5 years. Therefore, the 100 m column appears to be the more suitable column for future oil analyses. The only significant drawback of the new column is the increased time required for analytes to travel the increased column length. Total sampling and analysis time is approximately 2 hours per sample, and while this is not unreasonable we are experimenting with increased column pressure flows and modified temperature programs in an effort to reduce total analysis time without sacrificing the improved resolution.

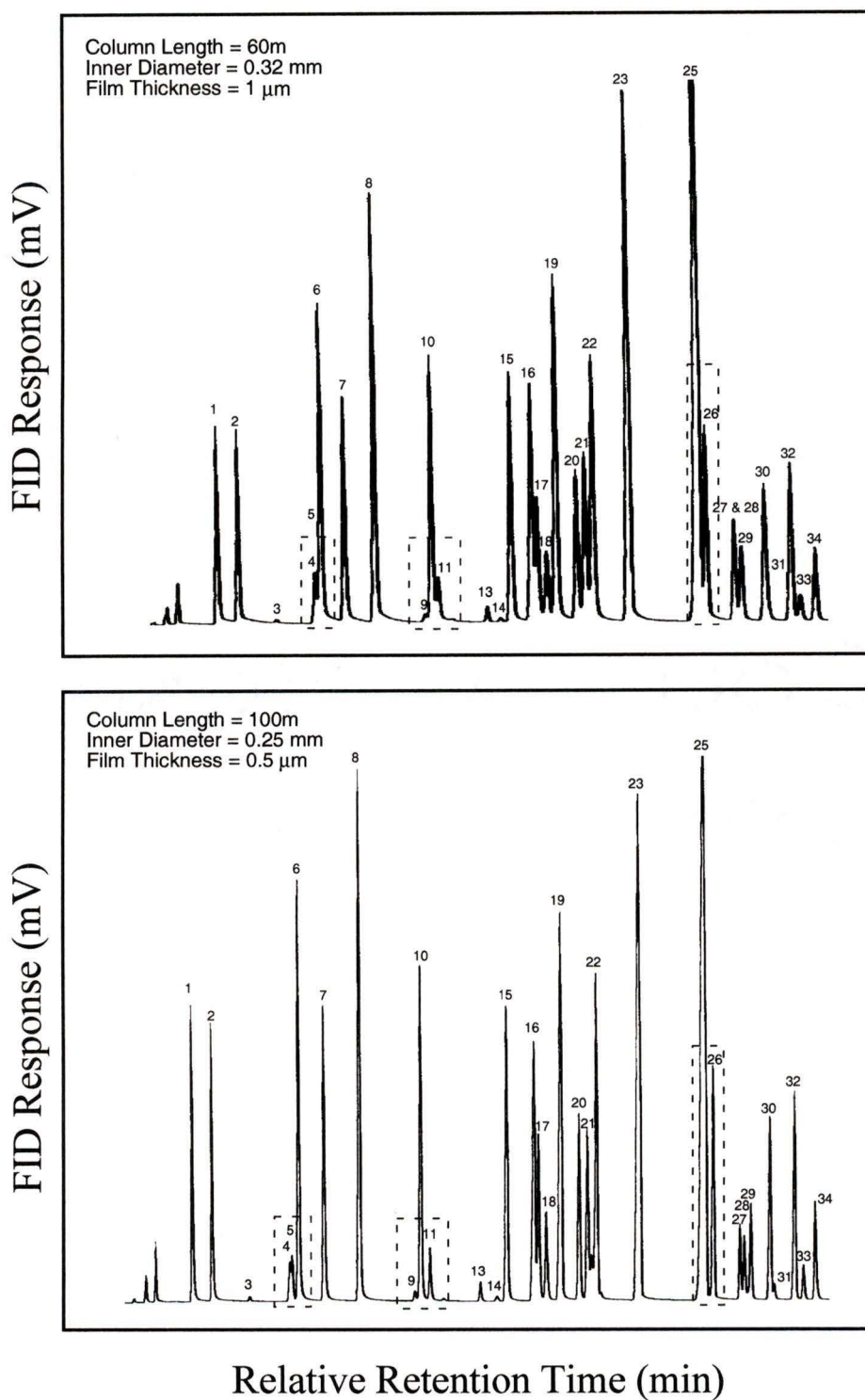


Figure 3.9 Comparison of capillary columns for separating gasoline range compounds. Note the improved separation of 23DMC4, MCYC5, and MCYC6 using the 100m column.

Chapter 4- Compound Specific Isotope Correlation (CSIC): Examples from Central and Southern Alberta

Samples and Geologic Background

In this study, a suite of 27 oils primarily of Devonian age from the WCSB were chosen for CSIC by CF-IRMS analysis of gasoline range compounds (Table 4.1). Most were sampled from Nisku formation reservoirs in central/southern Alberta in an area dominated by the Rimbey-Meadowbrook (RMT) and Bashaw Reef (BRC) complexes (Fig. 4.1). The samples were stored at the Geochemical Petroleum Archive of the Geological Survey of Canada-Calgary prior to analysis at the University of Victoria. Samples were chosen based on the assumption that all could be attributed to a common source rock, the Upper Devonian Duvernay Formation.

The Duvernay is part of the Upper Devonian Woodbend Group of the WCSB (Figure 4.2), and has long been considered a source for numerous oil reservoirs throughout the basin. Detailed discussions of structure, sedimentation, and depositional history of Woodbend-Winterburn successions can be found in Switzer et al. (1994), and will be briefly summarized here. Woodbend strata were deposited during a gradual deepening of the entire WCSB, resulting in development of thick aggradational successions of carbonates with large relief differences between shelf and basin areas. Numerous reef complexes formed at this time, and these features divide the basin into several distinct areas. Winterburn deposits were dominated by a shallowing/infilling of the basin by large amounts of shale mixed with lesser amounts of carbonate.

Table 4.1 List of selected Western Canada Sedimentary Basin oils

Sample No.	Location	GSC Smpl#	Field	Pool	Formation	Smpl top (m)	Smpl Base (m)	Abbrev.
1	09-05-029-26W4	2123	Acme	Inverness	Wabuman			Acme
2	14-01-041-23W4		Bashaw	Nisku G	Nisku	1717.5	1722.0	Bashaw1401
3	13-09-041-23W4	2079	Bashaw	Nisku G	Nisku			Bashaw1309
4	11-35-041-23W4		Bashaw	Nisku G	Nisku			Bashaw1135
5	13-09-042-23W4		Bashaw	Nisku G	Nisku			Bashaw42
6	03-32-047-13W5	1652	Brazeau River	Nisku Q	Nisku	3364.0	3380.8	BrazRiv
7	15-23-042-24W4		Chigwell	Leduc C				Chigwell
8	03-27-014-16W4	1662	Enchant	Arcs	Arcs	1352.0	1372.5	Enchant
9	16-03-056-24W4	944	Excelsior	Nisku A	Nisku	1194.2	1197.3	Excelsior
10	16-19-036-21W4	1586	Fenn-Big Valley	Nisku A	Nisku	1781.3	1782.5	FennBV
11	09-22-035-20W4	1143	Fenn-BigValley	Nisku A	Nisku	1599.0	1605.1	FennBV 922
12	01-03-037-20W4	1558	Fenn-BigValley	Nisku A	Nisku	1785.2	1785.8	FennBV 103
13	16-16-041-02W5	2037	Gilby	Nisku D	Nisku	2431.0	2442.0	Gilby
14	06-22-050-26W4	874	Leduc-Woodbend	Nisku A	Nisku	1364.0	1364.3	LeducWood
15	02-30-036-21W4	1557	Lousana	Nisku	Nisku	1785.2	1785.8	Lousana
16	01-13-039-02W5		Medicine River	Mississippian	Pekisko			MedRiv
17	16-03-036-22W4	2222	Mikwan	Nisku I	Nisku	1817.0	1821.0	Mikwan
18	14-22-020-12W4	1598	Princess	Jefferson A	Jefferson	No Sample	No Sample	
19	02-30-040-15W4	2257	Red Willow	Camrose F	Camrose	1704.0	1713.0	RedWill
20	16-28-028-02W4	1278	Sibbald	Nisku A	Nisku	1016.5	1021.0	Sibbald
21	13-12-029-24W4	1236	Swalwell	Nisku A	Nisku	1967.2	1972.1	Swalwell 1312
22	08-14-029-24W4	1665	Swalwell	Nisku A	Nisku	1972.1	1973.0	Swalwell 814
23	06-11-029-24W4	2051	Swalwell	Nisku C	Nisku	1982.5	1985.5	Swalwell C
24	10-15-029-24W4	2052	Swalwell	Nisku D	Nisku	1972.0	1984.0	Swalwell D
25	03-22-023-15W4	1559	Verger	Arcs A	Arcs	1370.0	1375.0	Verger
26	15-30-044-04W4	1182	Wainwright	Camrose Tongue A	Camrose	655.0	661.0	Wainwright
27	04-24-028-21W4		Wayne	Nisku A	Nisku	1700.0	1744.0	Wayne
28	14-25-031-10W4	1144	Youngstown	Arcs	Arcs	1130.0	1133.9	Youngstown

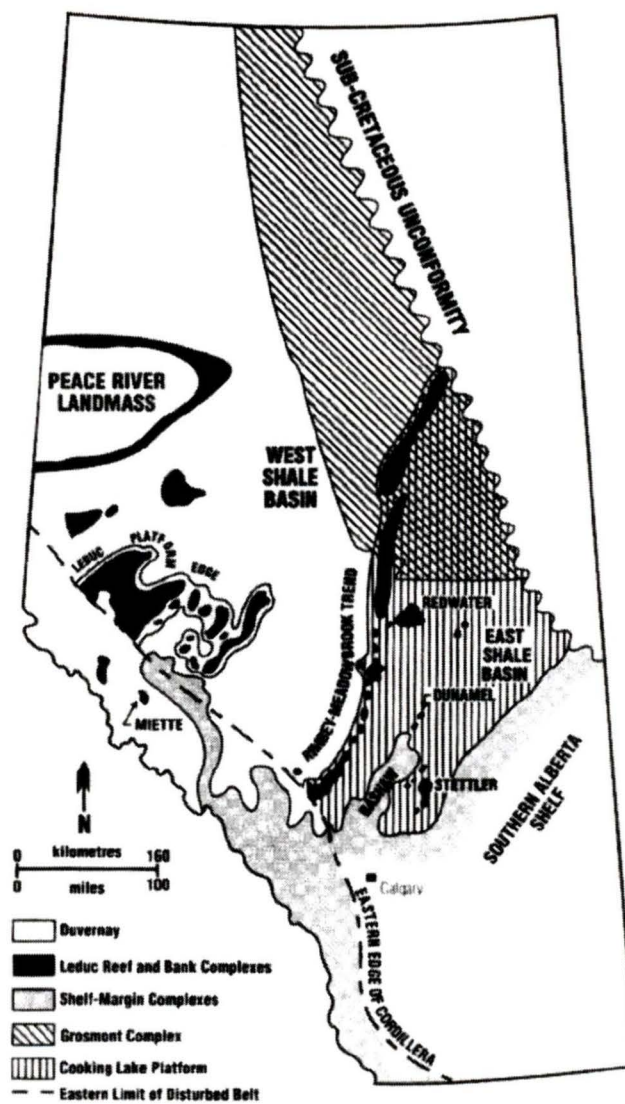
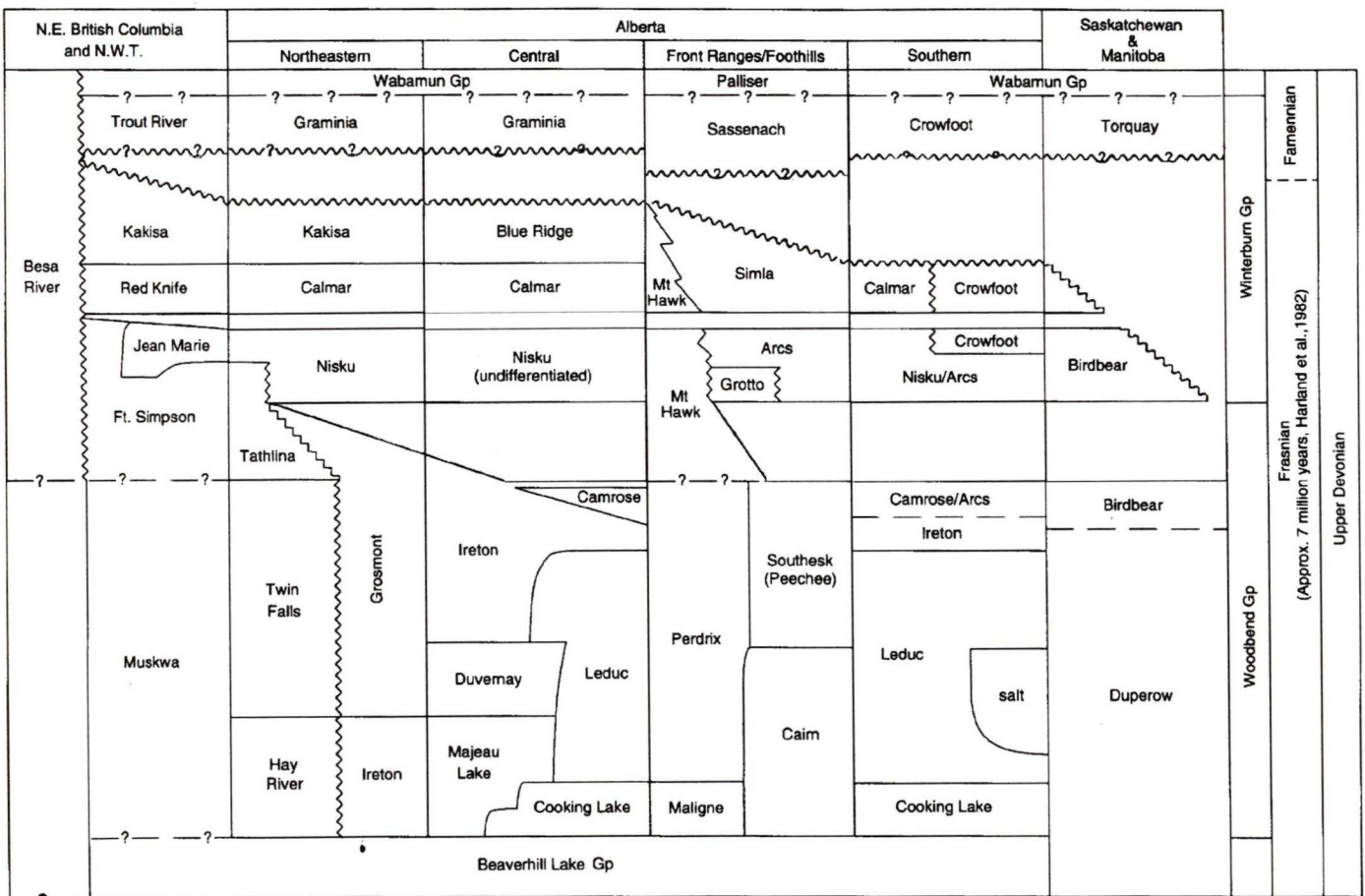


Figure 4.1 Map of province of Alberta showing distribution of major environmental facies of the Woodbend group. Major reef complexes are also shown, including lateral distribution of the Upper Devonian Duvernay formation. (From Chow et al., 1995)

Figure 4.2 Stratigraphy of Upper Devonian Woodbend-Winterburn groups. Duvernay and Nisku formations are predominantly in Central Alberta. (From Switzer et al., 1994)



Oils sourced by the Duvernay account for higher initial conventional oil in place reserves than any other petroleum system in Alberta and B.C. (Chow et al, 1995). They have migrated widely across the basin and are found predominantly in mid to late Devonian age pools. The exception to this is Lower Cretaceous sediments in east-central Alberta where Duvernay oils have been identified in a few Lower Cretaceous Mannville pools (Allan and Creaney, 1991). Duvernay sourced oils are found throughout the Bashaw complex and in the RMT where they have migrated extensively into Leduc buildups, passing into overlying Nisku platform carbonates (e.g. Leduc-Woodbend, Golden Spike, Chigwell) (Creaney et al., 1994). Duvernay oils have also been recovered in Swan Hills and Slave Point reefs, platforms of the Beaverhill Lake group, Gilwood sandstones (Watt Mountain Formation) and Keg River carbonates of the Elk Point Group (Chow et al., 1995). However, the Devonian Keg River formation is the dominant source for hydrocarbons found in Keg River reefs and the Rainbow, Zama, and Shekile subbasins of northern Alberta (Creaney et al., 1994). Oils expelled from Cynthia shales are found only in adjacent Nisku pools (Allan and Creaney, 1991), but this is not definitive due to the low TOC of these sediments (Creaney et al., 1994). Overall, there has been limited escape of Devonian sourced oils from Devonian age rocks over the course of the basin's evolution.

Duvernay sourced oils were first described by Stoakes and Creaney (1985), who classified organic matter within the Duvernay as unstructured, type II (oil-prone) kerogen, resulting from a marine planktonic origin. The geochemical characteristics of Duvernay and neighboring Cynthia Shale sourced oils are very similar, both having low sulphur content (<0.5%) and Pr/Ph ratios of ~1.5 attributed to source rock deposition

under normal marine salinities in anoxic, sediment starved environments (Allan and Creaney, 1991). Oils recovered from Nisku pools are similar in composition to those from Leduc pools with Duvernay sources, but many oils have not been directly correlated to either a Duvernay or Cynthia source (Creaney et al., 1994).

Results

In the current CSIC study, gasoline range compounds in oil samples are analyzed to determine both their molecular and isotopic compositions. The rationale for doing this is to determine if both stable isotope ratios and molecular compositions can be used to correlate oils. Previous results indicate that the molecular composition of an oil is highly susceptible to secondary alteration effects such as biodegradation and water washing, thereby limiting its diagnostic value. However, in unaltered samples these parameters may provide important genetic information about the oil. Gasoline range analytes are sampled using the SPME method discussed earlier (Chapter 3), except for the molecular analysis of 14 oils that were deemed high priority samples by PanCanadian. These oils were analyzed immediately upon arrival at UVic by the P&T method, as the SPME technique was still under development.

Molecular Variability

Gas chromatograms for the 14 high priority oils illustrate a wide range of molecular compositions (Figure 4.3). All oils were analyzed at least twice to ensure reproducible results. All samples had abundant n-alkane concentrations, with varying amounts of

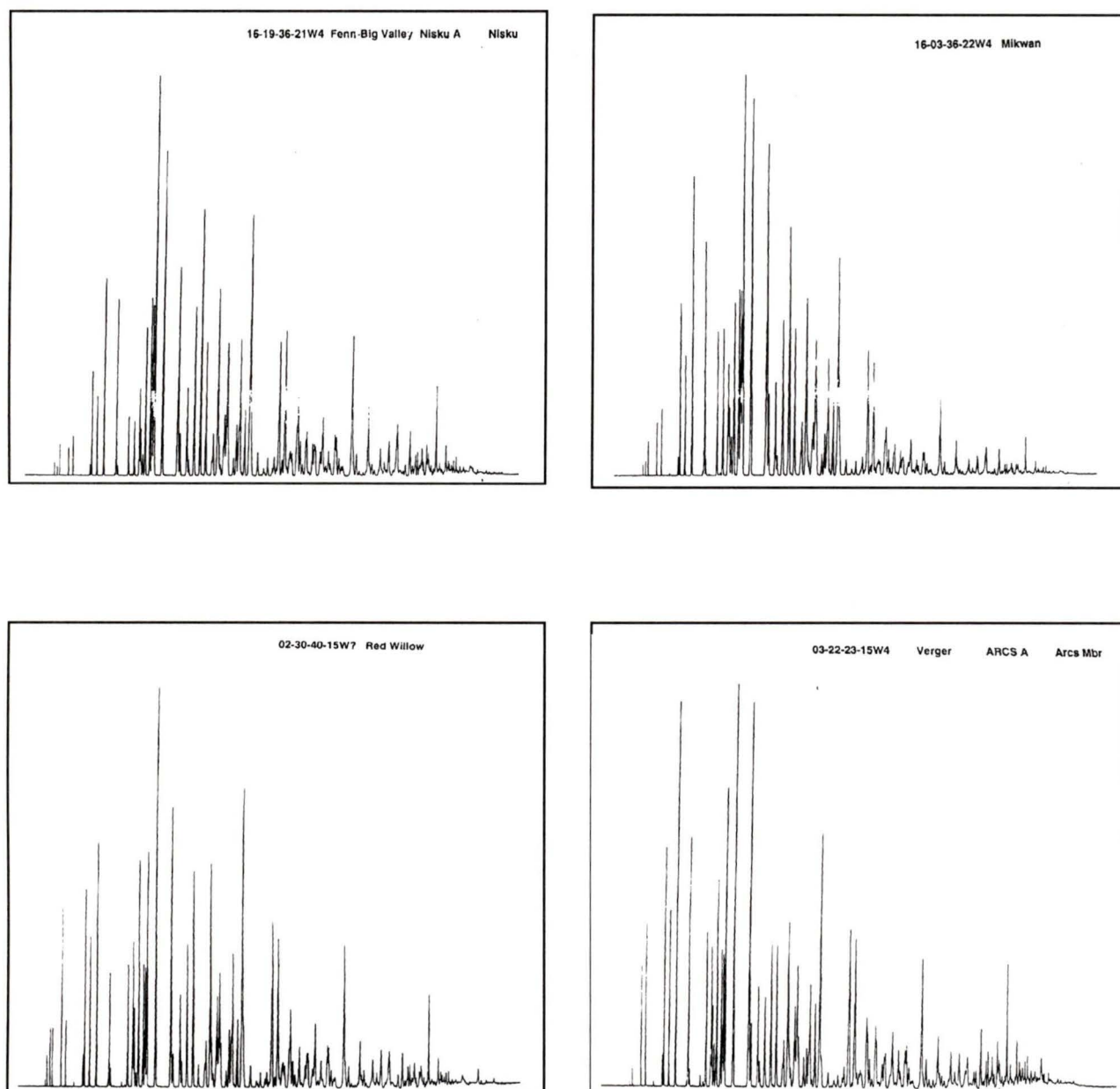


Figure 4.3 Chromatograms for 14 WCSB Oils showing diversity in composition for gasoline range compounds.

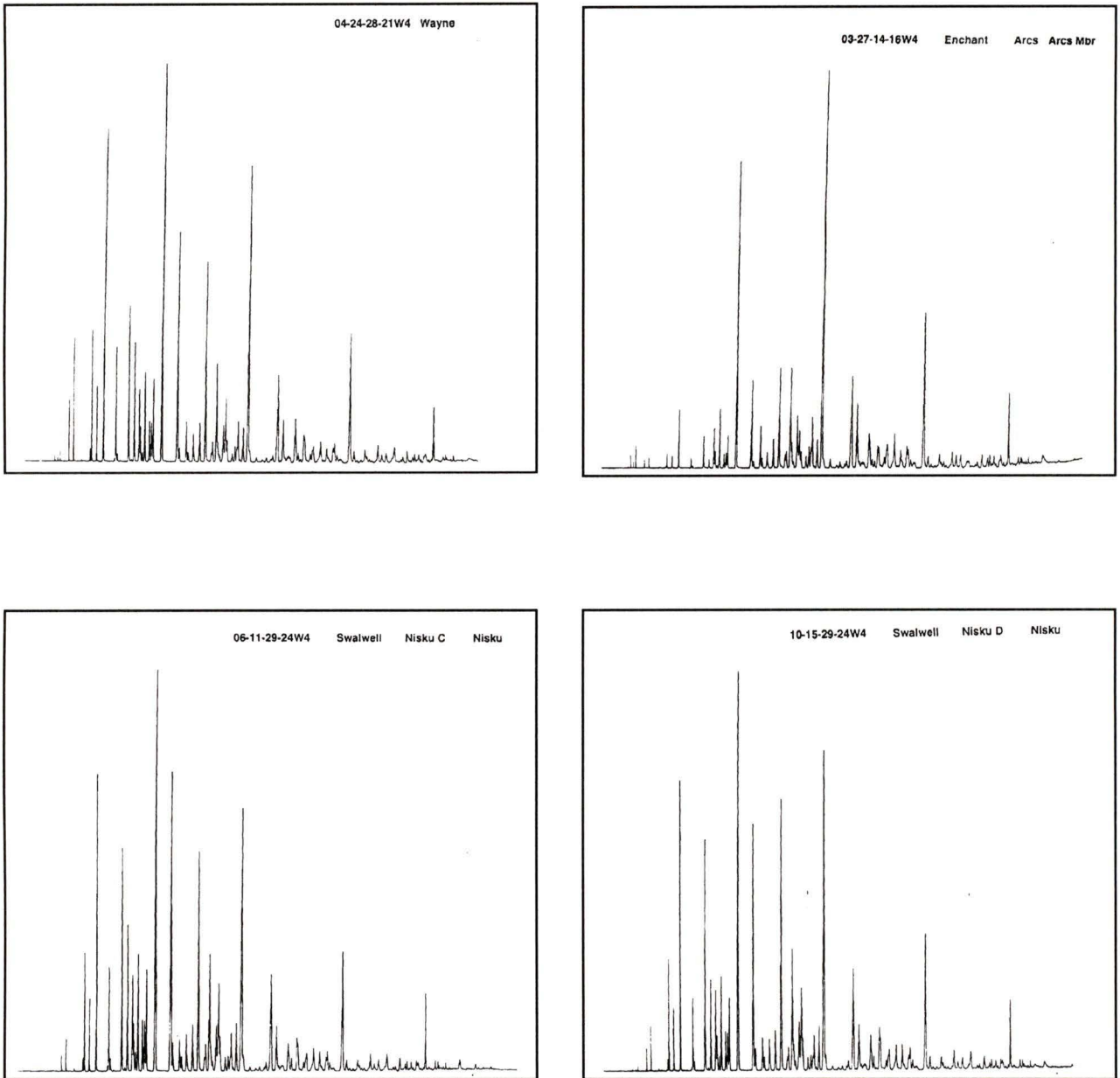


Figure 4.3 (continued) Chromatograms for 14 WCSB Oils showing diversity in composition for gasoline range compounds.

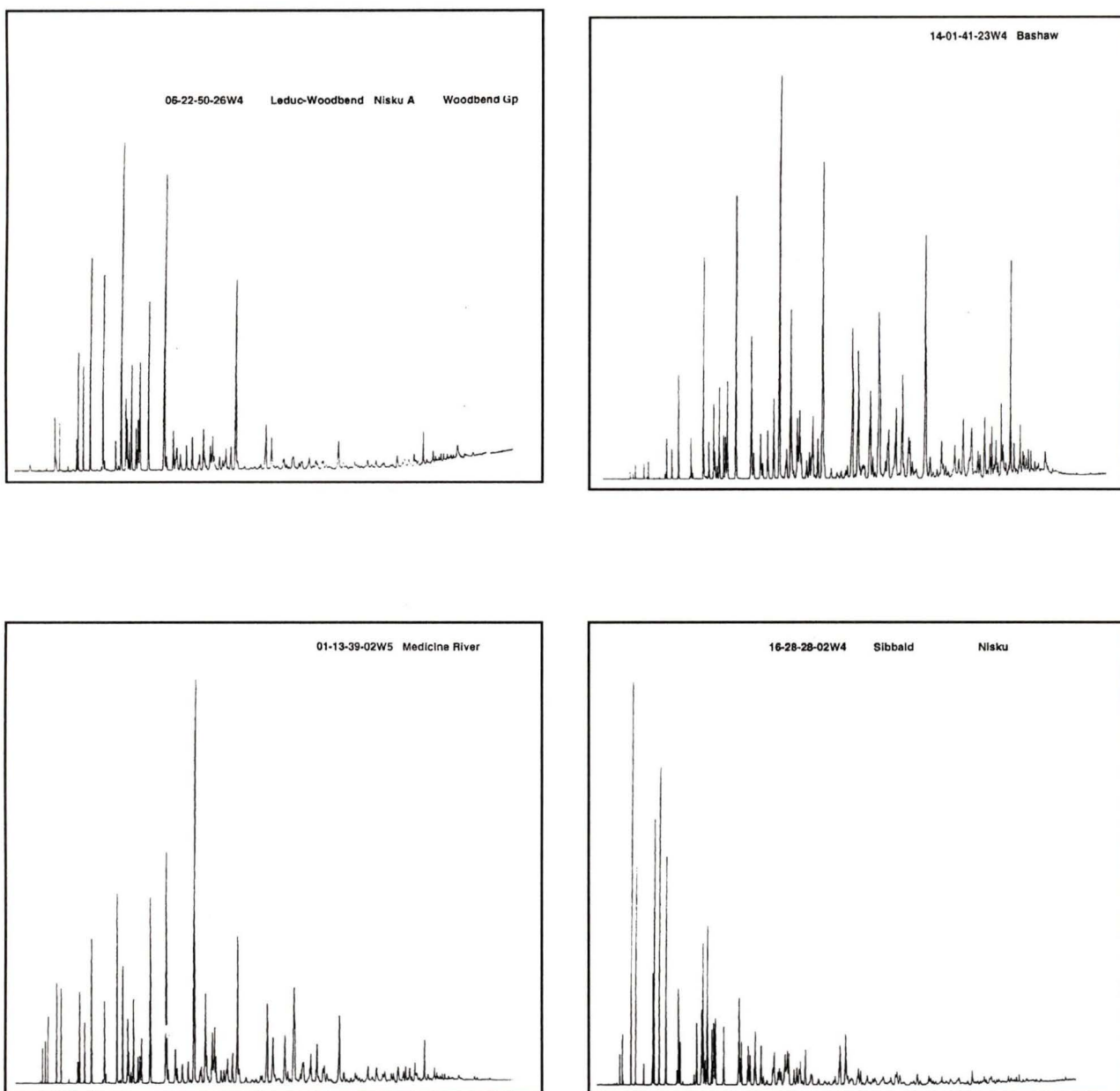


Figure 4.3 (continued) Chromatograms for 14 WCSB Oils showing diversity in composition for gasoline range compounds.

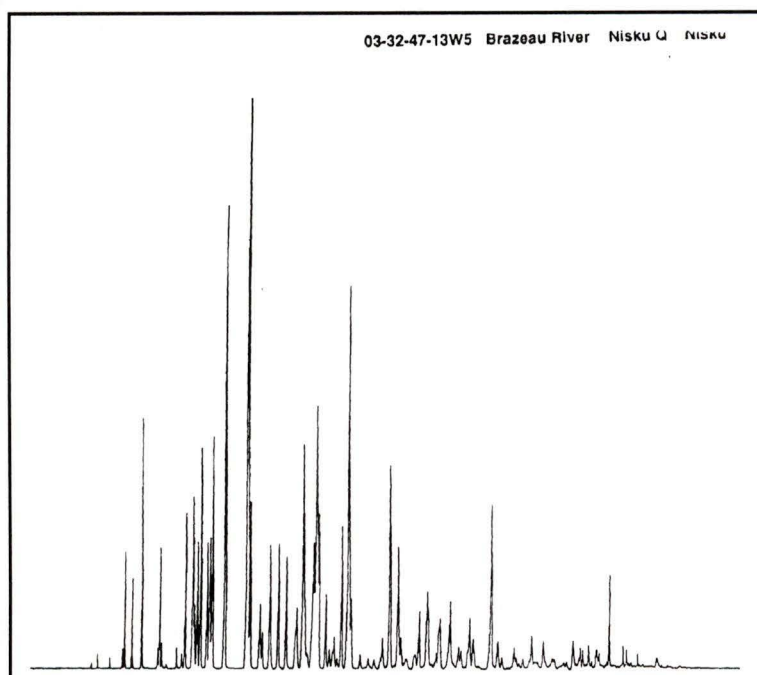
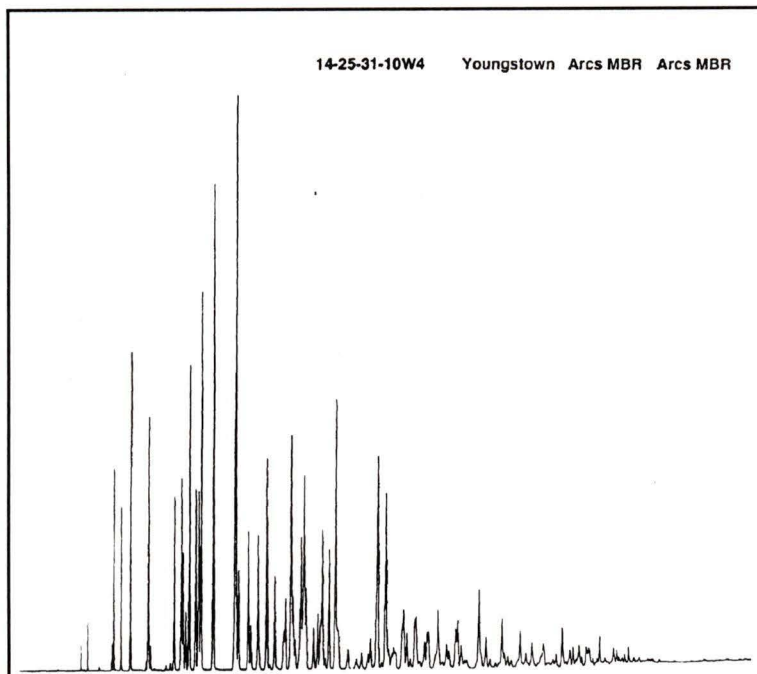


Figure 4.3 (continued) Chromatograms for 14 WCSB Oils showing diversity in composition for gasoline range compounds.

branched, cyclic, and aromatic components. The most abundant gasoline range compound in the majority of the samples is either nC7, MCYC6, Toluene, or nC8. An exception to this are the Fenn Big Valley oils that are dominated by a triplet composed of 1c3DMCYC5, 1t3DMCYC5, and 1t2DMCYC5. Another notable exception is the Sibbald oil, dominated by iC5 and 3MC6. In many cases, it is possible to visually distinguish similar oils simply by examining their GC traces. However, in the case of oils such as Sibbald, Leduc-Woodbend or Brazeau River that may have undergone some form of secondary alteration (e.g. biodegradation), the GC trace is not indicative of the original oil composition. It was hoped that stable isotope ratios would not be affected by these processes.

Statistical Analysis

To develop initial groupings of oils based on similar molecular composition, the 14 oils analyzed by the P&T method were statistically analyzed by computer using a Hierarchical cluster method. Cluster analysis is a multivariate procedure for detecting groupings in data, and is a good technique to use when the sample set is not expected to be homogenous in content (e.g. oils from different sources). Hierarchical clustering starts by setting up the appropriate experimental design algorithm and determining the closest or most similar pair of cases according to a distance measure, and combines them to form a cluster. The algorithm continues comparing cases until all the data are in one large cluster. The sequence followed by the algorithm can be displayed in an agglomeration

schedule. The method is hierarchical in that clusters formed in later stages of the analysis build upon or contain the initial clusters from earlier in the analysis.

There are several different similarity or distance measures used by the Hierarchical analysis for defining how different or alike two cases are. The measure most often used when cases have variables of the same units is the squared Euclidean distance, defined as the sum of the squared distances over all variables. An example of this for comparing oils would be:

Table 4.2 – Example Data Set for Determining Squared Euclidean Distance

Oil Name	IC ₅ (‰)	nC ₅ (‰)	2MC ₅ (‰)	3MC ₅ (‰)	nC ₆ (‰)	MCYC ₅ (‰)	Benzene (‰)	CYC ₆ (‰)	nC ₇ (‰)
Oil 1 (X _i)	-28	-29	-30	-31	-32	-31	-30	-29	-28
Oil 2 (Y _i)	-30	-32	-30	-29	-33	-32	-31	-30	-30
X _i -Y _i	2	3	0	2	1	1	1	1	2

$$\text{Squared Euclidean distance} = \sum_i (X_i - Y_i)^2 = 2^2 + 3^2 + 0^2 + 2^2 + 1^2 + 1^2 + 1^2 + 1^2 + 2^2 = 25$$

The smaller the distance, the greater the similarity between oils. It is important to distinguish between distance and similarity, as the two values are inversely related to each other. Hierarchical clustering computes a “Distance Matrix” with entries for distances between every pair of cases. A more convenient method to display the formation of clusters is a dendrogram. In this format, the distance between cases is rescaled to a “distance cluster combine coefficient” (DCC) ranging between 0 to 25, with smaller values indicative of greater similarity. Samples are listed in the order given in the agglomeration schedule, and similar cases are joined by vertical lines.

There are also numerous methods for deciding which cases or clusters should be combined at each step of the analysis. One of the simplest and most common is the single linkage or nearest neighbor technique, taking the cases that have the smallest distance between them, and designating them as the first cluster. The distance between this cluster and the remaining individual cases is computed based on the minimum distance between an individual case and a case in the cluster. This next smallest or closest distance is then added to the cluster. I employ the average linkage between groups method, because it defines the distance between two clusters as the average of the distances between all pairs of cases in which one member of the pair is from each of the clusters (Norusis, 1994). An example of this is comparing a cluster containing oils A, B,C, and another cluster of oils D,E, F. The distance between the two clusters is the average of distances between the following pairs of cases: (A,D) (A,E) (A,F) (B,D) (B,E) (B,F) (C,D) (C,E) (C,F). The important difference between this method and others (e.g. single linkage) is that it utilizes all pairs of distances, not just the nearest or furthest.

Molecular Correlations

The 14 oils analyzed by the P&T method were statistically analyzed using the raw area counts for 29 peaks, each representing the molecular abundance of a specific gasoline range compound. I utilize a greater number of peak data in molecular versus isotopic analysis because I can measure reproducible peak areas for compounds that co-elute as doublets or triplets even though they produce isotopic signatures that are of little or no diagnostic value. The 29 peaks chosen range from C₅ to C₁₀, and the raw area counts for each peak area are once again normalized to that of a common peak (nC₇)

Table 4.3 Peak Areas normalized to Heptane for 14 WCSB Oils

Peak	Enchant	Mikwan	FennBV	Wayne	Verger	SwalwellC	SwalwellD
iC5	0.02	0.05	0.03	0.06	0.11	0.03	0.02
Pentane	0.04	0.07	0.07	0.12	0.15	0.05	0.04
23DMC4 or CY	0.00	0.03	0.03	0.03	0.07	0.03	0.02
2MC5	0.07	0.22	0.27	0.19	0.34	0.14	0.15
3MC5	0.06	0.16	0.22	0.12	0.27	0.09	0.09
Hexane	0.27	0.43	0.53	0.54	0.60	0.39	0.43
MCYC5	0.07	0.41	0.50	0.21	0.46	0.16	0.12
Benzene	0.08	0.22	0.12	0.31	0.02	0.29	0.42
CYC6	0.07	0.30	0.16	0.25	0.32	0.27	0.18
2MC6	0.13	0.27	0.26	0.16	0.32	0.18	0.17
11DMCYC5	0.06	0.14	0.14	0.08	0.18	0.08	0.07
23DMC5	0.00	0.08	0.07	0.02	0.10	0.04	0.03
3MC6	0.21	0.42	0.47	0.21	0.48	0.22	0.21
1c3DMCYC5	0.06	0.46	0.60	0.09	0.32	0.10	0.08
1t3DMCYC5	0.08	0.48	0.62	0.11	0.35	0.11	0.10
1t2DMCYC5	0.14	0.96	1.33	0.20	0.71	0.20	0.16
Heptane	1.00	1.00	1.00	1.00	1.00	1.00	1.00
MCYC6	0.39	1.06	0.90	0.67	1.13	0.83	0.67
1c2DMCYC5	0.02	0.18	0.13	0.03	0.17	0.05	0.05
25DMC6	0.17	0.23	0.30	0.12	0.28	0.10	0.09
24DMC6	0.03	0.05	0.05	0.03	0.07	0.04	0.03
223TMC5	0.06	0.45	0.55	0.09	0.27	0.10	0.09
Toluene	0.26	0.43	0.29	0.58	0.40	0.63	0.75
3MC7???	0.19	0.25	0.26	0.13	0.29	0.16	0.15
3MC7??	0.14	0.57	0.61	0.23	0.50	0.31	0.27
1c4DMCYC6	0.09	0.21	0.21	0.11	0.26	0.15	0.13
Octane	1.20	0.78	0.78	1.03	0.84	1.10	1.09
Nonane	0.49	0.36	0.47	0.55	0.55	0.68	0.52
Decane	0.15	0.11	0.16	0.18	0.29	0.34	0.15

Peak	BrazRiv	LeducWood	Bashaw1401	RedWill	Youngstown	MedRiv	Sibbald
iC5	0.01	0.14	0.03	0.21	0.01	0.19	2.03
Pentane	0.01	0.11	0.04	0.10	0.03	0.19	1.17
23DMC4 or CY	0.02	0.17	0.02	0.07	0.04	0.10	1.19
2MC5	0.09	0.41	0.09	0.25	0.19	0.28	2.32
3MC5	0.07	0.39	0.07	0.22	0.17	0.20	3.02
Hexane	0.24	0.81	0.24	0.35	0.34	0.49	2.19
MCYC5	0.11	0.86	0.14	0.25	0.37	0.32	1.06
Benzene	0.03	0.14	0.58	0.01	0.01	0.78	0.00
CYC6	0.17	1.65	0.15	0.33	0.33	0.53	0.82
2MC6	0.31	0.39	0.23	0.31	0.35	0.31	1.13
11DMCYC5	0.09	0.29	0.08	0.18	0.22	0.15	2.27
23DMC5	0.18	0.16	0.05	0.04	0.12	0.06	0.40
3MC6	0.37	0.59	0.30	0.52	0.58	0.41	2.50
1c3DMCYC5	0.20	0.24	0.15	0.29	0.35	0.13	0.85
1t3DMCYC5	0.22	0.36	0.17	0.33	0.40	0.16	1.23
1t2DMCYC5	0.35	0.64	0.36	0.60	0.79	0.23	1.09
Heptane	1.00	1.00	1.00	1.00	1.00	1.00	1.00
MCYC6	1.54	1.96	0.66	0.92	1.55	1.41	1.78
1c2DMCYC5	0.31	0.07	0.11	0.10	0.26	0.06	0.97
25DMC6	0.15	0.26	0.20	0.31	0.37	0.21	0.83
24DMC6	0.08	0.31	0.06	0.09	0.12	0.09	0.71
223TMC5	0.32	0.13	0.22	0.48	0.40	0.14	1.40
Toluene	0.35	0.24	1.68	0.08	0.36	2.60	0.18
3MC7???	0.30	0.20	0.31	0.43	0.52	0.37	0.65
3MC7??	0.75	0.11	0.41	0.61	0.84	0.44	1.27
1c4DMCYC6	0.38	0.17	0.19	0.27	0.41	0.20	0.96
Octane	1.38	1.50	1.66	1.40	1.05	1.08	0.36
Nonane	0.80	0.28	1.47	1.19	0.71	0.59	0.29
Decane	0.29	0.22	0.65	0.53	0.26	0.25	0.05

(Table 4.3). This normalization establishes a relative concentration for a specific compound compared to the other gasoline range analytes. Heptane is again chosen as the common peak because it is in high abundance in all samples.

The agglomeration schedule and corresponding dendogram for 14 oils displays the stages of cluster combinations along with the distance measure (Coefficient) between cases (Figure 4.4). The actual value of the coefficient depends on both the distance measure and linkage method used to compare cases. The sample names and case numbers are listed in the dendogram. The agglomeration schedule also lists at what stage of the algorithm cases are first compared (Stage Cluster 1st Appears) and the next stage the same case is combined in a new cluster (Next Stage). Examination of the dendogram shows 3 major groups of oils and 1 oil (Sibbald) that has little or no similarity to others:

Group 1 - Wayne, SwalwellC, SwalwellD, Enchant

Group 2 – FennBV, Mikwan, Verger, BrazRiv, Youngstown, RedWill

Group 3 - LeducWood, Bashaw1401, MedRiv

When interpreting the dendogram, I establish boundaries based on the overall distribution of cases within the cluster. As most samples cluster within a DCC value of 5, it is easiest simply to group all oils except Sibbald into one large group. However, if we subdivide the oils based on 1 DCC unit intervals, then the more select groupings listed above emerge. Statisticians are unclear on where to “draw the line” in determining definite similarity in dendograms, with some favouring a value of 5 to 10 while others choose 10 to 15 (Norusis, 1994). Based on the structure of this data set, an interval of 1 to 3 can be used to distinguish between groups.

Agglomeration Schedule using Average Linkage (Between Groups)

Stage	Clusters Cluster 1	Combined Cluster 2	Coefficient	Stage Cluster 1st Appears Cluster 1	Cluster 2	Next Stage
1	11	13	.087232	0	0	2
2	10	11	.125477	0	1	4
3	4	7	.308670	0	0	5
4	3	10	.518928	0	2	9
5	4	12	.554452	3	0	8
6	2	14	.685073	0	0	7
7	2	8	1.113976	6	0	8
8	2	4	1.469084	7	5	9
9	2	3	2.130610	8	4	11
10	1	6	3.151214	0	0	12
11	2	5	5.051740	9	0	12
12	1	2	5.539639	10	11	13
13	1	9	41.616070	12	0	0

Dendrogram using Average Linkage (Between Groups)

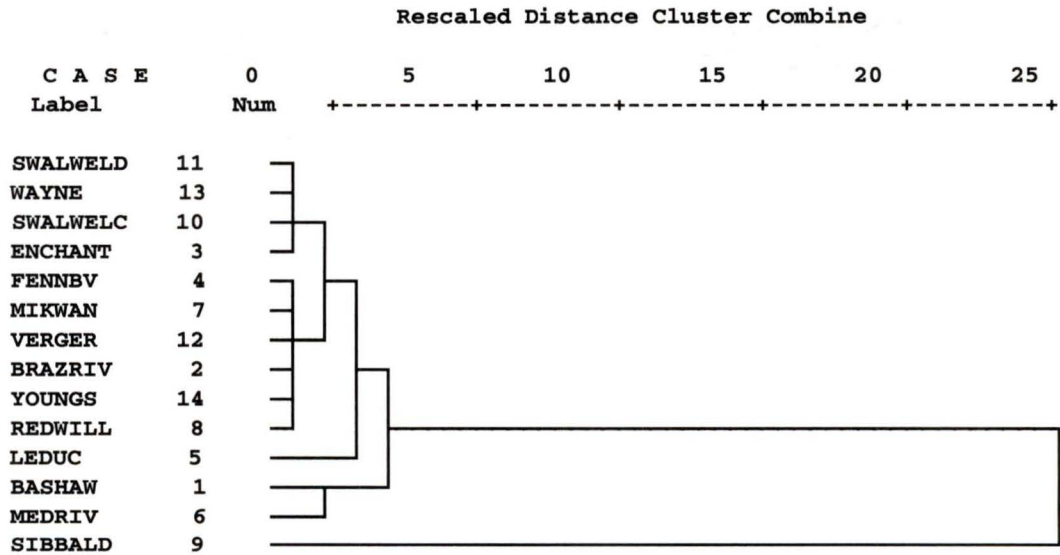


Figure 4.4 Agglomeration schedule and corresponding dendrogram for hierarchical cluster analysis of molecular concentrations for 14 WCSB oils.

Comparison of the raw data shows that all the oils are remarkably similar in composition except for the Sibbald sample. Group 2 and 3 oils contain (on average) higher concentrations of branched or iso-alkanes such as 3MC5, 2MC6, 3MC6, and 25DMC6 compared to group 1 oils. These two groups also show greater MCYC6 concentrations. Other compound classes such as n-alkanes and aromatics display highly variable concentrations both within and between groups. Visual comparison of the chromatograms (Figure 4.3) further demonstrates the unique characteristics of the Sibbald oil, although Enchant and LeducWood also have distinctive GC traces. The LeducWood sample contains very low total concentrations of all gasoline range hydrocarbons making analysis difficult.

I must also factor into the proposed correlations the geographic location and regional geology where samples are taken from. Based on their close geographic proximity to each other, certain oils may be expected to exhibit some similarity in their molecular composition due to generation and limited migration from a common source (i.e. Duvernay) (Figure 4.5). An example of this is Group 1 oils such as Wayne, SwalwellC, SwalwellD, and Enchant that comprise an area from Ranges 16-24W4 and Townships 14-29. All reservoirs are located in Nisku strata, but strangely the Verger oil taken from the same formation as Enchant does not correlate directly with this group. In addition, the Enchant well is located within a large carbonate shelf complex running throughout southern Alberta, and this area is considered to have a regional geology that is vastly different from the “simple” reef structures in central Alberta. Therefore while group 1 is a plausible correlation, its members are probably from different sources. This

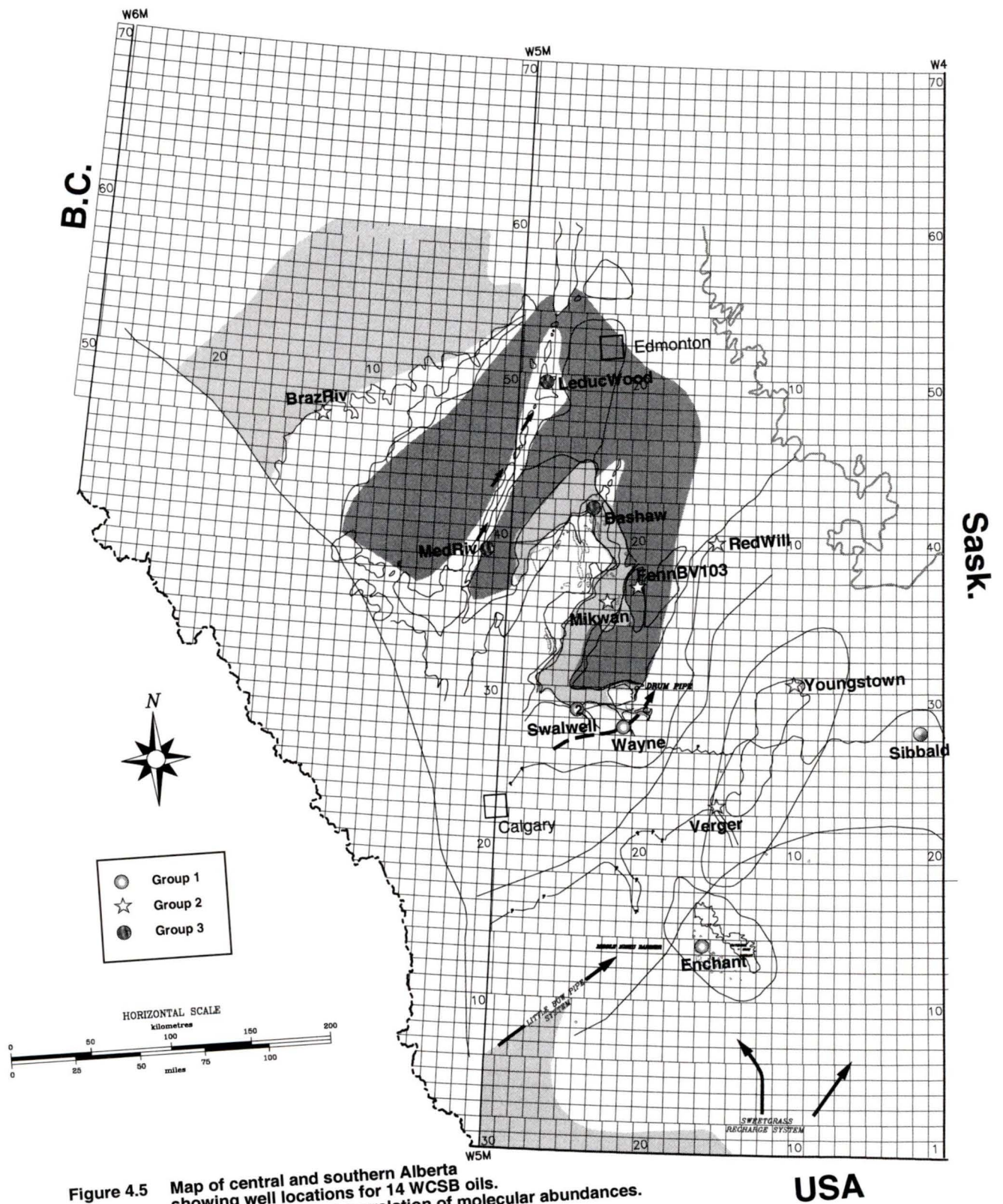


Figure 4.5 Map of central and southern Alberta showing well locations for 14 WCSB oils. Groups are based on correlation of molecular abundances.

should not imply that I manipulate data to fit a geographic or geologic interpretation, but, rather use it to eliminate unlikely groupings in the cluster analysis.

An example of this process of elimination occurs with Group 2 oils. The group represents a substantial area spanning Ranges 10W4 to 13W5 and Townships 23-47. The probability that these samples are all from the same source is highly unlikely, not only due to the long distance of migration involved, but also the fact that the sediments of the suspected source (Duvernay) has attained different levels of thermal maturity throughout the East and West Shale basins of central Alberta (Creaney et al., 1994). This would result in oils with variable molecular compositions and these oils may also have been influenced from localized Nisku source beds located in the East Shale Basin. The Brazeau River oil is also unique in that it may have undergone Thermochemical Sulfate Reduction (TSR), and this may substantially alter its molecular and isotopic composition (Manzano et al., 1997; Whiticar and Snowdon, 1998). Since the cluster analysis is not biased by other criteria in developing groupings for oils, the Brazeau River sample may show a molecular composition similar to Youngstown, but the probability of this oil retaining its original composition is low.

Group 3 are all located on or near the RMT, and communication between reservoirs in this area has been proposed (e.g. Stoakes and Creaney, 1985). However, the MedRiv oil is located in Mississippian not Devonian age strata, and therefore an unlikely member of this group. LeducWood and Bashaw oils are considered Duvernay sourced.

Compositional Relationships

Samples were analyzed to determine if any systematic correlation or relationship exists between molecular concentrations of gasoline range compounds (Figure 4.6, 4.7). Compounds with corresponding carbon numbers from different classes are compared with varying degrees of scatter observed. A strong linear correlation is evident between concentrations of straight chain and branched alkanes for C₆ and C₇ compounds (Figure 4.6a,b). Previous work on the origin of light hydrocarbons by Mango (1987, 1990b, 1997b) showed an invariance in the ratios of concentrations of specific iso-alkanes for homologous (same source) oils due to a pressured steady state catalytic process that is responsible for their formation. These products along with dimethylcyclopentanes and methylcyclohexanes can be derived from straight chain precursors (Mango, 1990b). This is evident by a good correlation between nC₆-MCYC5 ($r^2 = 0.9197$) and nC₇-MCYC6 ($r^2 = 0.8827$) (Figure 4.6c,d). In a group of papers on the origin of light cycloalkanes in petroleum, Mango (1990b, 1994) suggested that the ratio of nC₇/MCYC6 would show minor variance in petroleums and would not be altered due to thermal decomposition of polycyclic natural precursors or MCYC6 itself. Any variance in this ratio was more consistent with a hypothesis in which both products were formed by steady-state catalytic process. Mango (1990b) added that since MCYC5 is derived from catalytic decomposition of a straight chain parent, its concentration would be determined in a similar manner.

Somewhat unusual is the weaker correlation of nC₆ and CYC₆ ($r^2 = 0.6915$) (Figure 4.7a). Mango (1994) discussed how during carbocyclic ring closures in light

hydrocarbon formation, n-alkanes are transformed by catalysts that will preferentially promote ring closures of a specific carbon number forming disproportionate concentrations of isoalkanes, cyclopentanes, and cyclohexanes. He called this effect a ring preference (RP). However, Mango (1994) found a paradox in his explanation, in that a group of oils from a common source rock that he expected to show no RP still exhibited widely varying concentrations of isoalkanes, cyclopentanes and cyclohexanes (analogous to what I observe with this data). One would expect oils of a uniform overall composition reflecting a static system would show similar or fixed light hydrocarbon concentrations, but instead they show varying concentrations that reflects a dynamic system (Mango, 1994). Therefore, a poor correlation between n-C₆ and CYC₆ may be expected. There also appears to be no relationship between n-alkanes and their aromatic counterparts, as evidenced by the poor correlations of nC₆-Benzene and nC₇-Toluene (Figure 4.7b,c). This could be due to the extremely low concentrations of benzene and toluene in several samples, indicating source control on the molecular composition of the oil. It is also interesting to note that iC₅ and nC₅ show little or no dependence to each other (Figure 4.7d). An explanation for this could be evaporative loss of these highly volatile compounds during sample collection, and therefore the initial concentration of these compounds in the oil is not preserved.

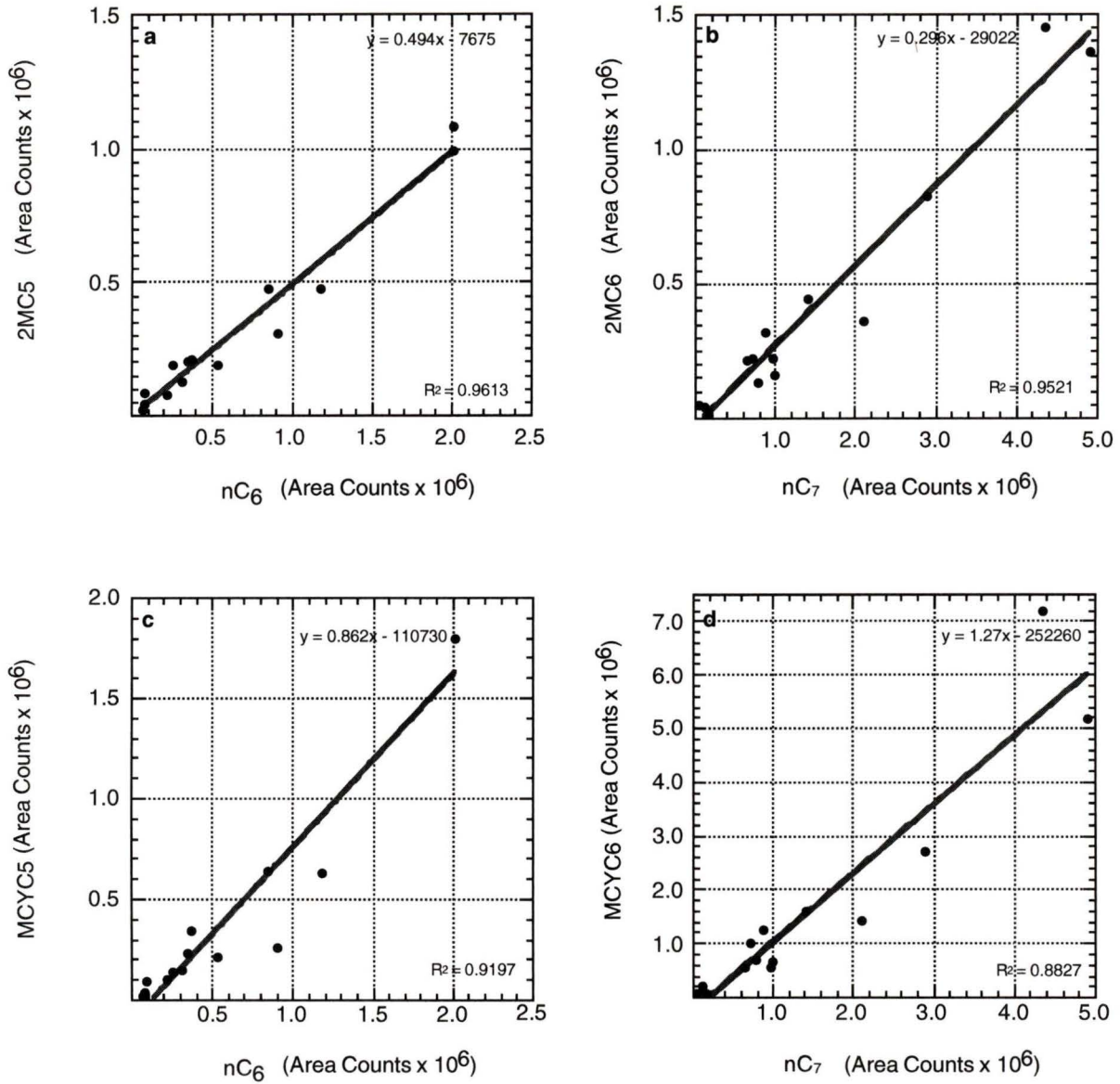


Figure 4.6 Cross-plots of the molecular concentrations for individual compounds illustrating interdependencies and relationships

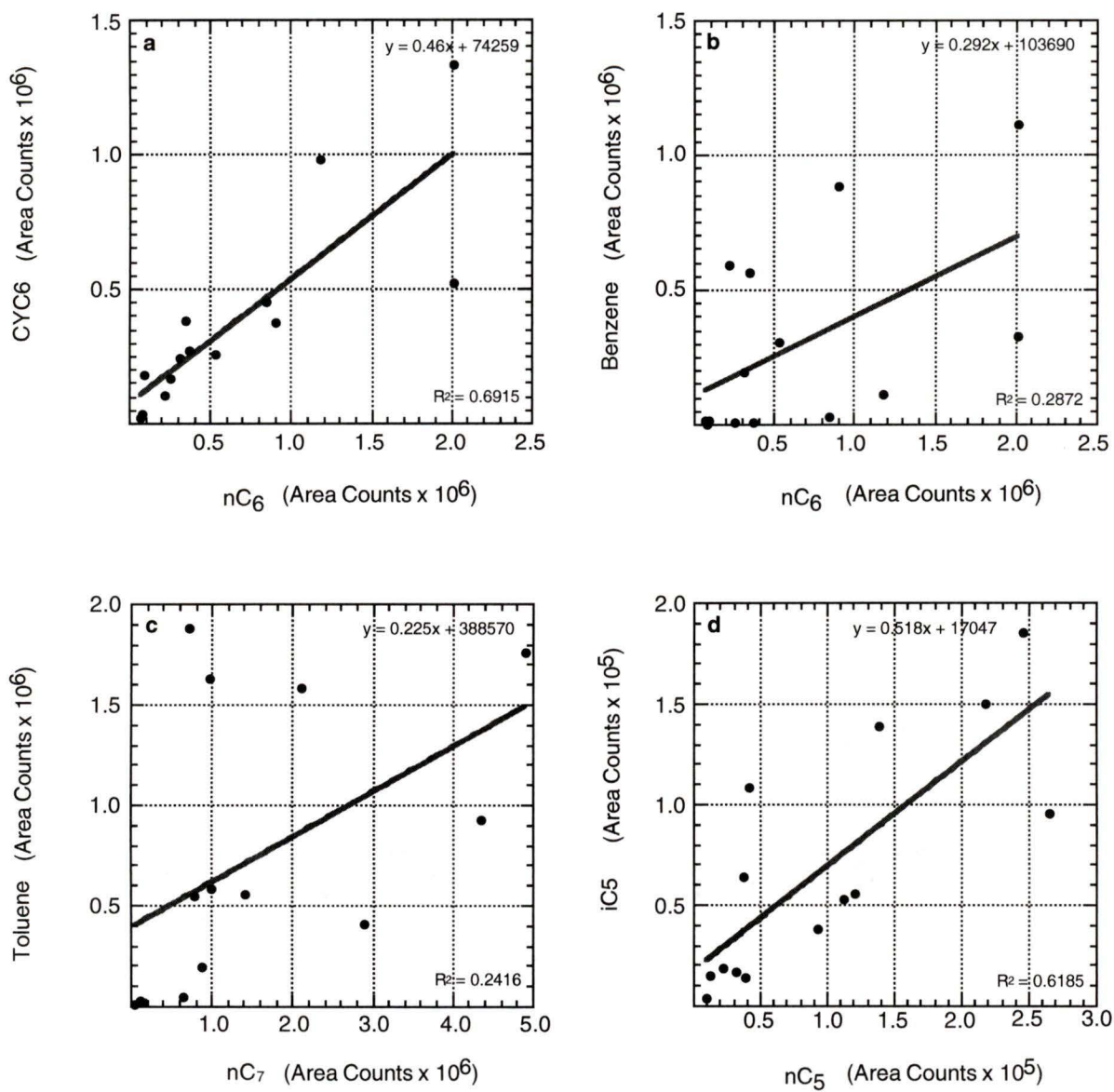


Figure 4.7 Cross-plots of the molecular concentrations for individual compounds illustrating interdependencies and relationships

A molecular approach to grouping or correlating oils appears to be limited in its usefulness. Although concentrations of certain gasoline range components have been used as possible indicators of biodegradation in oils and condensates (Osadetz et al., 1992), the majority of studies using light hydrocarbons for classifying oils have found molecular techniques impractical for these purposes (Snowdon and Osadetz, 1988; Osadetz et al., 1992; Whiticar and Snowdon, 1998). In light of this, I have focussed my efforts on utilizing stable isotope ratios as a more robust and diagnostic tool.

Stable Carbon Isotopes

When examining the isotopic data in conjunction with molecular abundances, it is important to remember that reproducible isotope ratios are measurable for a smaller number of compounds. When compounds co-elute their isotopic signatures blend together obscuring the original value for each individual compound. The main benefit of isotope ratios versus molecular abundances is that they are more resistant to secondary alteration process such as biodegradation or water washing, that can render the molecular signature of an oil unrecognizable (Murphy, 1995).

Isotopic Variability

Carbon isotopic ratios of individual hydrocarbons in the gasoline range fraction show significant and diagnostic diversity for the 27 oils from the WCSB (Table 4.4). Isotope ratios were measured by CF-IRMS using the SPME technique to extract analytes. Replicate analyses or “runs” of each sample were performed to ensure that reproducible

Table 4.4 Carbon Isotope Ratios of Oils for CSIC Study															
Well Name	iC5	Pentan	23DMC4	2MC5	3MC5	Hexane	MCYC5	Benzene	CYC6	Heptane	MCYC6	Toluene	1c4DM	Octane	Nonan
Mikwan 1	-30.24	-31.29	-28.22	-31.30	-29.43	-33.15	-28.36	-35.96	-34.44	-34.72	-30.45	-34.48	-31.12	-34.12	-34.93
Mikwan 2	-30.06	-31.11	-28.50	-31.19	-28.92	-32.53	-28.68	-36.12	-34.62	-34.89	-30.39	-34.22	-31.84	-33.86	-34.62
MedRiv1	-28.76	-28.89	-26.46	-29.04	-28.42	-29.71	-27.67	-29.22	-29.30	-30.54	-27.91	-28.21	-31.82	-31.22	-30.75
MedRiv2	-28.70	-27.25	-26.81	-29.04	-28.71	-29.90	-27.68	-29.29	-27.84	-30.73	-27.72	-28.22	-28.88	-30.36	-30.70
MedRiv3	-28.48	-29.26	-26.56	-28.92	-29.13	-29.54	-27.54	-29.07	-27.72	-30.72	-28.00	-28.28	-30.61	-31.60	-31.34
Wayne 1	-29.84	-31.09	-27.53	-30.25	-28.35	-32.04	-29.23	-32.55	-32.65	-32.83	-30.78	-32.60	-29.72	-32.81	-32.94
Wayne 2	-29.64	-30.83	-27.59	-30.04	-28.40	-31.93	-29.13	-32.37	-32.96	-32.97	-30.75	-32.33	-29.41	-32.69	-32.80
Bashaw 1401 1	-28.64	-29.75	-25.54	-29.25	-27.26	-30.51	-28.14	-29.48	-32.02	-32.14	-29.91	-31.08	-29.76	-31.52	-31.81
Bashaw 1401 2	-28.62	-29.67	-25.62	-29.20	-27.20	-30.36	-28.04	-29.41	-31.96	-30.77	-29.63	-30.83	-29.67	-31.32	-31.74
Verger 1	-29.14	-30.99	-26.52	-30.08	-28.30	-31.75	-28.10	-30.56	-31.98	-32.29	-29.89	-30.76	-29.92	-32.25	-31.74
Verger 2	-29.34	-30.98	-26.54	-30.05	-28.08	-31.84	-28.56	-29.42	-32.43	-31.17	-29.61	-31.43	-29.61	-31.63	-31.78
FennBV1	-30.09	-31.43	-28.60	-31.17	-28.96	-32.80	-27.65	-35.67	-32.73	-34.88	-29.16	-33.14	-29.95	-33.04	-32.87
FennBV2	-30.11	-31.42	-28.39	-31.11	-28.65	-32.46	-27.54	-35.81	-32.75	-32.44	-29.31	-33.99	-30.23	-33.10	-32.83
RedWill1	-29.65	-30.61	-26.75	-30.23	-28.57	-31.85	-28.84	-30.02	-33.83	-33.66	-30.80	-29.55	-29.07	-32.47	-32.80
RedWill2	-29.52	-30.49	-26.97	-30.32	-28.68	-32.58	-28.63	-33.14	-33.83	-33.77	-30.73	-29.53	-30.23	-32.73	-32.75
Youngstown 1	-24.52	-26.15	-24.54	-28.16	-26.73	-30.04	-27.30	-32.33	-31.57	-32.05	-28.96	-29.16	-29.42	-31.74	-31.50
Youngstown 2	-24.52	-26.15	-24.82	-28.57	-27.16	-30.16	-27.39	-27.36	-31.77	-30.90	-28.29	-29.50	-28.36	-30.99	-31.29
BrazRiv1	-24.37	-23.81	-22.36	-25.71	-25.31	-26.68	-22.65	-23.68	-27.92	-28.43	-26.31	-26.44	-25.57	-29.99	-30.42
BrazRiv2	-24.37	-23.81	-22.40	-25.41	-24.73	-26.70	-22.71	-23.60	-27.84	-28.43	-26.31	-26.37	-25.57	-29.99	-30.42
Enchant 1	-30.88	-30.76	-27.79	-31.25	-29.75	-31.17	-30.18	-33.13	-33.64	-31.05	-31.00	-32.57	-28.52	-30.97	-30.59
Enchant 2	-31.07	-30.94	-27.63	-31.32	-29.62	-31.16	-30.33	-33.11	-32.99	-31.09	-31.41	-32.59	-28.22	-31.01	-30.87
SwalwellC 1	-27.68	-28.18	-24.96	-28.33	-27.01	-30.06	-27.00	-28.80	-30.73	-31.23	-29.47	-29.62	-27.74	-31.60	-31.52
SwalwellC 2	-27.73	-27.70	-24.48	-28.33	-26.82	-30.03	-27.03	-28.83	-30.67	-31.32	-29.57	-29.61	-26.66	-31.97	-31.76
SwalwellD 1	-28.53	-29.45	-25.25	-28.98	-27.77	-31.00	-27.85	-30.03	-31.23	-31.87	-29.89	-30.20	-27.24	-32.15	-32.14
SwalwellD 2	-28.35	-29.43	-24.99	-28.91	-27.54	-30.90	-27.86	-29.82	-31.09	-31.66	-29.87	-30.08	-27.19	-32.16	-32.06
Sibbald 1	-29.43	-29.60	-27.29	-29.99	-28.41	-30.15	-27.26	-31.98	-30.61	-31.16	-28.15	-32.58	-32.17	-22.84	-27.95
Sibbald 2	-29.43	-29.35	-26.89	-30.07	-28.25	-29.94	-26.77	-30.25	-30.62	-30.12	-28.11	-30.25	-29.17	-22.44	-29.72
LeducWood1	-26.88	-28.19	-23.89	-28.64	-26.70	-28.19	-24.76	-24.44	-28.34	-28.63	-27.50	-27.99	-27.14	-30.54	-30.18
LeducWood2	-28.27	-26.85	-22.69	-27.56	-25.61	-29.08	-25.53	-25.61	-28.64	-28.41	-27.50	-27.70	-27.01	-30.14	-29.84
Gilby 1	-28.55	-29.63	-24.99	-29.39	-27.57	-31.10	-26.55	-27.19	-30.45	-31.50	-29.66	-29.14	-28.11	-32.19	-30.99
Gilby 2	-28.47	-29.63	-25.12	-29.09	-27.04	-30.77	-26.23	-27.03	-30.33	-31.33	-29.78	-29.07	-28.12	-31.84	-30.73
Acme 1	-28.04	-28.27	-22.78	-28.19	-26.87	-29.29	-26.83	-24.73	-29.44	-29.62	-29.87	-29.55	-37.12	-30.75	-31.25
Acme 2	-28.52	-28.49	-24.13	-28.28	-27.03	-29.56	-26.65	-25.33	-29.59	-29.85	-30.48	-29.71	-42.19	-31.35	-30.88
Chigwell 1	-28.81	-30.09	-25.62	-29.32	-27.44	-31.04	-27.09	-28.68	-32.06	-32.13	-29.79	-30.54	-28.28	-33.69	-31.69
Chigwell 2	-28.60	-30.21	-25.06	-29.44	-27.64	-30.98	-26.99	-28.60	-31.98	-32.08	-29.71	-30.31	-26.40	-33.21	-31.52
Bashaw 42 1	-28.51	-29.82	-25.94	-29.37	-27.78	-31.12	-26.91	-28.38	-30.69	-31.71	-29.74	-29.99	-25.60	-32.61	-30.63
Bashaw 42 2	-28.46	-29.74	-25.39	-29.35	-27.32	-31.12	-26.72	-28.36	-31.64	-31.57	-29.86	-30.17	-28.44	-32.69	-31.46
Bashaw 1309 1	-28.22	-29.37	-24.71	-29.21	-27.27	-30.75	-26.59	-28.24	-31.29	-31.49	-30.71	-30.32	-29.32	-32.65	-31.32
Bashaw 1309 2	-28.66	-29.70	-26.24	-29.13	-27.43	-30.92	-26.81	-28.62	-31.24	-31.13	-31.42	-30.52	-30.44	-33.72	-31.88
Bashaw 1135 1	-28.79	-29.54	-25.57	-29.49	-27.11	-30.89	-26.87	-27.14	-31.18	-31.77	-30.66	-30.73	-28.47	-32.92	-31.87
Bashaw 1135 2	-28.38	-30.08	-24.86	-29.45	-27.29	-30.86	-26.82	-26.07	-31.16	-31.73	-30.45	-30.46	-27.82	-32.82	-32.06
Lousana 1	-30.18	-31.50	-27.87	-31.49	-28.91	-32.50	-27.63	-35.27	-32.52	-33.20	-29.30	-24.97	-33.10	-33.10	-34.53
Lousana 2	-30.21	-31.18	-29.06	-30.97	-28.55	-32.86	-27.17	-35.41	-33.97	-32.24	-31.73	-31.35	-33.78	-33.10	-34.53
Lousana 3	-30.09	-31.18	-30.17	-30.72	-28.57	-32.89	-27.26	-35.95	-33.06	-32.01	-32.00	-30.30	-33.01	-33.10	-34.53
Lousana 4	-30.40	-31.42	-30.85	-31.05	-28.89	-32.98	-27.60	-35.60	-34.85	-32.97	-32.33	-30.66	-29.10	-36.47	-32.88
Swalwell814 1	-29.75	-30.74	-27.20	-29.93	-29.03	-31.67	-28.70	-32.02	-31.73	-31.93	-31.81	-30.91	-25.61	-31.45	-30.90
Swalwell814 2	-29.55	-30.96	-27.87	-29.65	-28.39	-31.47	-28.28	-31.54	-32.05	-31.86	-31.57	-30.91	-25.61	-31.45	-30.90
Swalwell1312 1	-29.26	-30.16	-26.90	-29.75	-28.09	-31.69	-28.48	-31.52	-33.92	-32.72	-36.64	-31.12	-26.37	-34.44	-32.15
Swalwell1312 2	-29.33	-30.71	-27.19	-29.70	-28.20	-31.60	-28.53	-32.74	-32.64	-32.09	-36.36	-31.09	-25.97	-34.15	-32.09
Wainwright 1	-26.26	-26.71	-25.84	-26.90	-26.38	-27.73	-31.55	-29.21	-28.82	-28.30	-30.52	-26.95	-30.35	-29.55	-28.24
Wainwright 2	-25.80	-26.77	-26.15	-27.08	-26.76	-27.89	-32.47	-33.23	-29.05	-28.01	-29.78	-25.68	-32.80	-30.42	-28.24
Wainwright 3	-26.29	-26.36	-26.53	-26.82	-26.61	-28.02	-32.73	-35.17	-29.03	-28.49	-29.90	-26.72	-34.04	-30.17	-28.24
FennBV 103 1	-28.41	-29.69	-27.10	-29.83	-28.61	-32.10	-28.35	-32.06	-34.00	-32.00	-37.17	-34.15	-31.56	-36.71	-36.56
FennBV 103 2	-28.93	-30.03	-27.41	-29.88	-28.20	-32.10	-28.34	-31.99	-33.29	-32.11	-35.27	-32.03	-28.36	-35.45	-36.56
FennBV 922 1	-24.27	-25.01	-25.71	-28.29	-26.75	-29.75	-26.75	-30.20	-34.48	-30.50	-31.08	-29.69	-26.11	-31.56	-31.97
FennBV 922 2	-23.76	-24.89	-26.12	-28.86	-27.15	-30.57	-27.32	-30.08	-32.37	-32.21	-29.14	-30.85	-27.55	-31.56	-31.97
Execelsior 1	-22.00	-23.53	-24.27	-27.22	-25.45	-29.74	-30.08	-28.12	-33.45	-28.23	-29.83	-24.67	-28.42	-31.39	-33.44
Execelsior 2	-22.63	-23.80	-25.12	-27.51	-26.21	-29.38	-28.53	-28.09	-31.97	-30.24	-34.16	-25.14	-28.56	-34.72	-37.30

ratios are measured for each of the 16 compounds discussed in development of the SPME method (Chapter 3). Peak reproducibilities are the same as those encountered in SPME trials, and similar caution must be used when interpreting results for Benzene, MCYC5, 1c2DMCYC5, and 1c4DMCYC6. It was decided that due to anomalous $\delta^{13}\text{C}$ values for 1c2DMCYC5 in a majority of samples, this compound should be removed from the final data set entirely. Isotopograms are generated for each oil to illustrate the isotopic variability of the samples (Figure 4.8). Variations of up to $>10\%$ are observed between oils (e.g. BrazRiv – Mikwan) and for different compounds within a particular oil (e.g. Excelsior). Internal sample reproducibility is high enough to reliably distinguish between oils.

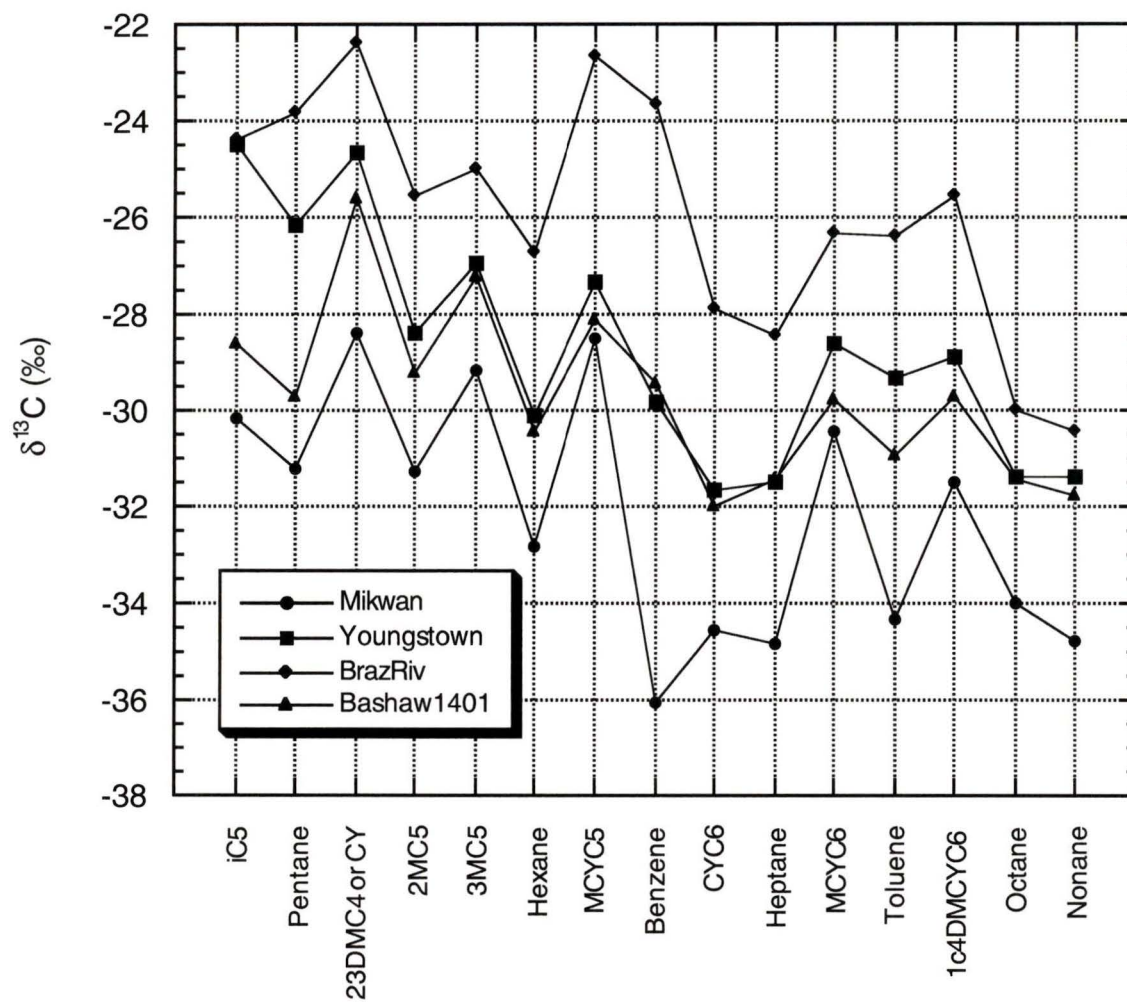


Figure 4.8 Isotopograms of 4 WCSB oils illustrating the carbon isotope ratio of 15 individual gasoline range hydrocarbons. Significant diversity is evident between oils.

Preliminary Analysis

When grouping or classifying oils based on carbon isotope ratios, it is often useful to visually compare isotopograms prior to statistical analysis. This is because oils from the same geographic location/field may be expected to exhibit nearly identical isotopic signatures. An example of this is the Bashaw oils drawn from the Nisku G formation (Figure 4.9). Isotope ratios for iC_5 , nC_5 , $2MC_5$, $3MC_5$, and nC_6 have a standard deviation of 0.3‰ between the 4 oils. The deviation increases from 0.5 to 1‰ for CYC_6 , nC_7 , $MCYC_6$, Toluene, nC_9 . The remaining compounds all show poor reproducibility (>1‰) and problems with them have already been discussed. These oils are all attributed to a Duvernay source rock and their isotopic similarities appear to confirm this suggestion.

Another example of oils from the same field that may be expected to show similar isotopic composition are the Swalwell samples from the Nisku A-D formations (Figure 4.10a). Unexpectedly, these 4 oils show significant variability, with a minimum 2‰ offset between end member oils (SwalwellC – Swalwell 1312) for all gasoline range compounds. Two subgroups also appear to be present, with the Swalwell C and D oils distinctly separated from Swalwell 814 and 1312. The variation within the subgroups is small, as ratios for several compounds exhibit only minor offsets of 0.1-0.5‰.

The Fenn Big Valley samples are the best example of substantial isotopic variability for oils from a common field (Figure 4.10b). Ratios for iC_5 , Benzene, $MCYC_6$ and nC_9 show a 6‰ offset from FennBV922 to other oils. Overall, there is little isotopic similarity between any of the 4 samples, except for minor variations of 1-2‰ for C_5 and C_6 compounds of FennBV, FennBV103 and Lousana. The differences are

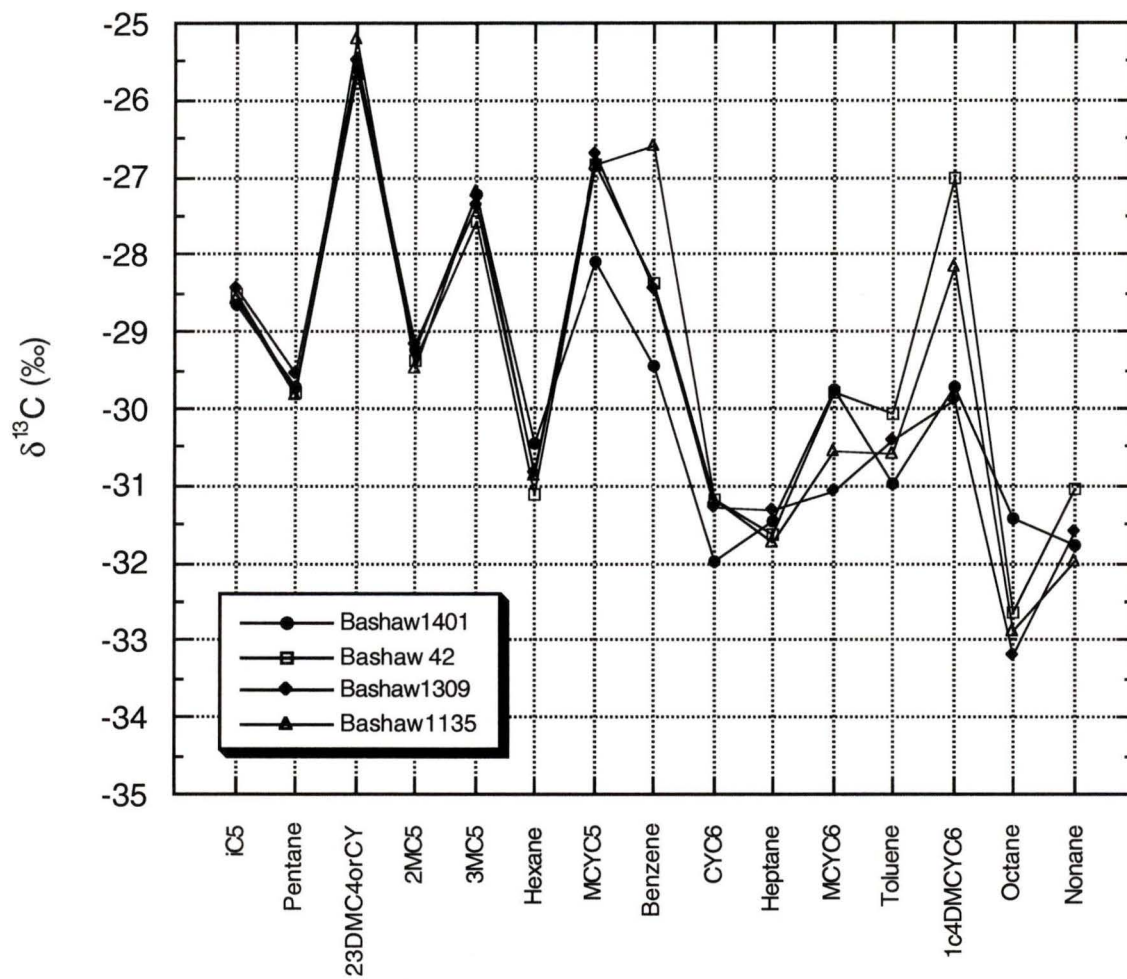


Figure 4.9 Comparison of the isotopograms of 4 Bashaw oils illustrating their similar isotopic composition. Note that some compounds (Benzene, 1c4DMCYC6) show poor reproducibility (>1‰) even for oils from the same field.

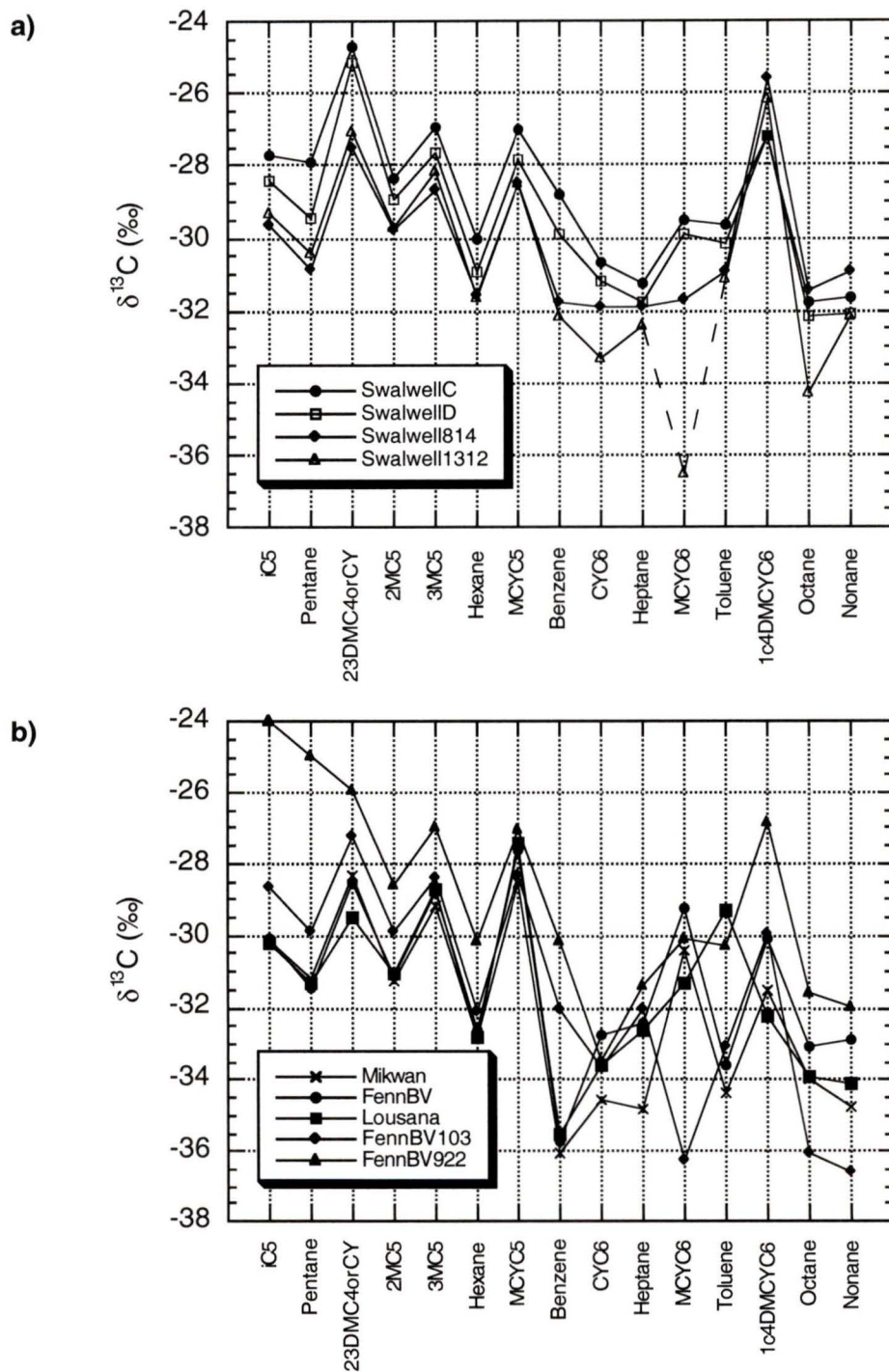


Figure 4.10 Isotopograms for a) Swalwell and b) Fenn Big Valley oils showing non-homogenous isotopic composition between samples. Mikwan and Lousana oils are included with Fenn Big Valley samples as they are often considered to be in the same field.

attributed to oils being sourced from different facies or from Duvernay sediments of different maturities, with varying degrees of influence from localized Nisku source rocks (M. Fowler, Pers. Comm.). Reef structures in this area are also distinct and separate and it is unclear if there is any communication between them through underlying strata.

Hierarchical Cluster Analysis

For statistical analysis of the stable isotope data, a data set including replicate analyses of the 27 individual oils was analyzed. All 15 compounds are included as variables at the beginning of the analysis, and compounds that are characterized by low reproducibility are removed sequentially to determine what effect this has on the resulting correlations.

The most important feature to recognize in Figure 4.11 is the pairing of replicate runs for each oil. This must be expected, and is an important confirmation of analytical reproducibility. Oils that do not meet this requirement (Chigwell, Bashaw 1309, Bashaw42, Lousana) illustrate the need to remove compounds with low reproducibility to ensure that multiple analyses of the same oil will cluster together and allow us to reliably match carbon isotope signatures.

After examination of the raw data, I removed Nonane, 1c4DMCYC6, and 23DMC4 as variables from the cluster analysis. This was because $\delta^{13}\text{C}$ ratios for these compounds exhibit poor reproducibilities of up to 2‰ between replicate analyses of the same oil. Also removed were two case analyses of the Lousana oil (Lousana 1 and 4). This was because the other two analyses (Lousana 2 and 3) show the predicted replicate

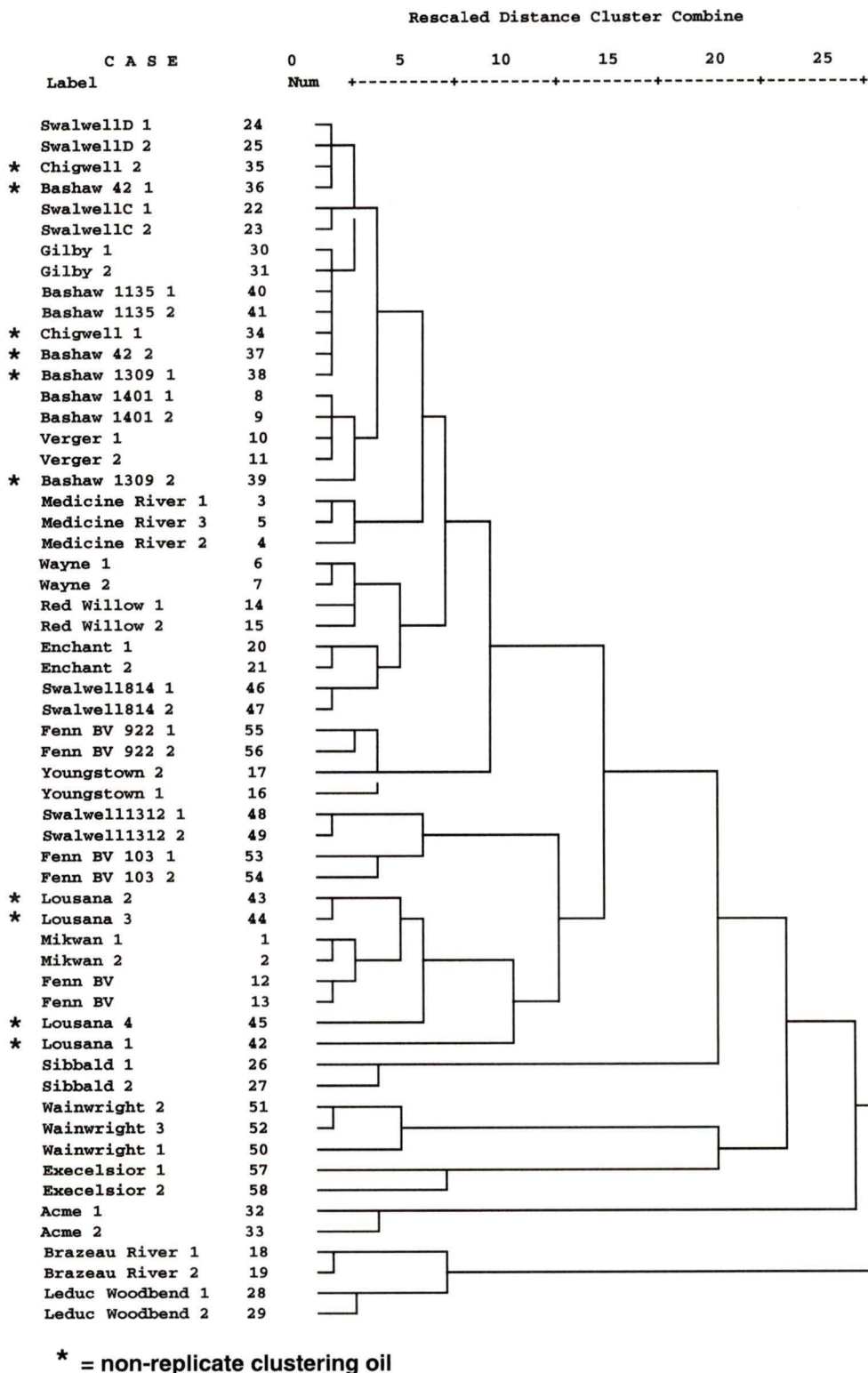


Figure 4.11 Hierarchical cluster analysis dendrogram using average linkage (between groups) method. Note the clustering of replicate analyses for all oils except Chigwell, Bashaw 1309, Bashaw 42, Lousana.

clustering and therefore are a reproducible sample of the oil composition. The resulting dendrogram with this new variable set displays all oils clustering together except for replicates of Youngstown that now show minor variation between analyses. This is highly unusual as the previous dendrogram showed these runs clustering together, but indicates that minor differences in ratios for certain compounds possess greater weight with the reduced number of variables. Thus, I remove Benzene and Toluene as low concentrations of these compounds in several oils may also lead to inaccurate isotope ratios. This results in a dendrogram showing replicate clustering for all oils (Figure 4.12a).

It is difficult to compare this dendrogram to that from the cluster analyses of molecular abundances. Obviously a much larger number of oils (cases) are being compared, but at the same time a smaller number of variables (compounds) are used. There is also the question of deciding what range of DCC values are indicative of similarity between cases. Due to the greater number of clusters generated, I raised the DCC significance level (1 to 10) from the 1 to 3 range in molecular clustering so as to classify oils in a more manageable number of groups. I settled on the following six divisions:

- Group A: Bashaw1401, Bashaw1309, Bashaw1135, Bashaw42, Chigwell, Acme, SwalwellC, SwalwellD, MedRiv, Gilby (Duvernay)
- Group B: FennBV, Lousana, Mikwan, RedWill, Wayne, Swalwell814, Verger, Enchant (Duvernay-Nisku)
- Group C: Swalwell 1312, FennBV103 (Mixed Duvernay)
- Group D: FennBV922, Youngstown, Excelsior (Duvernay-Biodegraded?)
- Group E: BrazRiv, LeducWood (Duvernay-Altered)
- Group F: Wainwright, Sibbald (Exshaw-Biodegraded)

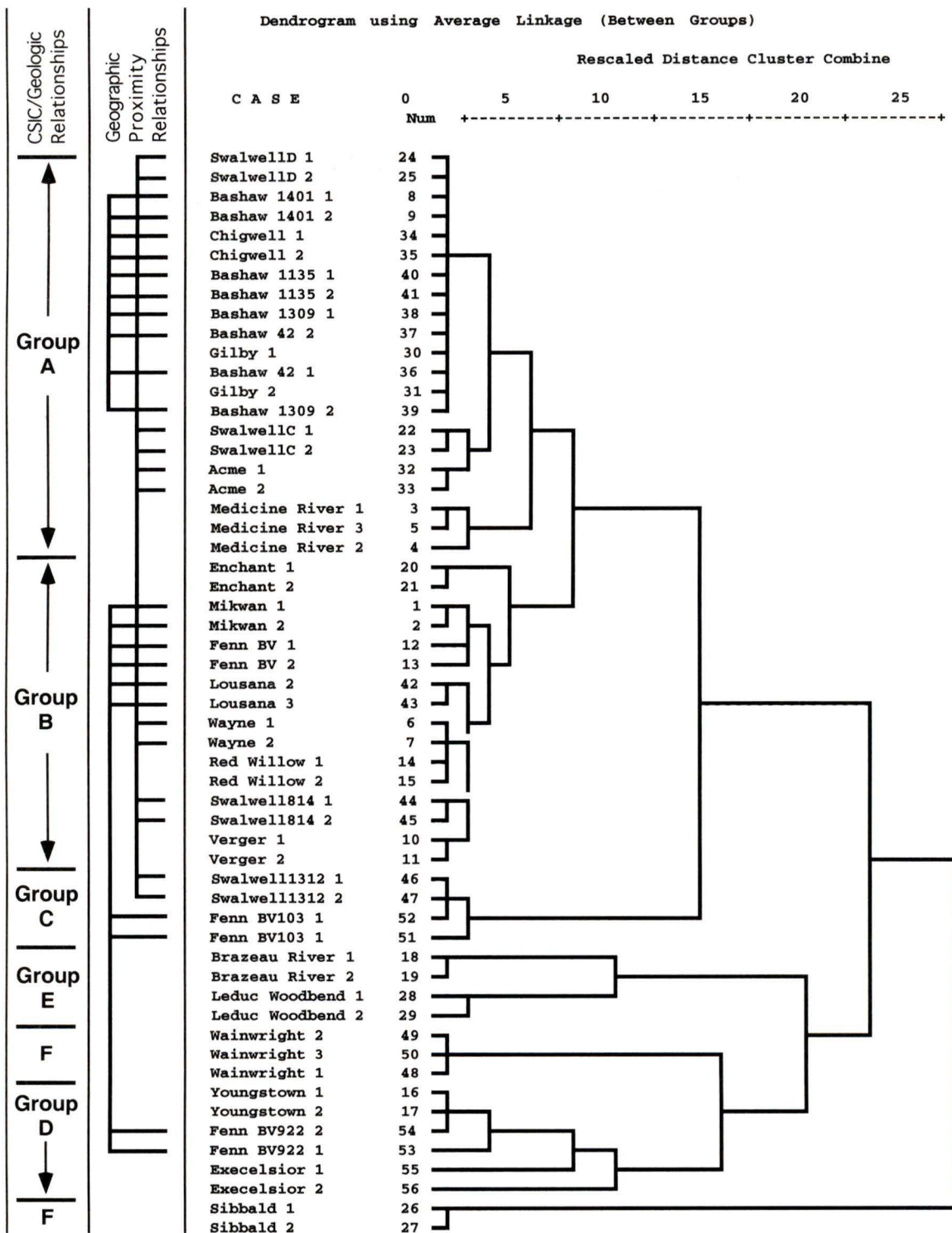


Figure 4.12a Hierarchical cluster analysis dendrogram using average linkage (between groups) method (right side). Note that isotope ratios for 23DMC4, 1c4DMCYC6, Nonane, Benzene and Toluene are not included as variables to ensure clustering of replicate analyses. Expected geographic proximity relationships along with CSIC and inferred geologic relationships are also shown (left side).

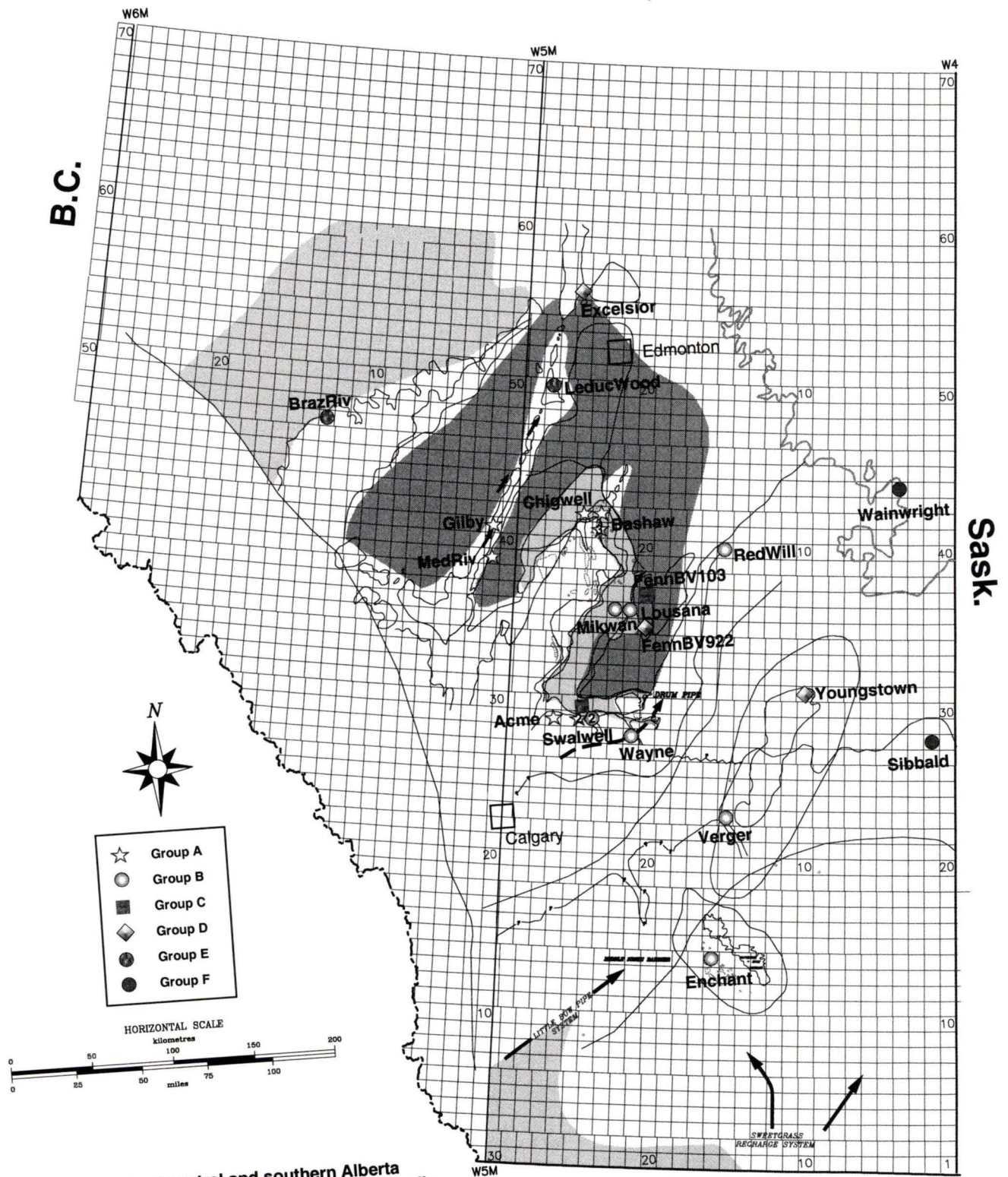


Figure 4.12b Map of central and southern Alberta showing well locations for 27 WCSB oils. Groups are based on correlation of stable isotope ratios of individual gasoline range compounds.

The suspected source rock for each group is listed in brackets, along with any secondary alteration effects that may aid in characterizing each group. Each group will be discussed separately in the next section. These groupings are based on results of the statistical cluster analysis, along with proposed geologic relationships between samples.

Correlations expected based on the geographic proximity of samples to each other are also shown in Figure 4.12a.

Examination of Figure 4.12b shows the location of all the wells along with their new classifications. For those oils common to both molecular and isotopic cluster analysis, few of those original groupings are preserved. SwalwellC and SwalwellD now group with Bashaw oils, while Wayne and Enchant now correlate to FennBV, Mikwan, RedWill and Verger. Other samples such as BrazRiv and Youngstown now belong to smaller more select groups. The only oil to consistently show distinct similarity from all others is the Sibbald sample, taken from the Nisku carbonate shelf in East Central Alberta.

Oil-Oil/Oil-Source Correlations

Group A oils all exhibit high similarity to each other, with the MedRiv, Acme, and SwalwellC samples forming smaller clusters offset from the main group. This similarity is also evident when comparing their isotopic compositions shown in Figure 4.13. Most of these oils are attributed to a mid maturity Duvernay source, encompassing an area covering most of the BRC and parts of the RMT. The MedRiv sample is an unlikely

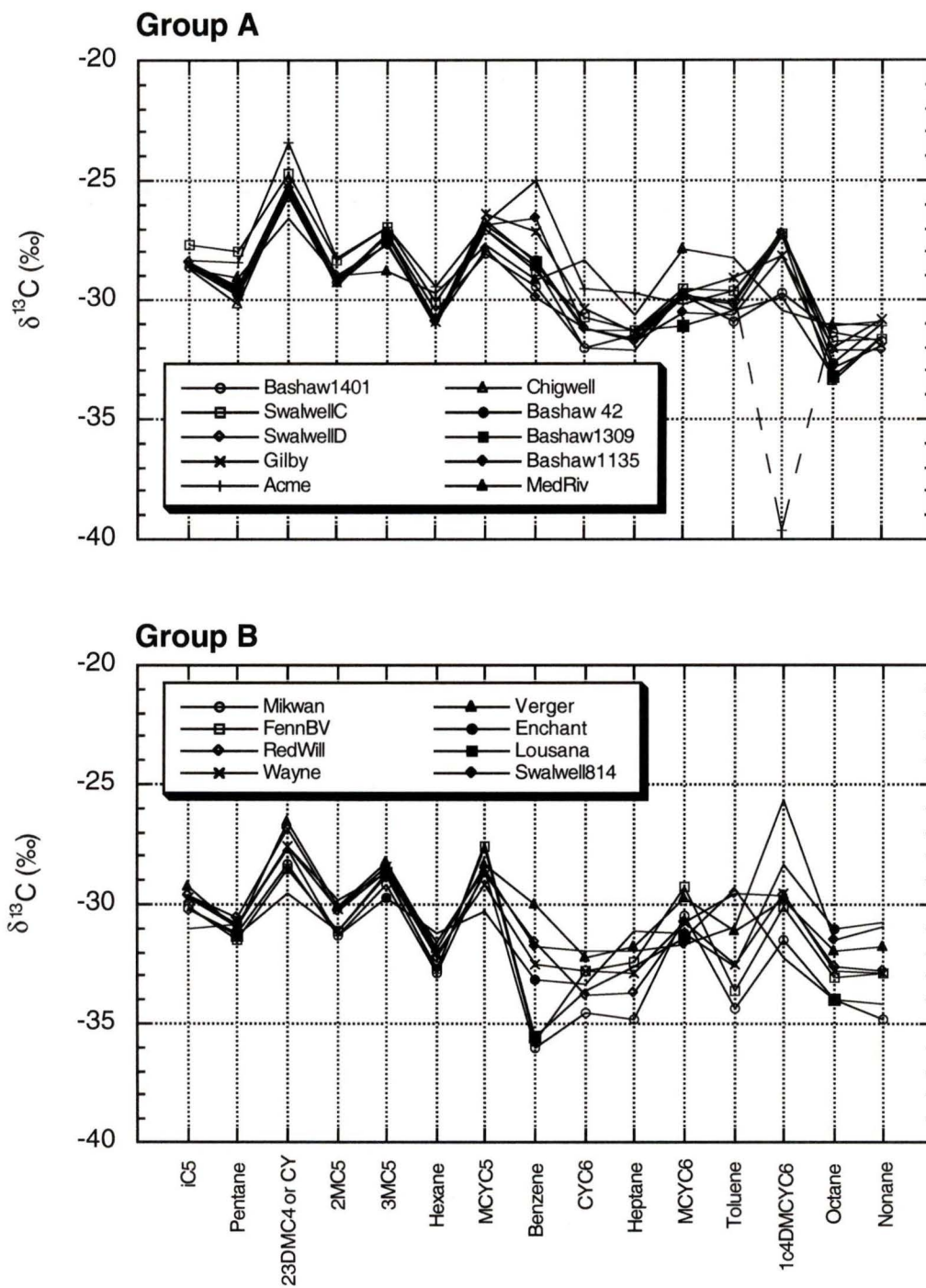


Figure 4.13 Isotopograms for Group A and B oils displaying a high degree of similarity in isotopic composition.

member of the group, given that it is taken from Mississippian age strata (Pekisko Fm.) and relatively isolated from Devonian strata below. If this oil is genetically related to others in the group it is likely due to a separate generation event rather than long distance migration. The suspected source rock for this oil is the Mississippian Exshaw Shale (Whiticar and Snowdon, 1998). The Gilby sample is from the same area as MedRiv but is located on the RMT and is probably sourced from mature Duvernay strata located near the reef trend. The Bashaw and Chigwell samples would be expected to group together given their close geographic proximity, along with the Acme and 2 Swalwell oils. It is reasonable to assume that all 4 Swalwell oils would group together, but a closer examination of the area shows that the reef facies containing the Nisku C and D pools is trapped and separated from the A pool by a north-south channel cutting through the reef and filled with shallow water evaporites (Hunter, 1996). Overall, group A and B oils display similar isotopic compositions, but group A oils are more likely from a slightly more mature facies of the Duvernay. This may be shown by a 1 to 2‰ enrichment in ^{13}C for all gasoline range compounds in these samples versus group B oils. This maturity effect may also be expressed in $\delta^{13}\text{C}$ ratios for HMW hydrocarbons.

Group B oils span a large area in the East Shale Basin extending into southern Alberta between T15-40W4. I classify these oils as having a low maturity Duvernay source, with a substantial Nisku source overprint (Figure 4.13). Southern Alberta oils such as Enchant are thought to be generated entirely from Nisku source beds (see Appendix for details). Mikwan is also attributed to a localized Nisku source, while Lousana, FennBV and RedWill are classified as low maturity Duvernay (M. Fowler, Pers. Comm.). This is surprising as other samples analyzed from the Lousana field more

closely reflect a Nisku rather than Duvernay source (Whiticar and Snowdon, 1998). In the area of Fenn Big Valley, several isolated Nisku reef structures provide excellent reservoirs for oil accumulation, but mapping/interpreting them involves using a layered model as reservoir heterogeneity is caused by lateral and vertical changes in sedimentary facies (Dolph, 1996?). Therefore, communication between reservoirs may be limited, resulting in separate sources for different reservoirs. If Nisku source rocks are responsible for contributing partially or completely to some of these oils, it is possible that this isotopic signature is masked by that produced from the Duvernay. It is tempting to lump group A and B oils into one large cluster, but significant facies variations of the Duvernay and Nisku throughout central Alberta dictates a more cautious approach. In order to definitively classify oils between the two sources, other parameters (e.g. biomarkers) should be examined in conjunction with gasoline range analyses.

Swalwell1312 and FennBV103 show an equally poor statistical correlation with group A and B oils. I classify them as a separate group (C) and propose a mixed Duvernay facies source. The isotopic signature is similar to either group A or B oils, but the $\delta^{13}\text{C}$ ratios appear to be intermediate values between the two groups (Figure 4.14). This could represent mixing of oils generated from low and high maturity Duvernay facies, as is thought to occur in the Swalwell area (M. Fowler, Pers. Comm.).

Group D oils are all classified as Duvernay sourced, but appear to have been subject to some degree of secondary alteration (Figure 4.14). This is evidenced by GC traces that show extremely low concentrations of gasoline range compounds. This effect may be caused by biodegradation resulting in loss of straight chain or branched alkanes, but more likely by evaporation due to improper sample handling. There is also a significant

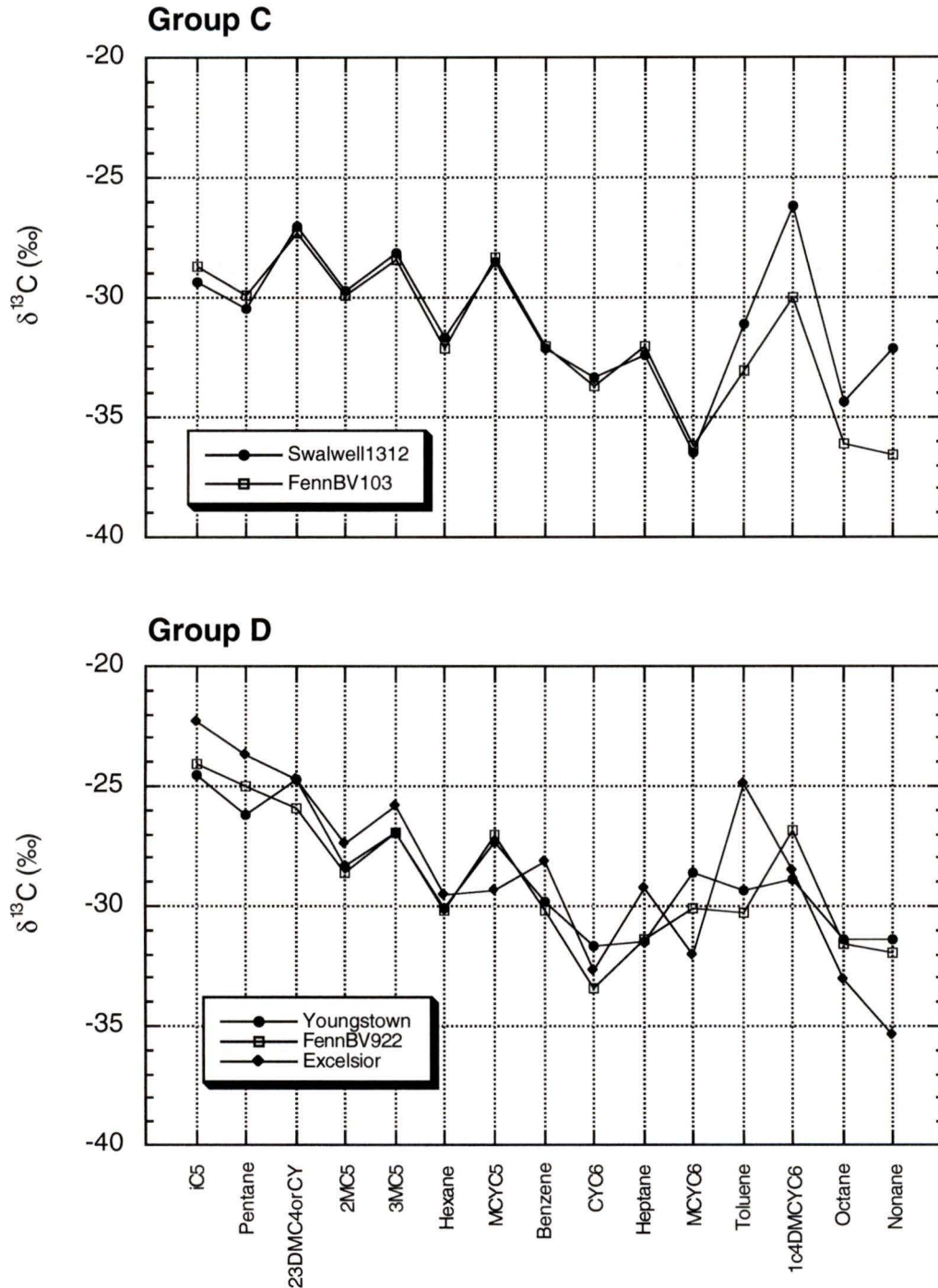


Figure 4.14 Isotopograms for Group C and D oils. Group C is characterized by signatures similar to those of Groups A and B. Group D shows significant enrichment in ^{13}C for $i\text{C}_5$ and $n\text{C}_5$ relative to other compounds in the C_{6-9} range.

enrichment in ^{13}C is observed for iC5 and nC5 compared to C₆₋₉ compounds, further suggesting that evaporation may have occurred. The samples are unrelated with respect to geographic and geologic setting. Further experiments are required to confirm that biodegradation or evaporation does not affect the $\delta^{13}\text{C}$ ratios of gasoline range compounds (Murphy, 1995).

In the case of Group E oils, both the Brazeau River and Leduc Woodbend samples are Duvernay sourced oils that have definitely undergone some form of secondary alteration, (Figure 4.15). As discussed earlier, some Brazeau River samples have undergone TSR and this may result in significant changes to the molecular and isotopic composition of an oil. Manzano et al. (1997) reported an increase in the $\delta^{13}\text{C}$ ratio of the saturate fraction in Brazeau River oils with increasing TSR, along with a decrease in the overall saturate/aromatic ratio, increase in abundance of organo-sulphur compounds, and $\delta^{34}\text{S}$ values approaching those for anhydrite of the Nisku formation in that area. However, Manzano et al. (1997) did not rule out the possibility that the ^{13}C enrichment could be due to thermal maturity effects, illustrating the limitation of measuring isotope ratios on bulk oil fractions. In a CSIC study of 6 Brazeau River oils/condensates, Whiticar and Snowdon (1998) showed that TSR affected $\delta^{13}\text{C}$ values of several individual gasoline range compounds. A ^{13}C enrichment shifted ratios up to 10‰ relative to samples less or unaffected by TSR. Isotope signatures for the latter group of samples were more representative of Nisku oils/condensates. The shift was apparent for the entire C₅ to C₈ range, but the enrichment was greatest in lower carbon number compounds in condensate samples (Whiticar and Snowdon, 1998). Our sample was taken from the Nisku Q pool, considered a low maturity sample in Manzano et al. (1997) (Figure 10 in Manzano et al.,

1997). Therefore, while it is not definitive if TSR resulted in a ^{13}C enrichment for this sample, it is a reasonable assumption because its $\delta^{13}\text{C}$ ratios are among the heaviest for any oils in the current study. The Leduc Woodbend sample also shows significant ^{13}C enrichment for several compounds, and this may be because the sample was damaged (i.e. dropped) and suffered extreme evaporation prior to arrival at our laboratory for analysis (M. Fowler, Pers. Comm.). If this is true, and you remove the sample from the cluster analysis entirely so that it does not bias the results, the only change observed in the dendrogram is the BrazRiv oil showing no correlation with any of the other oils.

The Sibbald and Wainwright oils show little or no similarity to each other nor any of the other samples in the study (Figure 4.15). There is a minor statistical correlation between Wainwright and Group D oils, but the DCC value is >15 so they are not grouped together. Both Sibbald and Wainwright are attributed to a Mississippian Exshaw shale source rock, and so we group them together based on this fact alone. These oils have also have undergone some degree of biodegradation, as evidenced by extremely low concentrations of straight chain and branched alkanes.

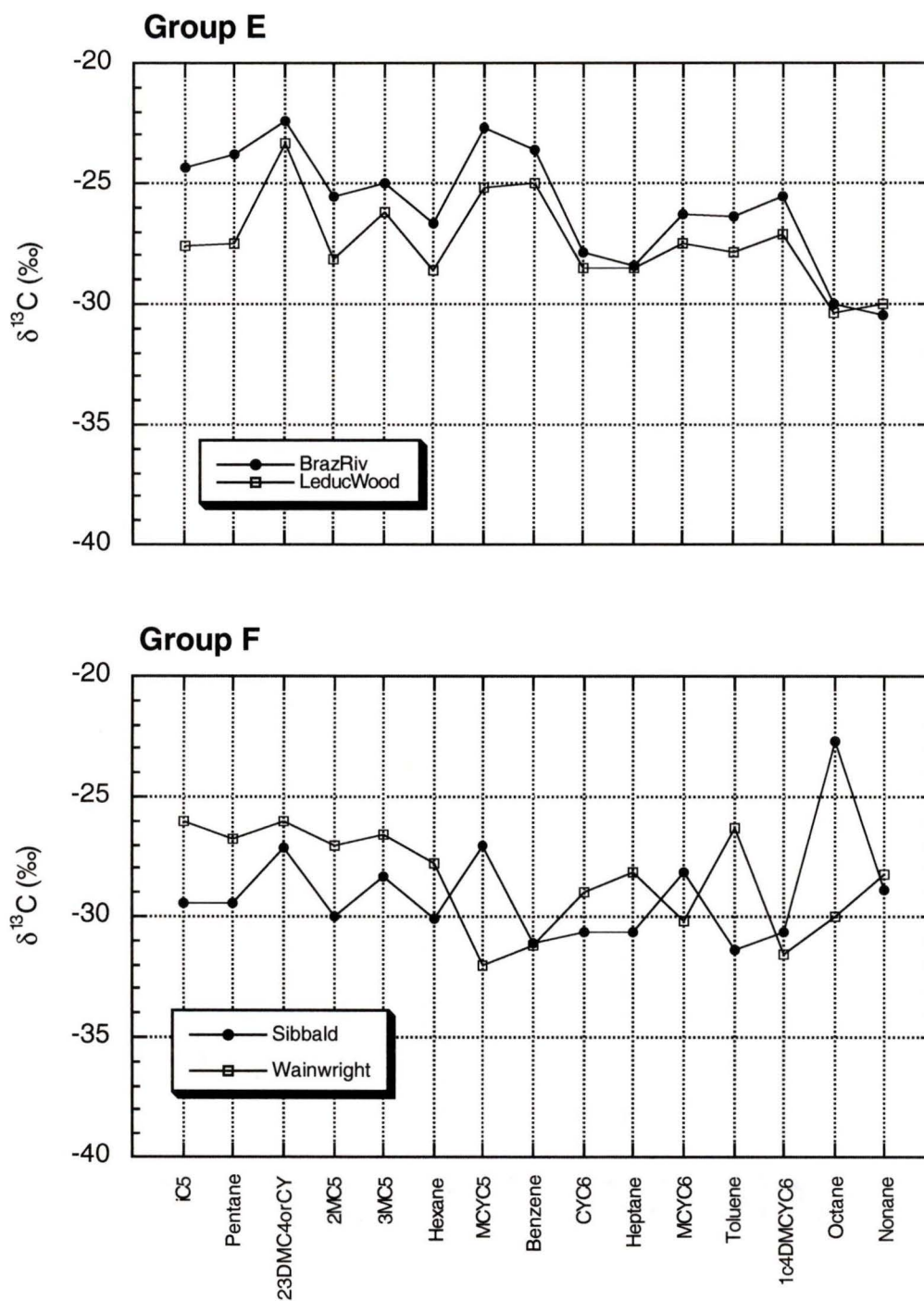


Figure 4.15 Isotopograms for Group E and F oils. Group E is characterized significant enrichment in ^{13}C for all compounds especially the BrazRiv sample that may have undergone TSR. Group F oils display unique signatures and do not correlate well with each other or any of the other oils in this study.

Compositional Relationships

It is often useful to look for systematic isotope ratio differences, both between oils and individual gasoline range compounds. Whiticar and Snowdon (1998) observed several such differences, both within and between homologous series in the gasoline range fractions. They found differences were most pronounced for highly branched dimethylalkanes, and less so for other straight chain, branched, cyclic aliphatics or aromatic compounds. LMW compounds were depleted in ^{13}C relative to heavier compounds. Whiticar and Snowdon (1998) add that evidence of systematic isotopic distributions among isomers of the same carbon number suggests that the formation of gasoline range hydrocarbons is linked to the isotopic composition of the precursor material, not by thermodynamic processes as originally thought.

Figure 4.16a shows the $\delta^{13}\text{C}$ ratios of n-alkanes from nC₅-nC₉ for all 58 analyses in the study. An enrichment in ^{13}C is observed for n-pentane versus other n-alkanes in most oils, with Sibbald the lone exception. The difference in ratios between the different n-alkanes ($\Delta\delta^{13}\text{C}_{x-y}$) indicates that this enrichment is relatively consistent for group A, B, and C oils ($\delta^{13}\text{C}_5 - \delta^{13}\text{C}_6 \sim 1\text{-}2\text{‰}$, $\delta^{13}\text{C}_5 - \delta^{13}\text{C}_7 \sim 2\text{-}3\text{‰}$, $\delta^{13}\text{C}_5 - \delta^{13}\text{C}_8 \sim 3\text{-}4\text{‰}$, $\delta^{13}\text{C}_5 - \delta^{13}\text{C}_9 \sim 2\text{-}4\text{‰}$) (Figure 4.16b). However, group D oils show a significant enrichment between 5 to 14‰ for n-nonane relative to n-pentane (Excelsior). Sibbald shows a 7‰ depletion in ^{13}C for n-octane versus n-pentane, but this may be the result of an incorrect $\delta^{13}\text{C}$ calculation for n-octane due to its low concentration in this oil. The consistent offset between n-alkanes for Groups A, B, and C indicates a common source for these oils.

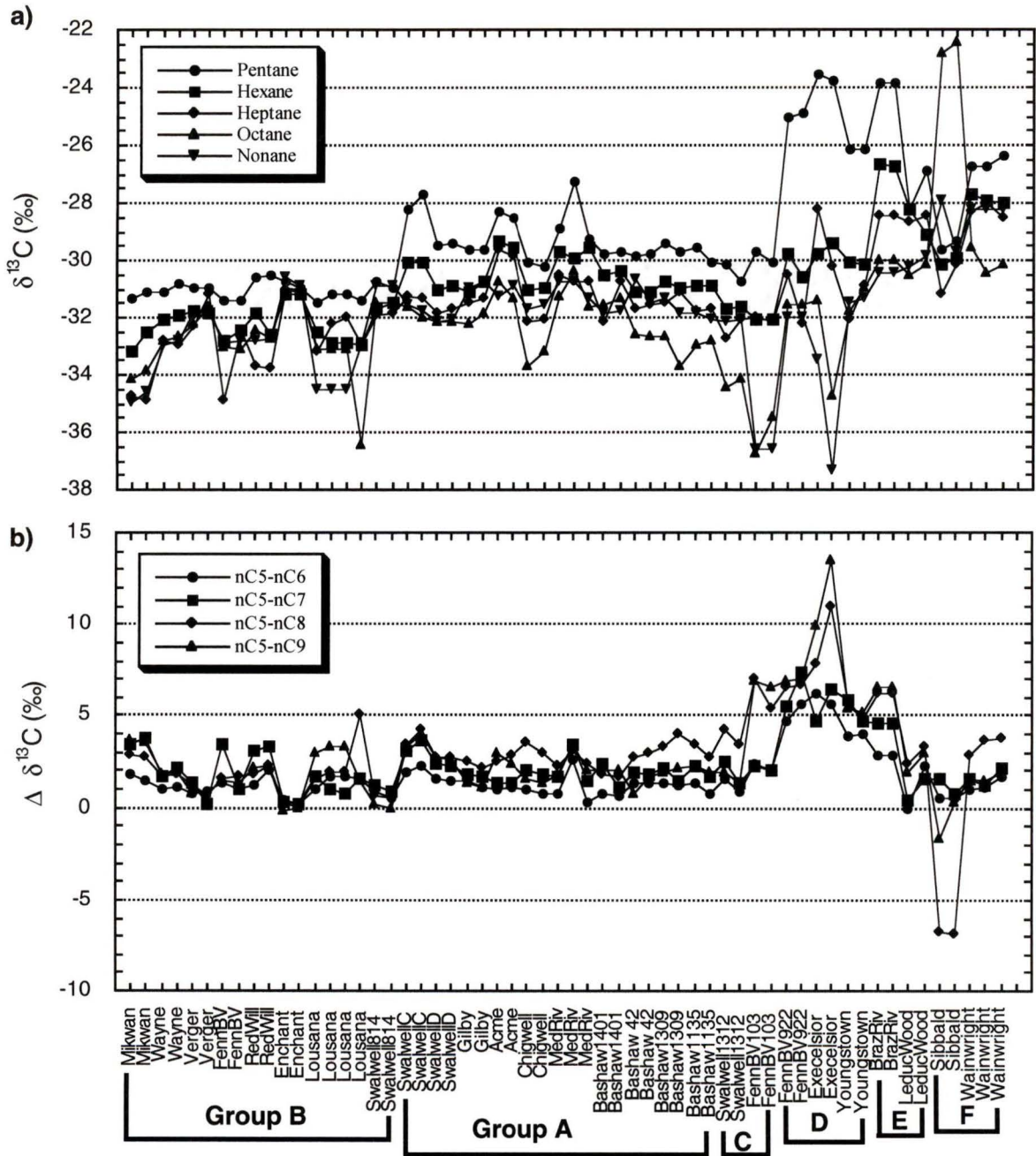


Figure 4.16 a) Comparison of carbon isotope ratios for C₅-C₉ n-alkanes between the oil sample suite. b) The magnitude of ¹³C enrichment for nC5 (pentane) versus other n-alkanes is quite consistent for Group A, B, C oils.

To determine if the offset between n-alkanes applies to other non-straight chain hydrocarbons, ratios of individual compounds with either similar carbon number or chemical structure are compared in Figure 4.17-4.18. For most oils, C₅ compounds show a depletion in ¹³C for nC₅ versus iC₅, however the magnitude of depletion is inconsistent between oil groups (Figure 4.17a). A similar pattern is observed for C₆ compounds, with 23DMC4 consistently enriched in ¹³C (up to 8‰) relative to benzene, hexane, CYC6, 2MC5, 3MC5, MCYC5 (Figure 4.17b). It is interesting to note that the offset between compounds is most irregular for groups D, E and F, each comprised of oils that may be subject to secondary alteration. The Brazeau River sample that may be affected by TSR is distinguished by significant ¹³C enrichment for all gasoline range compounds relative to other oils. However, TSR appears to only have significant effect on δ¹³C ratios of specific light hydrocarbons dependant upon the compound class (Rooney, 1995). Comparison of ratios for C₇ compounds shows that n-heptane is generally depleted in ¹³C relative to MCYC6 and Toluene, however the depletion is inconsistent both within and between oil groups (Figure 4.17c).

Branched or iso-alkanes also exhibit a isotopic offset between compounds, with a majority of oils having 23DMC4 most enriched in ¹³C followed in order by 3MC5, iC₅, and 2MC5 (Figure 4.18a). If these carbon isotope distributions are based on thermodynamic reactions, one would not expect a systematic isotope difference between two isomers such as 2MC5 and 3MC5 (Whiticar and Snowdon, 1998). If this offset were due to maturity, we would expect the lower molecular weight compound (iC₅) to be more enriched in ¹³C than 3MC5. Since neither case is prevalent, this implies that some isotopic control is exerted by the precursor material that generated the oil. This topic will

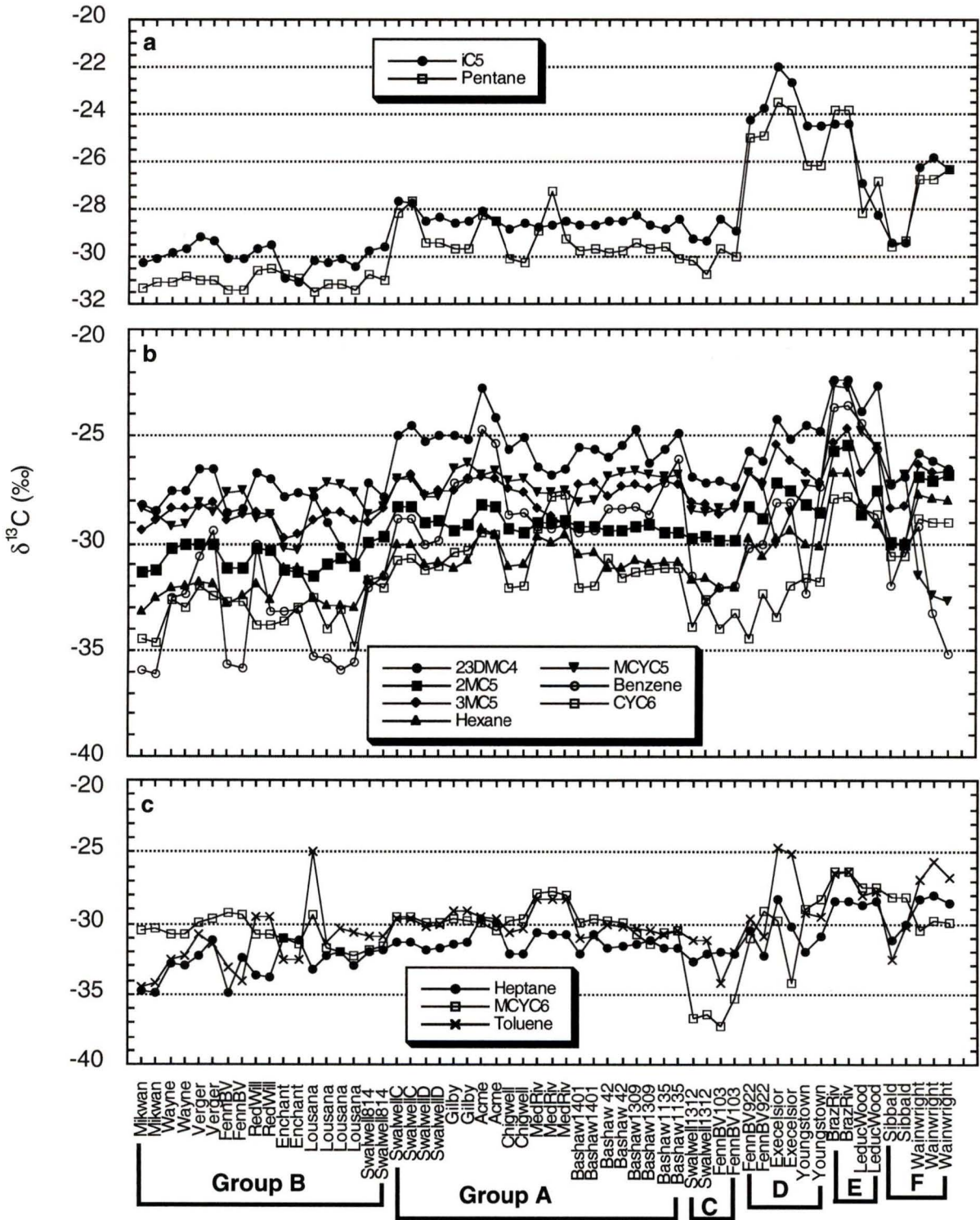


Figure 4.17 Comparison of carbon isotope ratios for specific compounds between the oil sample suite. In some cases, there are clear and consistent isotopic shifts observed between compounds with similar carbon numbers

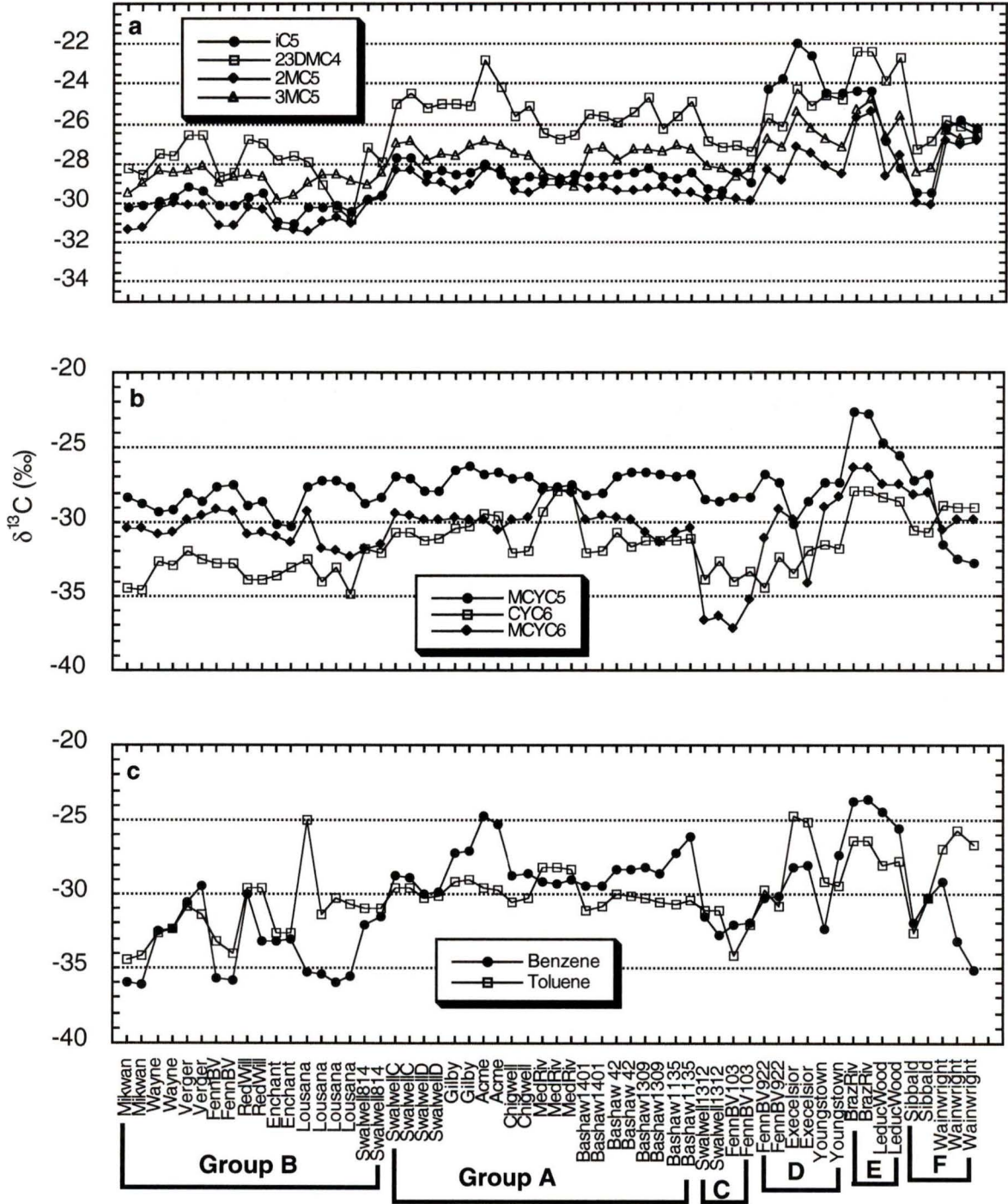


Figure 4.18 Comparison of carbon isotope ratios for specific compounds between the oil sample suite. In some cases, there are clear and consistent isotopic shifts observed between compounds with similar chemical structure.

be discussed more in the next section. The offset between iso-alkanes is reasonably consistent for most oils (except group F), perhaps indicative of a common source. However, this offset is not apparent for cyclic or aromatic compounds (Figure 4.18b,c). High variability is observed between ratios of MCYC5 and MCYC6 (2-8‰) in addition to Benzene and Toluene (0-10‰) both within and between oil groups.

Causal relationships between hydrocarbons can also be shown by direct comparison of isotope ratios for individual compounds with similar carbon number or chemical structure. Figures 4.19-4.21 show linear regressions for several compound pairs, and comparison of n-alkanes indicates that for most oils a linear relationship exists ($r^2 = 0.5-0.8$, Figure 4.19a-d). It is interesting to note that this correlation between $\delta^{13}\text{C}$ ratios of n-alkanes is limited to pairs separated by only 1 carbon atom in length (e.g. nC5 vs. nC6; nC6 vs. nC7). However, more useful information can be derived from the isotopic separation between n-alkanes (first noted in Figure 4.16b). This relationship (Figure 4.19e) can distinguish oils of a common source, because homologous oils may be expected to have a systematic offset between n-alkanes based on generation from similar kerogen types and thermal history.

Similar to results of molecular abundance data, a linear correlation is evident between ratios of straight chain and branched alkanes (Figure 4.20a-d). This relationship was not previously expressed for C₅ compounds (iC₅ – nC₅, Figure 4.20a), but as mentioned these compounds are highly susceptible to evaporative losses that may have affected their molecular abundance. This illustrates the more robust nature of isotope ratios versus molecular concentrations. Methylpentanes (2MC5 and 3MC5) also track well together (Figure 4.20d), similar to results of dimethylhexanes reported by Whiticar and Snowdon

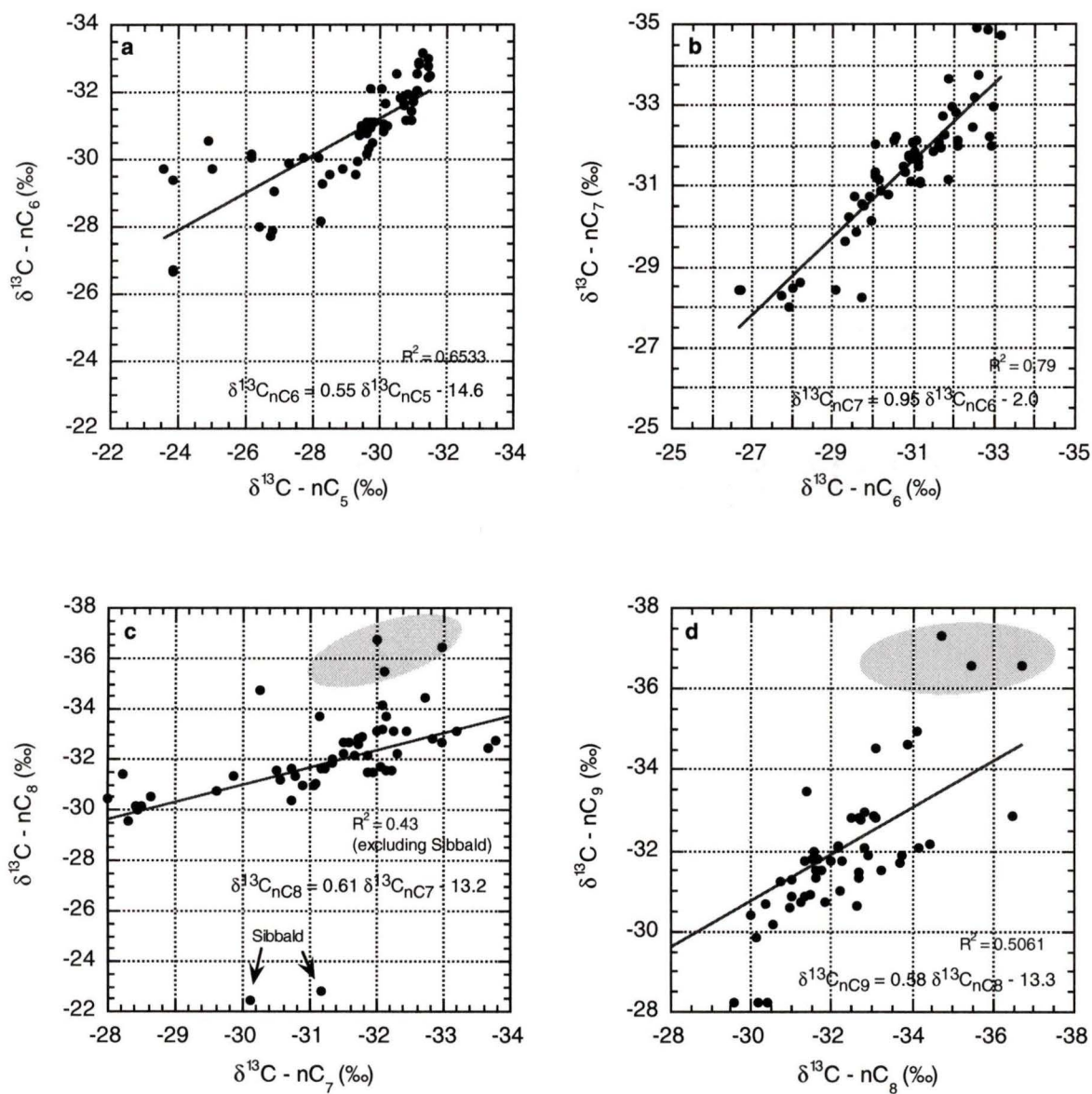


Figure 4.19 Cross-plots of the isotopic ratios for individual gasoline range compounds illustrating interdependencies and relationships. For explanation of shaded areas, refer to page 131.

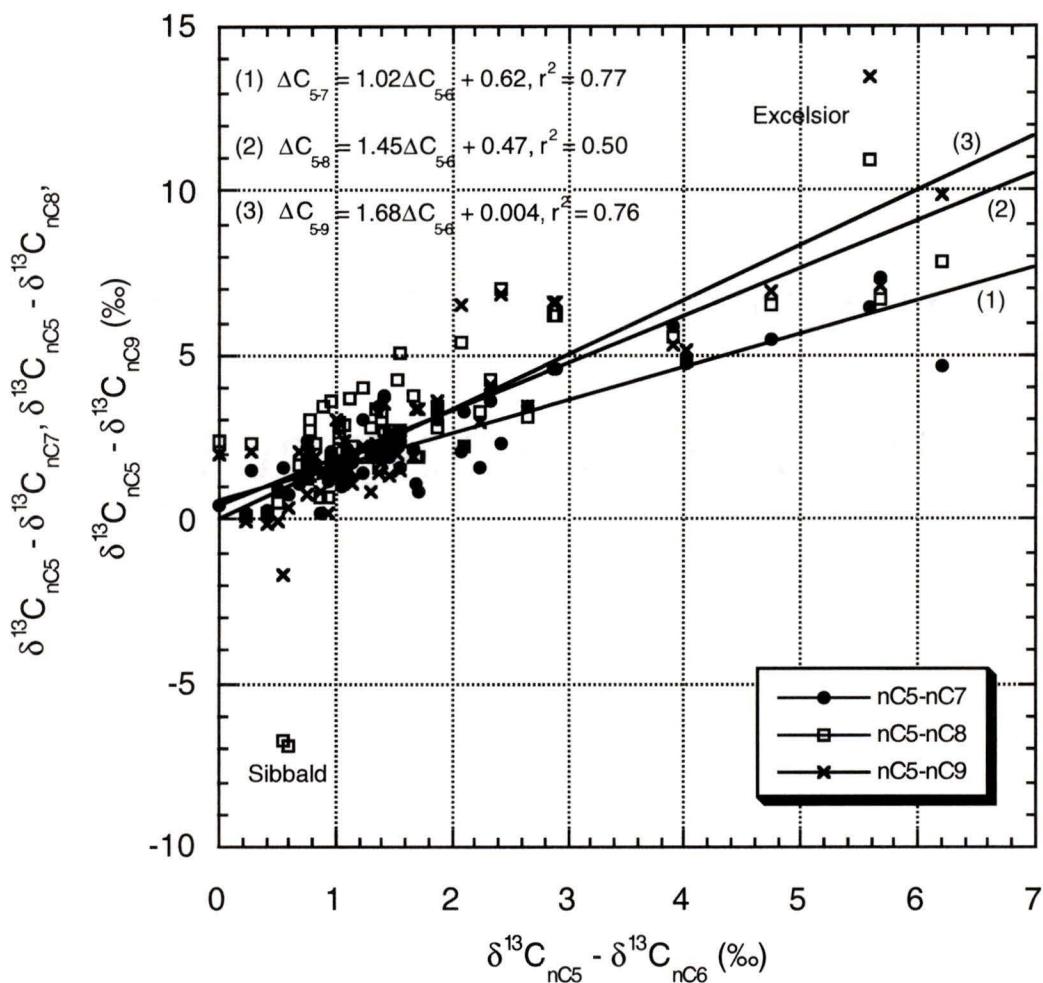


Figure 4.19e Systematic carbon isotope offset between C₅, C₆, C₇, C₈ and C₉ n-alkanes. There are good linear relationships between the isotopic ratios of the n-alkane pairs except for Excelsior and Sibbald oils.

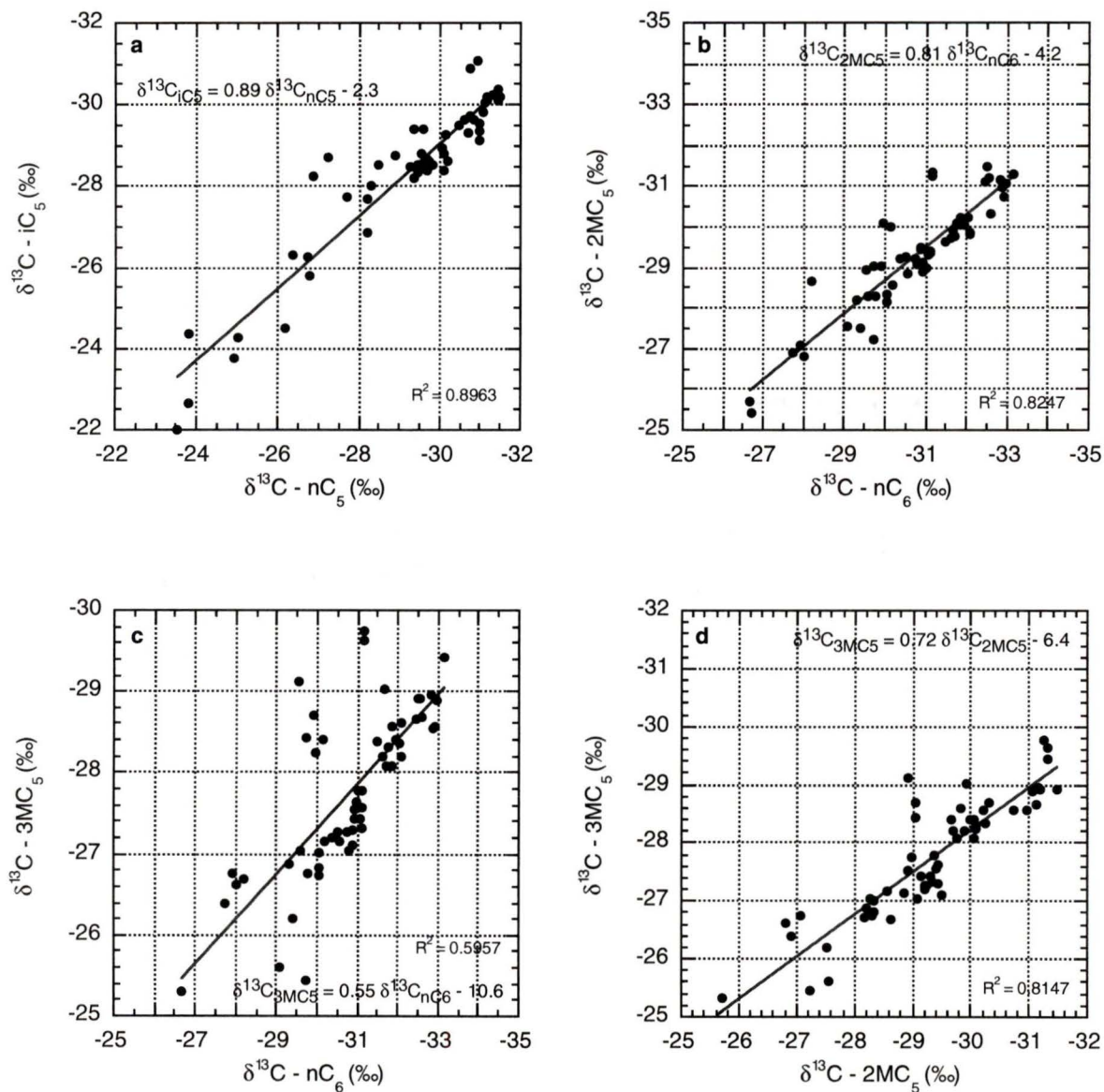


Figure 4.20 Cross-plots of the isotopic ratios for individual gasoline range compounds illustrating interdependencies and relationships

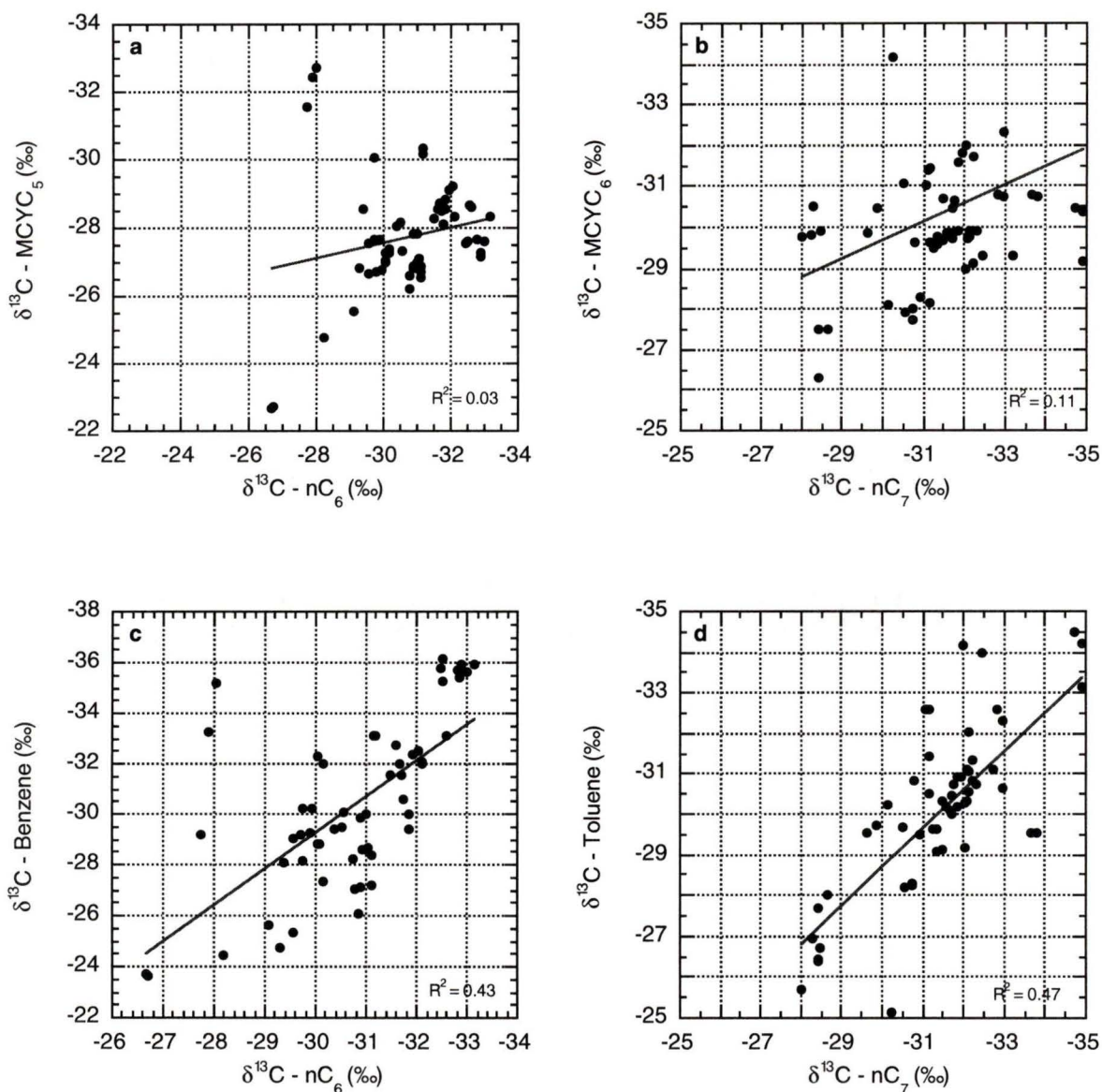


Figure 4.21 Cross-plots of the isotopic ratios for individual gasoline range compounds illustrating interdependencies and relationships

(1998). The slope of the regression line for iC5-nC5 approaches a 1:1 relationship, while those for the other pairs are offset by up to 10‰.

Contrary to previous molecular analyses, a poor correlation appears to exist between $\delta^{13}\text{C}$ ratios of n-alkanes and methyl-cyclic compounds (Figure 4.21a,b). This is surprising based on reaction series proposed by Mango (1990b) for the generation of methylcyclohexanes from straight-chain precursors (discussed earlier). The correlation of ratios between n-hexane and CYC6 is similar to molecular results ($r^2 = 0.64$), although $\delta^{13}\text{C}_{\text{CYC6}}$ does not correlate well with other C_6 compounds like benzene ($r^2 = 0.40$). The relationship between ratios of the aromatics and same carbon number n-alkane first observed by Murphy (1995) is also not clearly evident with these oils (Figure 4.21c,d). It is highly probable that poor reproducibility resulting from co-elution or low concentrations are responsible for some of the scatter observed with this data set (see below).

Discussion

The cause(s) for the relationships or lack there of between gasoline range compounds are unclear. In establishing what determines the isotope ratios of individual compounds, it is necessary to understand what processes are responsible for their generation. Work by Mango (1990a,b, 1994, 1997) has shown invariant ratios in concentrations of isoheptanes $[(2\text{MC6} + 23\text{DMC5})] / [(3\text{MC6} + 2,4\text{DMC5})]$ for homologous oils based on a steady-state kinetic reaction scheme whereby various C_7 hydrocarbons are derived from specific precursors. Mango (1990b) notes that these ratios are significantly removed

from values predicted by thermodynamic reaction series. If one applies Mango's theories on an isotopic level, then straight chain precursors should produce branched or cyclic alkanes with similar $\delta^{13}\text{C}$ signatures. I do observe a strong correlation between ratios for straight chain and branched alkanes (Figure 4.20), in addition to that between methylpentanes. However, the weaker correlation between cyclic and straight chain hydrocarbons implies that there may be other variables to consider.

The most likely explanation is that source rock or precursor organic matter composition is the other dominant influence on stable isotope ratios. For example, differences in bulk $\delta^{13}\text{C}$ ratios between oils sourced from marine versus terrestrially derived kerogens are well documented (e.g. Hunt, 1996). Facies variations (e.g. shallow vs. deep water) between similar source rocks could also account for some variability seen in $\delta^{13}\text{C}$ signatures. Mango (1990b) noted that his invariance ratios are kerogen-specific, and each source generates its own ratio. During light hydrocarbon generation, the kerogen's structure impresses kinetic control over the competing kinetic pathways or reactions (Mango, 1997b), therefore each source may be expected to imprint its own molecular and isotopic ratios. Mango (1990b) adds that analyses on light hydrocarbons extracted from source rocks and those generated by thermal cracking experiments of HMW oil fractions show invariant ratios of isoheptanes suggesting that light hydrocarbons may be generated within the kerogen itself prior to petroleum expulsion. This would further indicate that the isotopic signature of the structural precursor is imparted into the light hydrocarbons. However, Mango (1990b) questions the validity of the oil simulations, based on a lack of active catalysts to drive the reactions. Mango (1997b) adds that although several gasoline range compounds can be derived from

biological precursors, it is doubtful that the amounts of these precursors in sediments can explain the concentrations of isoalkanes and cycloalkanes seen in oils. In order to determine what effect precursor material has on the isotopic composition of the gasoline range, it may be necessary to analyze potential source rock extracts to try and determine their light hydrocarbon compositions for comparison. This is a similar approach to Odden et al. (1998), however, these extracts do not often yield sufficient concentrations of gasoline range hydrocarbons for analysis. Thus a new approach may have to be developed.

A final possibility is that $\delta^{13}\text{C}$ ratios for specific gasoline range compounds in some of the oils may be imprecise due to an analytical oversight. At the time samples were analyzed, the CF-IRMS system was operated maintaining a low level of free oxygen (O_2) in the microcombustion oven ($\ll 0.1\text{ V}$) to minimize the amount of O_2 reaching the IRMS source. It was thought that excess O_2 levels ($>0.1\text{ V}$) would oxidize the tungsten filament thereby causing it to deteriorate at an accelerated rate. In discussions with other laboratories doing CF-IRMS analyses, it was learned that the source filament can be operated at higher oxygen levels ($0.2 - 0.4\text{ V}$) without significant risk of damage. Therefore, it is possible that while operating under the pre-existing low O_2 conditions, there was insufficient oxygen present in the system to properly combust some analytes to CO_2 producing false $\delta^{13}\text{C}$ ratios. The Cu/Pt wires in the microcombustion oven release free oxygen at a rate dependant on temperature and amount of oxygen sorbed on the wires prior to each analysis. As we did not re-oxidize the oven in between analyses, the oxygen concentration would certainly diminish both over the course of multiple analyses and likely during an individual run. Therefore, as gasoline range compounds sequentially

elute off the GC column, the C₇-C₉ analytes eluting in the largest concentrations and longest retention times may not react with enough O₂ to undergo complete combustion. It is less likely that C₅-C₆ compounds would be affected as they elute at the beginning of analyses when oxygen levels are highest or have been replenished. Typically these compounds also elute in smaller quantities relative to C₇-C₉ analytes and therefore require less O₂ to undergo complete combustion.

To test this hypothesis, $\delta^{13}\text{C}$ ratios for several gasoline range compounds are compared with their corresponding peak area determined from the CF-IRMS mass 44 trace (Table 4.5, Figure 4.22a-d). Comparison of n-alkanes shows $\delta^{13}\text{C}$ ratios becoming progressively depleted in ^{13}C with increasing peak area (Figure 4.22a). This trend may indeed be a result of high concentrations of nC₇, nC₈ or nC₉ in some oils combusted at insufficient O₂ levels resulting in erroneously low $\delta^{13}\text{C}$ measurements (depleted in ^{13}C). However, I would accept this as a factor for only 4 oils (Wainwright, FennBV103, FennBV922, Excelsior), that show a significant depletion in ^{13}C for $\delta^{13}\text{C}_{\text{nC8}}$ or $\delta^{13}\text{C}_{\text{nC9}}$ (-34 to -37‰) These samples were the last to be analyzed in this suite and therefore were probably run at very low O₂ concentrations. All of these oils also contain extremely high concentrations of heptane, octane or nonane relative to the other gasoline range compounds. This required multiple analyses at different injector split ratios to obtain a merged data set of peak areas and $\delta^{13}\text{C}$ ratios for all the desired analytes. This sometimes resulted in only one measurement of $\delta^{13}\text{C}_{\text{nC9}}$ for some oils (Table 4.3), and is the main reason why nonane is removed as a variable from the hierarchical cluster analysis. If one excludes these erroneous values for $\delta^{13}\text{C}_{\text{nC8}}$ and $\delta^{13}\text{C}_{\text{nC9}}$, then the isotopic composition of n-alkanes appears to be independent of concentration (Figure 4.22a), and is derived from

Table 4.5 Peak Areas of Oils for CSIC Study															
Well Name	iC5	Penta	23DMC	2MC5	3MC5	Hexan	MCYC	Benze	CYC6	Heptan	MCYC	Tolue	1c4D	Octan	Nona
Mikwan 1	7.28	11.71	2.47	8.06	5.22	11.98	13.68	2.58	7.67	12.66	13.55	6.80	2.27	9.94	9.2
Mikwan 2	9.30	15.27	3.25	10.90	7.94	17.09	18.92	3.57	10.74	17.86	19.40	9.82	3.32	14.48	13.24
MedRiv1	1.99	3.18	1.24	3.97	2.54	8.20	4.25	9.37	7.04	16.14	18.02	43.63	2.45	19.25	21.08
MedRiv2	3.82	5.87	2.10	6.65	4.16	13.30	6.66	14.51	11.57	24.49	27.19	64.25	4.06	29.32	31.37
MedRiv3	2.17	3.57	1.36	4.32	2.76	8.96	4.57	10.23	8.02	17.18	19.23	46.41	2.57	20.11	21.93
Wayne 1	12.24	20.79	3.56	11.82	7.43	28.60	14.38	9.66	16.13	34.00	23.25	19.91	2.85	31.72	30.86
Wayne 2	9.85	17.36	3.22	10.85	6.90	26.98	13.82	9.32	15.48	33.73	23.10	19.74	2.86	31.07	28.75
Bashaw 1401 1	12.95	20.91	4.86	16.52	11.97	31.53	17.51	15.58	12.38	31.48	20.87	27.34	3.02	25.05	21.19
Bashaw 1401 2	14.16	22.66	5.18	17.75	12.86	33.77	18.81	16.71	13.26	35.08	22.31	29.20	3.20	26.60	22.63
Verger 1	3.88	5.08	1.52	5.84	4.28	9.41	8.58	0.20	5.26	12.17	12.29	5.82	2.39	11.32	11.63
Verger 2	7.84	11.29	3.00	11.60	9.49	18.75	16.96	0.40	10.13	25.13	23.96	11.33	4.61	22.17	23.22
FennBV1	8.56	14.19	3.27	10.15	7.41	15.19	23.33	1.82	6.37	16.48	16.93	6.27	3.20	13.16	11.42
FennBV2	10.03	16.35	3.73	11.38	9.24	17.73	25.93	2.03	7.05	20.29	18.57	6.74	3.53	14.58	12.98
RedWill1	13.00	11.11	3.56	14.29	11.86	20.38	13.31	0.13	13.42	26.19	22.40	1.29	4.46	23.99	21.54
RedWill2	11.30	9.62	3.11	12.52	10.40	17.00	10.11	0.11	11.88	23.61	20.08	1.17	3.89	22.06	21.35
Youngstown 1	3.59	5.90	1.08	5.34	5.06	9.32	10.35	0.12	8.97	22.98	32.11	7.27	6.79	22.06	18.49
Youngstown 2	3.59	5.90	1.66	8.27	7.83	14.39	15.72	0.19	13.64	37.44	49.10	10.98	11.11	34.23	28.68
BrazRiv1	4.90	2.09	1.12	4.85	3.79	6.51	6.63	0.78	12.41	7.48	13.17	29.25	3.34	15.60	21.35
BrazRiv2	4.90	2.09	0.96	4.08	3.22	5.55	5.64	0.65	10.41	37.37	13.17	24.67	3.34	15.60	21.35
Enchant 1	5.39	12.67	2.46	8.72	7.21	24.58	7.96	4.84	5.40	33.09	9.80	12.91	1.48	32.16	27.04
Enchant 2	5.35	12.74	2.55	8.87	7.37	25.55	8.29	5.20	5.84	34.96	10.23	13.73	1.53	33.52	26.9
SwalwellC 1	3.09	3.55	1.38	5.38	3.34	12.47	7.28	6.40	11.10	24.55	19.91	20.15	2.88	28.37	29.13
SwalwellC 2	2.72	3.10	1.17	4.37	2.85	10.63	6.18	5.41	9.39	20.64	16.74	16.89	2.50	23.69	24.13
SwalwellD 1	6.86	11.23	2.19	8.36	5.40	19.54	9.42	10.03	12.79	26.26	19.64	21.65	2.61	25.54	24.45
SwalwellD 2	7.05	11.50	2.22	8.44	4.73	19.58	9.41	10.16	12.74	25.88	19.46	21.46	2.58	24.97	22.59
Sibbald 1	10.14	6.48	4.92	11.04	14.54	11.19	5.18	0.08	4.52	6.46	9.09	1.64	1.06	2.96	21.45
Sibbald 2	14.53	9.47	7.06	15.66	20.68	15.93	7.20	0.11	6.21	9.62	12.38	2.41	1.75	4.24	14.53
LeducWood1	0.08	0.09	0.17	0.51	0.46	1.25	1.08	0.88	2.26	4.86	5.20	6.07	1.14	7.77	11.8
LeducWood2	0.06	0.07	0.14	0.43	0.40	1.12	0.97	0.82	2.09	4.64	4.91	5.87	1.08	7.49	11.16
Gilby 1	5.36	9.92	2.03	9.16	6.25	17.75	11.52	5.31	8.29	21.69	19.19	10.10	3.52	18.37	16.56
Gilby 2	5.26	9.72	1.97	8.89	6.07	17.16	11.11	5.14	7.97	20.80	18.38	9.75	3.40	17.74	15.86
Acme 1	1.31	2.11	1.08	2.98	2.19	7.45	3.52	12.36	4.75	13.41	7.62	37.91	0.81	15.61	17.46
Acme 2	1.79	2.85	1.45	3.91	2.89	9.70	4.57	15.92	6.04	16.58	9.40	46.22	0.98	18.60	20.34
Chigwell 1	6.03	10.20	1.94	7.70	5.73	12.84	9.84	4.77	5.83	12.76	11.68	9.37	1.94	9.90	9.17
Chigwell 2	5.70	9.22	1.89	7.27	4.94	12.23	9.37	4.56	5.56	12.20	11.15	9.00	1.93	9.44	8.47
Bashaw 42 1	4.18	7.55	1.69	6.17	3.92	11.61	8.38	5.18	5.45	13.67	10.53	8.72	1.82	11.55	10.64
Bashaw 42 2	6.41	11.44	2.42	9.03	6.25	16.89	12.03	7.48	7.49	19.67	15.02	12.66	2.59	16.91	16.05
Bashaw 1309 1	8.49	15.26	2.86	11.34	7.58	21.71	13.48	6.73	8.90	24.19	17.73	13.40	2.86	19.15	16.62
Bashaw 1309 2	13.24	22.90	3.73	14.75	9.58	26.43	15.93	7.92	10.34	26.54	18.53	13.91	2.53	18.83	16.89
Bashaw 1135 1	1.94	2.83	0.69	3.37	2.31	6.45	5.35	0.24	3.86	12.47	11.46	2.49	3.09	18.54	27.71
Bashaw 1135 2	1.94	2.82	0.69	3.37	2.31	6.46	5.35	0.24	3.87	12.57	11.65	2.52	3.16	18.91	28.29
Lousana 1	4.93	7.17	1.95	5.95	4.71	8.54	14.12	0.85	4.08	10.97	11.80	3.26	2.45	10.28	10.91
Lousana 2	13.56	19.06	4.41	13.81	11.17	18.83	30.78	1.85	8.49	23.32	22.72	7.18	5.00	20.07	19.44
Lousana 3	9.59	14.16	3.77	11.57	9.67	16.63	27.82	1.71	7.99	22.56	21.69	7.20	4.75	19.83	20.54
Lousana 4	14.17	20.02	4.44	14.65	11.81	20.26	32.53	1.94	8.74	25.03	23.86	7.91	4.88	20.91	22.07
Swalwell814 1	9.35	13.74	2.44	8.82	5.09	20.77	10.68	10.34	12.88	29.04	21.20	19.80	2.69	29.90	30.02
Swalwell814 2	9.24	13.44	2.35	9.26	5.84	21.46	11.02	10.71	13.42	30.23	21.68	20.68	2.66	31.03	30.78
Swalwell1312 1	6.58	10.35	1.65	7.05	4.56	16.16	8.50	7.92	10.03	22.12	15.38	15.39	1.92	23.67	25
Swalwell1312 2	6.22	8.95	1.66	6.55	4.02	15.11	7.92	6.94	9.56	21.43	15.13	15.07	2.00	23.38	25.17
Wainwright 1	3.34	3.51	3.42	7.68	5.03	8.96	9.13	0.11	13.61	12.09	39.40	3.65	6.08	10.32	7.37
Wainwright 2	3.53	3.82	3.67	8.52	5.57	9.97	10.18	0.11	15.28	13.73	44.64	4.11	6.92	11.60	4.94
Wainwright 3	5.64	5.55	4.62	10.46	6.64	11.53	11.24	0.11	16.22	13.95	44.81	3.97	6.51	11.45	4.94
FennBV 103 1	1.35	2.15	1.00	4.07	3.33	7.97	9.97	5.00	7.48	20.49	17.52	20.38	3.67	25.12	26.49
FennBV 103 2	1.41	2.34	1.21	4.82	3.98	9.76	12.40	6.38	9.56	25.71	22.65	27.50	5.22	32.66	34.75
FennBV 922 1	0.35	0.62	2.08	9.65	10.42	13.50	31.94	4.88	26.05	42.51	62.12	33.75	17.31	62.33	81.38
FennBV 922 2	0.13	0.24	0.99	3.92	4.07	5.37	13.60	2.31	12.15	17.71	30.21	15.19	7.71	29.59	41.99
Execelsior 1	0.39	0.86	1.22	8.05	7.21	18.98	13.37	0.34	13.42	49.67	52.17	5.13	12.05	50.82	48.44
Execelsior 2	0.18	0.43	0.70	4.63	4.14	11.27	7.92	0.21	8.26	32.09	32.94	3.35	7.40	33.73	32.15

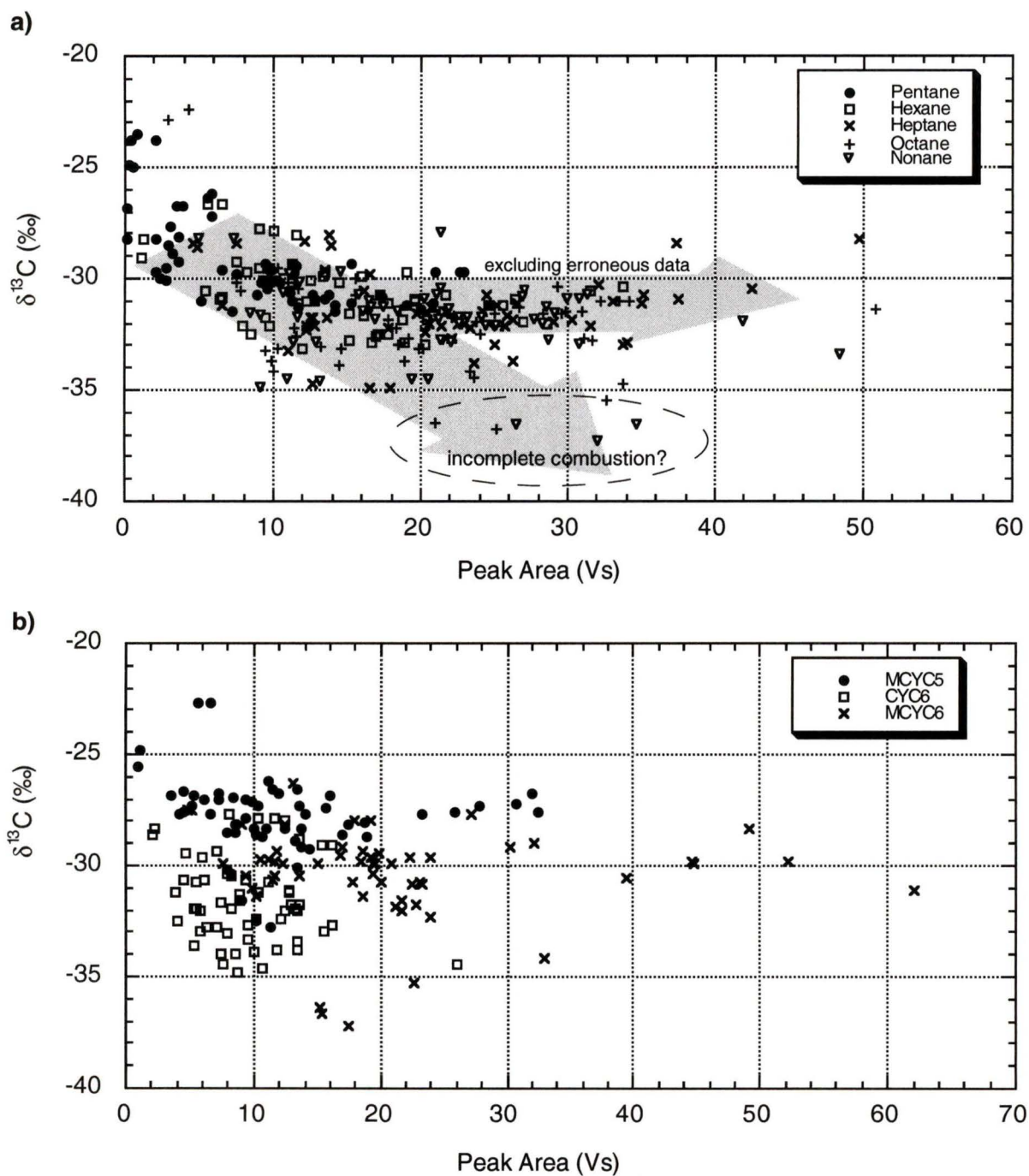


Figure 4.22 a) Comparison of carbon isotope ratios for C_5 - C_9 n-alkanes with peak area (concentration) to evaluate data quality. Erroneous measurements due to incomplete combustion are circled, and if these points are ignored then the trend of ^{13}C depletion with increasing concentration is not prevalent. b) Comparison of carbon isotope ratios for cyclic alkanes with peak area (concentration). Variable $\delta^{13}\text{C}$ ratios are observed independent of peak area.

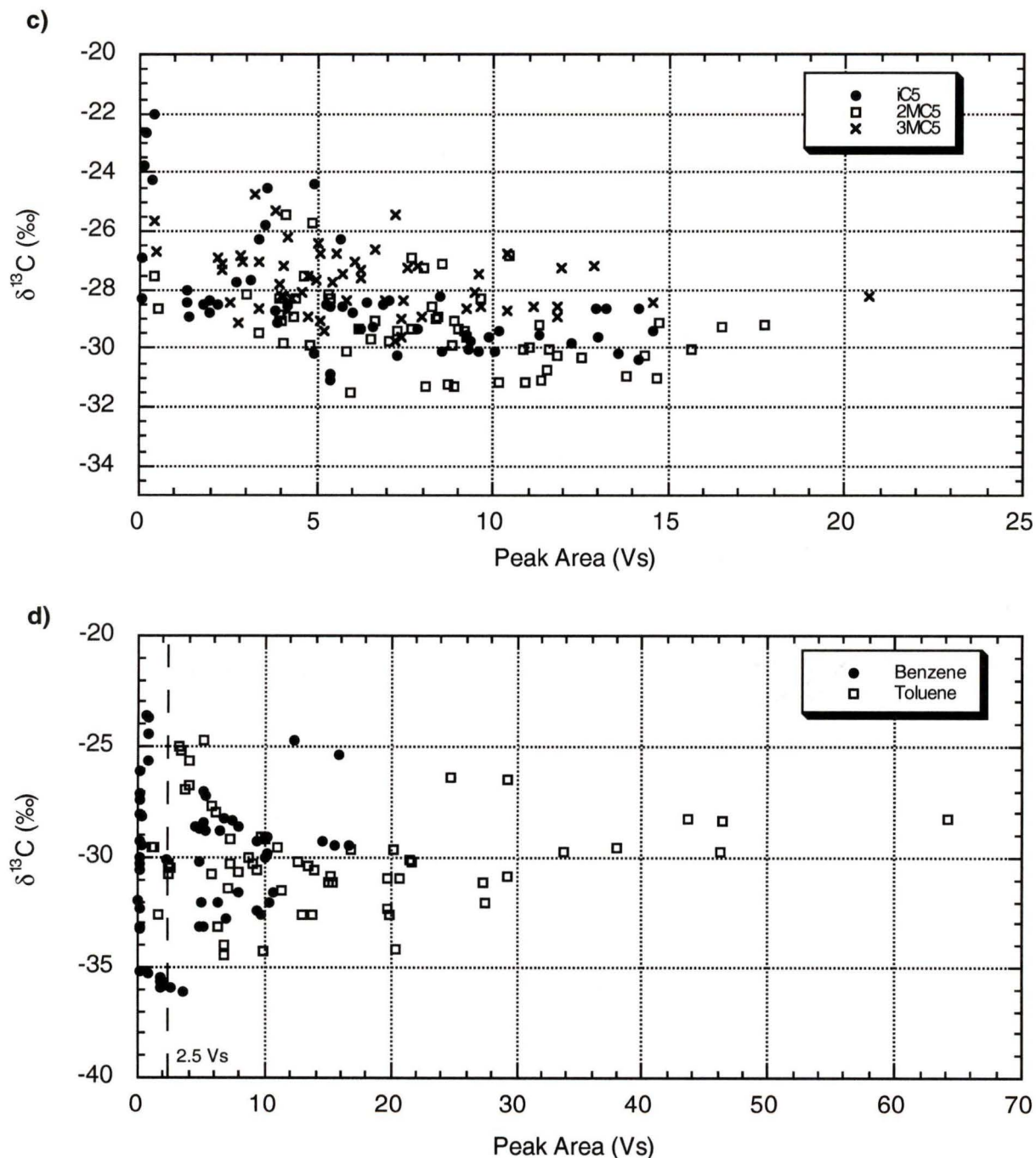


Figure 4.22 c) Comparison of carbon isotope ratios for methylcyclic alkanes with peak area to evaluate data quality. Variable $\delta^{13}\text{C}$ ratios are observed for all compounds independent of peak area.
 d) Comparison of carbon isotope ratios for aromatic compounds with peak area showing variable $\delta^{13}\text{C}$ ratios independent of peak area. The large scatter observed for compounds with peak areas < 2.5 Vs are a result of measurements made outside the dynamic range of the IRMS detectors.

either the biological precursors or kinetic pathways responsible for their generation.

The significant depletion in ^{13}C for $\delta^{13}\text{C}_{\text{nC8}}$ and $\delta^{13}\text{C}_{\text{nC9}}$ in 4 of the oils also accounts for some of the more extraneous data points (-34 to -37‰) observed in Figure 4.19c,d. Removing these points (shaded gray) would improve the correlation between compound pairs. This would also minimize some of the larger isotopic separations observed between n-alkanes in Figure 4.16 and 4.19e.

The trend of ^{13}C enrichment with decreasing peak area is not prevalent for other compound classes (Figure 4.22b,c,d). Despite increasing peak areas, cyclic compounds show a wide range in $\delta^{13}\text{C}$ values for C_6 and C_7 compounds, as do the branched alkanes and aromatics. As previously discussed, the $\delta^{13}\text{C}$ ratios of benzene and toluene often have poor reproducibility as a result of low concentrations in most oils. SPME trials (Chapter 3) showed that when compounds elute in small quantities below the dynamic range of the IRMS detectors (<0.5 V amplitude; <2.5 Vs area), the system is unable to measure a precise/ reproducible $\delta^{13}\text{C}$ value. This is evident by the large scatter in $\delta^{13}\text{C}$ values for peak areas < 2.5 Vs in Figure 4.22d.

Overall, the analytical difficulties of the CSIC technique do not appear to have significantly compromised the data quality. Certain oils should be re-analyzed to confirm if $\delta^{13}\text{C}$ values are accurate, however, those compounds whose ratios were questionable were removed as variables prior to the hierarchical cluster analysis. Source control still appears to be the dominant influence on the isotopic composition of the gasoline-range.

Chapter 5 – Outlook and Conclusions

Solid Phase MicroExtraction is an innovative technique for analyzing gasoline range hydrocarbons from the headspace above oil. It solves many of the traditional problems associated with other solventless analytical methods, such as evaporative loss of highly volatile analytes and the laborious task of determining the amount of sample required for CF-IRMS analysis. SPME is a relatively rapid, user-friendly sampling technique that produces reproducible and representative $\delta^{13}\text{C}$ ratios for $\text{C}_5\text{-C}_9$ hydrocarbons in numerous types of oils. This method has been demonstrated to be a more efficient technique than its P&T predecessor .

Experiments to test the veracity of molecular and stable isotope data have shown that it is important to ensure that instrument parameters such as flow rates, temperature programs, and combustion conditions are optimized for precise measurements. Injector split flows can be used to effectively control the amount of sample analyzed, and its effects on $\delta^{13}\text{C}$ ratios are minimal. Numerous sampling variables such as adsorption times, temperatures, and potential effects of a complex matrix must also be considered.

The CSIC technique uses the individual carbon isotope signatures of gasoline range compounds as a diagnostic fingerprint for oil-oil and oil-source correlations. The sample suite of 27 oils in this study can mostly be attributed to a common source rock, the Upper Devonian Duvernay Formation. It is still unclear if Nisku source beds have contributed partially or completely to some of these oils, and combining the CSIC results with other geochemical data (e.g. biomarkers) on these samples should help to clarify this issue. The 6 groups suggested by CSIC results all display distinct $\delta^{13}\text{C}$ signatures, however a more

detailed understanding of the regional geology for areas where these samples were taken from would also help establish their validity.

It is important to measure isotope ratios for all compound classes as the relationships between them may provide information on the origin of oils and light hydrocarbons. Straight-chain and branched hydrocarbons display both a molecular and isotopic relationship to each other, while cyclic and aromatic compounds display much more variable results. The data in this study support a steady-state or kinetic mechanism for oil generation, in contrast to previous thermodynamic models. Systematic isotopic offsets of individual compounds with similar carbon number or chemical structure both within and between oil groups point towards some form of source control on isotopic composition of oils. LMW compounds are generally depleted in ^{13}C relative to heavier compounds. Thermochemical Sulfate Reduction (TSR) appears to result in pronounced ^{13}C enrichment for several compounds relative to unaltered samples.

Future directions of study would include exploiting new advances in chromatography and mass spectrometry to analyze a greater number of gasoline range compounds. Co-elution effects must be minimized as they were the primary obstacle in obtaining quality results in this study. The CSIC technique has numerous potential applications outside the petroleum industry. Identifying the source of fugitive oil spills in either soils or open waters is a promising idea and should be developed. Other experiments examining the effects of how microbial alteration influences $\delta^{13}\text{C}$ signatures of gasoline range compounds would also aid in definitively establishing CSIC as another effective tool in petroleum exploration.

References

- Allan, J. and S. Creaney. 1991. Oil families of the Western Canada Basin. *Bulletin of Canadian Petroleum Geology*, 39, p. 107-122.
- Arthur, C.L., and Pawliszyn, J., 1990. Solid Phase MicroExtraction with thermal desorption using fused silica optical fibers. *Analytical Chemistry*, 62, 2145-2148.
- Arthur, C.L., Killam, L., Buchholz, K.D., and Pawliszyn, J., 1992a. Automation and optimization of Solid-Phase MicroExtraction. *Analytical Chemistry*, 64, 1960-1966.
- Arthur, C.L., Killam, L., Motlagh, S., Lim, M., Potter, D., and Pawliszyn, J., 1992b. Analysis of substituted benzene compounds in ground-water using SPME. *Environmental Science and Technology* 26, 979-983.
- Bailey, N.J.L., Krouse, H.R., Evans, C.R., and Rogers, M.A.. 1973. Alteration of crude oil by waters and bacteria - evidence from geochemical and isotope studies. *AAPG Bulletin*, 57, p. 1276-1290.
- Baylis, S.A., Hall, K., and Jumeau, E.J. 1994. The analysis of the C₁-C₅ components of natural gas samples using gas chromatography-combustion-isotope ratio mass spectrometry. *Organic Geochemistry*, 21, p. 777-785.
- Bigeleisen, J. 1961 Statistical mechanics of isotope effects on the thermodynamic properties of condensed systems. *J. Chem. Phys.* 34, p. 1485-1493.
- Bjørøy, M., Hall, K., and Jumeau, J. 1990. Stable carbon ratios analysis on single components in crude oils by direct GC-isotope analysis. *Trends Analytical Chemistry*, 9, p. 331-337.
- Bjørøy, M., Hall, K., Gillyon, P., and Jumeau, J. 1991a. Carbon isotope variations in n-alkanes and isoprenoids of whole oils. *Chemical Geology*, 93, p. 13-20.
- Bjørøy, M., Hall, P.B., Hustad, E. and Williams, J.A. 1991b. Variation in stable carbon isotope ratios of individual hydrocarbons as a function of artificial maturity. *Adv. in Organic Geochemistry*, 19, p.89-105.

Bjørøy, M., Hall, P.B., and Rita, P.M. 1993. Stable carbon isotope variation of n-alkanes in Central Graben oils. *Adv. in Organic Geochemistry*, 22, p.355-381.

Bjørøy, M., Hall, P.B., and Moe, R.P. 1994. Variation in the isotopic composition of single components in the C₄-C₂₀ fraction of oils and condensates. *Organic Geochemistry* 21, 761-776.

Boyd-Boland, A.A., Magdic S., and Pawliszyn, J. 1996. Simultaneous determination of 60 pesticides in water using Solid Phase MicroExtraction and Gas Chromatography-Mass Spectrometry. *Analyst*, 121, 929-937.

Carpentier, B., Ungerer, P., Kowalewski, I., Magnier, C., Courcy, J.P., and Huc. A.Y. 1996. Molecular and isotopic fractionation of light hydrocarbons between oil and gas phases. *Organic Geochemistry*, 24, 1115-1139.

Chung, H.M., Gormly, J.R., and Squires, R.M. 1988. Origin of gaseous hydrocarbons in subsurface environments: theoretical considerations of carbon isotope distribution. *Chemical Geology*, 71, p. 97-103.

Chung, H.M., Rooney, M.A., Toon, M.B., and Claypool, G.E. 1992. Carbon isotope composition of marine crude oils. *AAPG Bulletin*, 76, p. 1000-1007.

Chung, H.M., Claypool, G.E., Rooney, M.A. and Squires, R.M. 1994. Source characteristics of marine oils as indicated by carbon isotopic ratios of volatile hydrocarbons. *AAPG Bulletin*, 78, 396-408.

Chow, N., Wendte, J., and L.D. Stasiuk. 1995. Productivity versus preservation controls on two organic-rich carbonate facies in the Devonian of Alberta: sedimentological and organic petrological evidence. *Bulletin of Canadian Petroleum Geology*, 43, p. 433-460

Clayton, C.J. 1991. Effect of maturity on carbon isotope ratios of oils and condensates. *Org. Geochem*, 17, p. 887-899.

Clayton, C.J. and Bjørøy, M. 1994. Effect of maturity on ¹³C/¹²C ratios of individual compounds in North Sea oils. *Organic Geochemistry*, 21, p. 737-750.

Creaney, S., Allan, J., Cole, K.S., Fowler, M.G., Brooks, P.W., Osadetz, K.G., Macqueen, R.W., Snowdon, L.R. and C.L. Riediger. 1994. Petroleum generation and migration in the Western Canada Sedimentary Basin. In: Geological Atlas of the Western Canada Basin (G.D Mossop and I. Shetsen comps.) Canadian Society of Petroleum Geologists and Alberta Research Council. p. 455-468.

Curiale, J.A. 1994. Correlation of oils and source rocks – A conceptual and historical perspective. In: The Petroleum System – From Source to Trap: AAPG Memoir 60, Magoon, L.B. and Dow, W.G. eds. P. 251-260.

Dai Jinxing. 1992. Identification and distinction of various alkane gases. Science in China, 35, p. 1246-1257.

Dempster, H.S., Sherwood-Lollar, B., and Feenstra, S. 1997. Tracing organic contaminants in groundwater - a new methodology using Compound Specific Isotope Analysis. Submitted to Environmental Science and Technology

Dias, R.F., and Freeman, K.H. 1997. Carbon isotope analyses of semivolatile organic compounds in aqueous media using Solid-Phase Microextraction and isotope ratio monitoring GC/MS. Analytical Chemistry, 69, 944-950.

Dolph, J.A. 1996?. Reservoir heterogeneities in the Nisku formation in the Stettler, Stettler South and Fenn Big Valley North Lobe oil pools, Alberta. Gulf Canada Resources special report.

Dowling, L.M., Boreham, C.J., Hope, J.M., Murray, A.P. and Summons, R.E. 1995. Carbon isotopic composition of hydrocarbons in ocean-transported bitumens from the coastline of Australia. Organic Geochemistry, 23, p. 729-737.

Durand, B. and Espitalie, J. 1972. Formation et evolution des hydrocarbures de C₁ a C₁₅ et des gaz permanents dans les argiles du Toarcien du bassin de Paris. Advances in Organic Geochemistry, 1971. Int. Ser. Monogr. Earth Sci., 33, p. 455-468.

Dzou, L.I.P. and Hughes, W.B. 1993. Geochemistry of oils and condensates, K field, offshore Taiwan: a case study in migration fractionation. Organic Geochemistry, 4, p. 437-462.

- Erdman, J.G. and Morris, D.A. 1974. Geochemical correlation of petroleum. AAPG Bulletin, 58, p. 2326-2337.
- Faber, E. 1987. Zur isotopengeochemie gasformiger kohlenwasserstoffe. Erdol Erdgas und Kohle, 103, p. 210-218.
- Galimov, E.M. 1974. Organic geochemistry of carbon isotopes. In: Advances in Organic Geochemistry 1973. B.P. Tissot and F. Bienner eds. p. 439-452.
- Halpern, H.I. 1995. Development and applications of light-hydrocarbon based star diagrams. AAPG Bulletin, 79, p. 801-815.
- Hunt, J.M. 1980. Generation of light hydrocarbons in sedimentary rocks. Nature, v.288, no.5792, p.688-690.
- Hunt, J.M. 1984. Generation and migration of light hydrocarbons. Science, 226, p. 1265-1270.
- Hunt, J.M. 1996. Petroleum Geochemistry and Geology – 2nd Edition. W.H. Freeman and Company, New York. 745 p.
- Hunter, I.G. 1996. Nisku Formation in the Swalwell area of southern Alberta. CSPG Core Workshop.
- James, A.T. 1983. Correlation of natural gas by use of the carbon isotopic distributions between hydrocarbon components. AAPG Bulletin, 67, p. 1176-1191.
- James, A.T. 1990. Correlation of reservoir gases using the carbon isotopic compositions of wet gas components. AAPG Bulletin, 74, p. 1441-1458.
- James, A.T. and Burns, B.J. 1984. Microbial alteration of subsurface natural gas accumulations. AAPG Bulletin, 68, p. 957-960.

Jonathan, D., L'Hote, G., and Du Rochet, J. 1975. Analyse geochemiques des hydrocarbures legers par thermovaporisation. *Revue de l'institute Francais de Petrole*, 30, p. 65-88.

Koons, C.B., Bond, J.G., and Pierce, F.L. 1974. Effects of depositional environment and postdepositional history on chemical composition of Lower Tuscaloosa Oils. *AAPG Bulletin*, 58, p. 1272-1280.

Kvenvolden, , K.A. and Squires, R.M. 1967. Carbon isotopic composition of crude oils from Ellenburger Group (Lower Ordovician), Permian Basin, West Texas and eastern New Mexico. *AAPG Bulletin*, 51, p. 1293-1303.

Leythaeuser, D, Schaefer, R.G., Cornford, C. and Weiner, B. 1979a. Generation and migration of light hydrocarbons (C2-C7) in sedimentary basins. *Organic Geochemistry*, 1, p. 191-204.

Leythaeuser, D., Schaefer, R.G. and Weiner, B. 1979b. Generation of low molecular weight hydrocarbons from organic matter in source beds as a function of temperature and facies. *Chemical Geology*, v.25, p.95-108.

Louch, D., Motlagh, S., and Pawliszyn, J. 1992. Dynamics of organic compound extraction from water using liquid-coated fused silica fibers. *Analytical Chemistry*, **64**, 1187-1199.

MacGillivray, B., Pawliszyn, J., Fowlei, P., and Sagara, C. 1994. Headspace Solid-Phase MicroExtraction versus purge and trap for the determination of substituted benzene compounds in water. *Journal of Chromatographic Science*, 32, 317-322.

Magoon, L.B. and Claypool, G.E. (1983) Petroleum geochemistry of the North Slope of Alaska: Time and degree of thermal maturity. In *Advances in Organic Geochemistry*, eds. M. Bjoroy et al., New York: Wiley, 28-38

Mango, F.D. 1987. An invariance in the isoheptanes of petroleum. *Science*, v.237, p.514-517.

Mango, F.D. 1990a. The origin of light cycloalkanes in petroleum. *Geochimica et Cosmochimica Acta*, v.54, p.23-27.

Mango, F.D. 1990b. The origin of light hydrocarbons in petroleum: A kinetic test of the steady-state catalytic hypothesis. *Geochimica et Cosmochimica Acta*, v.54, p.1315-1323.

Mango, F.D. 1991. The stability of hydrocarbons under the time-temperature conditions of petroleum genesis. *Nature*, v.352, no.6331, p.146-148.

Mango, F.D. 1992. The stability of hydrocarbons under the time-temperature conditions of petroleum genesis. *Nature*, v.352, p.146-148.

Mango, F.D. 1994. The origin of light hydrocarbons in petroleum: Ring preference in the closure of carbocyclic rings. *Geochimica et Cosmochimica Acta*, v.58, no.2, p.1315-1323.

Mango, F.D. 1996. Transition metal catalysts in the generation of natural gas. *Organic Geochemistry*, 24, p. 977-984.

Mango, F.D. 1997a. The catalytic decomposition of petroleum into natural gas. *Geochimica et Cosmochimica Acta*, 61, p. 5347-5350.

Mango, F.D. 1997b. The light hydrocarbons in petroleum: a critical review. *Organic Geochemistry*, 26, p.417-440.

Mansuy, L., Philp, R.P., and Allen. J. 1997. Source identification of oil spills based on the isotopic composition of individual components in weathered oil samples. *Environ. Sci. Technol.*, 31, p. 3417-3425.

Manzano, B.K., Fowler, M.G., and Machel, H.G. 1997. The influence of thermochemical sulfate reduction on hydrocarbon composition in Nisku reservoirs, Brazeau River area, Alberta, Canada. *Organic Geochemistry*, 27, p. 507-521.

Moldowan, J.M., Seifert, W.K., and Gallegos, E.J. 1985. Relationship between petroleum composition and depositional environment of petroleum source rocks. *AAPG Bulletin*, 69, 1255-1268.

Murphy, D.E. 1995. GC-C-IRMS: A new technique to characterize and correlate oils and source rocks. Unpublished M.Sc. thesis, University of Victoria, 382 p.

Northam, M.A. 1985. Correlation of northern North Sea oils: The different facies and their Jurassic Source. In: *Petroleum Geochemistry in Exploration of the Norwegian Shelf*, eds. B.M. Thomas et al., London: Graham & Trotman for the Norwegian Petroleum Society, 93-99.

Norusis, M.J. 1994. SPSS Professional Statistics 6.1. SPSS Inc., USA, 385 p.

O'Malley, V.P., Abrajano, T.A., and Hellou, J. 1996. Stable carbon isotopic apportionment of individual polycyclic aromatic hydrocarbons in St. John's Harbour, Newfoundland. *Environmental Science and Technology*, 30, p. 634-639.

Odden, W., Patience, R.L., and Van Graas, G.W. 1998. Application of light hydrocarbons (C₄-C₁₃) to oil/source rock correlations: a study of the light hydrocarbon compositions of source rocks and test fluids from offshore Mid-Norway. *Organic Geochemistry*, 28, p. 823-847.

Osadetz, K.G., Brooks, P.W., and Snowdon, L.R. 1992. Oil families and their sources in Canadian Williston Basin (southeastern Saskatchewan and southwestern Manitoba). *Bulletin of Canadian Petroleum Geology*, 40, p. 254-273.

Osadetz, K.G., Snowdon, L.R., and Brooks, P.W. 1994. Oil families in Canadian Williston Basin (southwestern Saskatchewan). *Bulletin of Canadian Petroleum Geology*, 42, p. 155-177.

Peters, K.E., Moldowan, J.M., Driscoll, A.R., and Demaison, G.J. 1989. Origin of Beatrice Oil by co-sourcing from Devonian and Middle Jurassic source rocks, Inner Moray Firth, United Kingdom. *AAPG Bulletin*, 73, p. 454-471.

Philip, R.P. 1983. Correlation of crude oils from the San Jorge Basin, Argentina. *Geochimica et Cosmochimica Acta*, 47, p. 267-275.

Philippi, G.T. 1975. The deep subsurface temperature controlled origin of the gaseous and gasoline-range hydrocarbons of petroleum. *Geochim. Cosmochem. Acta*, 39, p. 1353-1373.

Philippi, G.T. 1977. On the depth, time and mechanism of origin of the heavy to medium-gravity naphthenic crude oils. *Geochimica et Cosmochimica Acta*, 41, p.33-52.

Philippi, G.T. 1981. Correlation of crude oils with their oil source formation, using high resolution GLC C6-C7 component analyses. *Geochim. Cosmochim. Acta*, 45, p. 1495-1513.

Potter, D. and Pawliszyn, J. (1994) Rapid determination of polyaromatic hydrocarbons and polychlorinated biphenyls in water using Solid Phase MicroExtraction and GC/MS. *Environmental Science and Technology*, 28, 298-305.

Ricci, M.P, Merritt, D.A, Freeman, K.H., and Hayes, J.M. 1994. Acquisition and processing of data for isotope-ratio-monitoring mass spectrometry. *Organic Geochemistry*, 21, p. 561-571.

Rooney, M.A. 1995. Carbon isotope ratios of light hydrocarbons as indicators of thermochemical sulfate reduction. In: *Organic Geochemistry: Developments and Applications to Energy, Climate, Environment and Human History, Selected Papers from the 17th International Meeting on Organic Geochemistry* (J.O. Grimalt and C. Dorronsoro eds.). p. 523-525.

Seifert, W.K, Moldowan, J.M., and Demaison, G.J. 1984. Source correlation of biodegraded oils. *Organic Geochemistry*, 6, p. 633-643.

Silverman, S.R. 1964. Investigation of petroleum origin and evolution mechanisms by carbon isotope studies. In: *Isotope and Cosmic Chemistry*, H. Craig, S.L. Miller, and C.J. Wasserburg (eds.), N. Holland Publishing, Amsterdam, p. 92-102.

Silverman, S.R. 1971. Influence of petroleum origin and transformation on its distribution and redistribution in sedimentary rocks. In: *Proceedings of the 8th World Petroleum Congress*, 2, p. 47-54.

Snowdon, L.R. and Osadetz, K.G. 1988. Geological processes interpreted from gasoline range analyses of oils from southeast Saskatchewan and Manitoba. In: *Current Research, Part D, Geological Survey of Canada, Paper 88-1D*, p. 33-40.

Sofer, Z. 1984a. Stable carbon isotope compositions of crude oils: Application to source depositional environments and petroleum alteration. *AAPG Bulletin*, 68, p. 31-49.

Sofer, Z. 1984b. Preparation of carbon dioxide for stable carbon isotope analysis of petroleum fractions. *Analytical Chemistry* 52, 1389-1391.

Sofer, Z. Zumberge, J.E., and Lay, V. 1985. Stable carbon isotopes and biomarkers as tools in understanding genetic relationship, maturation, biodegradation, and migration of crude oils in the Northern Peruvian Oriente (Maranon) Basin. *Adv. in Organic Geochemistry*, 10, p. 377-389.

Sofer, Z, Bjørøy, M., and Hustad, E. 1991. Isotopic composition of individual n-alkanes in oils. In: *Organic Geochemistry: Advances and Applications in Energy and the Natural Environment*, 5th Meeting of the EAOG Poster Abstracts. D.A.C. Manning, eds. p. 207-211.

Stahl, W.J. 1977. Carbon and nitrogen isotopes in hydrocarbon research and exploration. *Chemical Geology*, 20, p. 121-149.

Stahl, W.J. 1978. Source rock-crude oil correlation by isotopic type-curves. *Geochim. Cosmochim. Acta*, 42, p. 1573-1577.

Stahl, W.J., and Koch, J. 1974. Verhältnis nordeutscher Erdgase-Reifemerkmale ihrer Muttersubstanzen. *Erdöl und Kohle-Erdgas-Petrochemie*, 27, p. 10

Steffen, A. and Pawliszyn, J. 1996. The analysis of flavour volatiles using Headspace Solid Phase MicroExtraction. *J. Agricultural. Food Chem.*, 44, 2187-2193.

Stoakes, F.A. and Creaney, S. 1985. Sedimentology of a carbonate source rock: the Duvernay Formation of Alberta, Canada. In: *Rocky Mountain Carbonate Reservoirs – A core workshop*. M.W. Longman, K.W. Shanley, R.F. Lindsay, D.E. Eby (eds.). Society of Economic Paleontologists and Mineralogists, Core Workshop no. 7, p. 343-374.

Switzer, S.B., Holland, W.G., Christie, D.S., Graf, G.C., Hedinger, A.S., McAuley, R.J., Wierzbicki, R.A., and J.J. Packard. 1994. Devonian Woodbend-Winterburn Strata of the Western Canada Sedimentary Basin In: *Geological Atlas of the Western Canada Basin*

(G.D Mossop and I. Shetsen comps.) Canadian Society of Petroleum Geologists and Alberta Research Council. p. 165-202.

Ten Haven, H.L. 1996. Applications and limitations of Mango's light hydrocarbon parameters in petroleum correlation studies. *Organic Geochemistry*, 24, p. 957-976.

Thompson, K.F.M. 1979. Light hydrocarbons in subsurface sediments. *Geochimica et Cosmochimica Acta*, no.5, v.43, p.657-672.

Thompson, K.F.M. 1983. Classification and thermal history of petroleum based on light hydrocarbons. *Geochimica et Cosmochimica Acta*, v.47, no.2, p.303-316.

Thompson, K.F.M. 1987. Fractionated aromatic petroleums and the generation of gas condensates. *Organic Geochemistry*, v.11, p.573-590.

Thompson, K.F.M. 1988. Gas-condensate migration and oil fractionation in deltaic systems. *Marine and Petroleum Geology*, v.5, no.3, p.237-246.

Van Duin, A.C.T. and Larter, S.L. 1997. Unravelling Mango's mysteries: a kinetic scheme describing the diagenetic fate of C7-alkanes in petroleum systems. *Organic Geochemistry*, 27, p. 597-599.

Whiticar, M.J. 1994. Correlation of natural gases with their sources. In: *The Petroleum System – From Source to Trap: AAPG Memoir 60*, Magoon, L.B. and Dow, W.G. eds. p. 261-283.

Whiticar, M.J., Faber, E., and Schoell, M. 1984. Carbon and hydrogen isotopes of C1-C5 hydrocarbons in natural gases (abs.). *AAPG Research Conference on Natural Gases*, San Antonio, Texas, p. 31.

Whiticar, M.J. and Snowdon, L.R. 1998. Geochemical characterization of selected western Canada oils by Compound Specific Isotope Correlation. *Organic Geochemistry* (in press)

Wilhelms, A., Larter, S.R., and Hall, K. 1994. A comparative study of the stable carbon isotope composition of crude oil alkanes and associated crude oil asphaltene pyrolysate alkanes. *Organic Geochemistry*, 21, p. 751-759.

Williams, J.A. 1974. Characterization of Oil Types in Williston Basin. *AAPG Bulletin*, 58, p. 1243-1252.

Zhang, Z. and Pawliszyn, J. 1993a. Headspace Solid Phase MicroExtraction. *Analytical Chemistry* 65, 1843-1852.

Zhang, Z. and Pawliszyn, J. 1993b. Analysis of organic compounds in environmental samples using headspace Solid Phase MicroExtraction. *J. High Resolution Chromatography*, 16, 689-692.

Zhang, Z., Yang, M. and Pawliszyn, J. (1994) Solid Phase MicroExtraction: A new solvent-free alternative for sample preparation. *Analytical Chemistry* 66, 844A-853A.

Appendix A - Devonian Petroleum Systems (DPS) Report

A recent report by the DPS group provides updated thermal maturity, organic facies, and oil correlation data for Woodbend-Winterburn strata in the WCSB. The report is summarized here as it contains proprietary data that cannot be made available for publication at this time.

Facies Analysis

The organic facies of the Woodbend group showed a distinct regional pattern throughout central Alberta, especially in the East Shale Basin where deep and intermediate water depth facies dominate. Duvernay source rocks in the eastern extremity of the basin are enriched in terrestrial-derived macerals (e.g. sporinites, vitrinites). The DPS group suspects this may affect both kerogen quality and hydrocarbon generation. For the West Shale Basin including parts of northern Alberta and the Northwest Territories (NWT), Duvernay-Muskawa source rocks are dominated by more shallow water facies, a direct contrast to those for the East Shale Basin. Terrestrially derived inertinites and vitrinites are still the dominant constituents, with graptolites increasing in abundance as one approaches the Peace River and Western Alberta Arches.

A distinct, siliceous microfossil enriched unit is mixed with the shallow water facies of the Duvernay/Muskawa through most of northern Alberta and the NWT, indicating a potential hydrologic connection with a possible open marine shelf system to

the north. Since paleocirculation patterns in this area would have been more efficient than in central Alberta, the DPS group considered potential source rock deposition unlikely. However, Rock-Eval and TOC data of core samples from northern Alberta was undertaken to investigate if potential hydrocarbon source rocks occur in this largely unexplored area. Samples of the Muskawa Fm. show hydrocarbon source potential in several wells with higher than expected TOC. More work is being done in this area.

Source rock intervals in the Nisku and Camrose formations (Winterburn Group) overlying the Duvernay in eastern/central Alberta show an abundance of shallow and intermediate water depth facies that were considered deposited within a restricted marine platform environment. Most of the maceral assemblages in lower Nisku samples were of marine origin, with terrestrial input increasing as one approached the upper Nisku-Camrose member contact. In southern Alberta, potential source rock intervals in both formations showed influence from marine and terrestrial sources. The base of the Camrose was distinguished by deep water, open-marine, terrestrially influenced facies (stromatolites, prasinophytes), overlying organic facies of the Ireton Formation, similar in composition to the Duvernay. Moving into western/central Alberta, the Nisku becomes predominantly enriched in terrestrially derived macerals (sporinites, vitrinites), along with a high detrital quartz content. Since the more oil-prone amorphous and alginite macerals are less common in this area relative to central and southern Alberta, the quality of the kerogen found in Nisku samples was considered to be of lower quality relative to the Duvernay. Within many of the organic-rich zones of the Camrose member, sulfides were often associated with the kerogen in significant quantities, thereby diminishing its quality as well.

Thermal Maturity

Thermal maturity data (vitrinite reflectance %Ro) for the Woodbend Group and equivalent strata produced a pattern similar to that for the underlying Elk Point Group. Maturity zones trend parallel to the deformation belt throughout most of northern Alberta and the NWT, with most sediments increasing in maturity westwards from immature (<0.6 %Ro) to overmature (>1.2 % Ro). Between townships 30-80, Ranges 25W4 to 8W5 a significant NE-SW trending maturity deflection is observed corresponding to the area encompassing the Bashaw Reef Complex and Rimbey-Meadowbrook Reef Trend. This deflection places the area within the oil window (0.6 to 1.2 %Ro – marginally mature to thermally mature), thus highlighting its exploration potential. In contrast, data for the overlying Winterburn strata show a much more subtle deflection. Nonetheless, the maturity anomaly places the Nisku strata within the oil window, corresponding to known hydrocarbon accumulations in the Nisku and Camrose formations in southern Alberta (e.g. Hays-Enchant). Other anomalies suggested updip, as yet undiscovered reservoirs.

Source Rocks of the Nisku Formation

A section of the report is devoted to the geology and geochemistry of potential source rocks and oils found within the Nisku Formation in southern and central Alberta.

Based on an extensive collection of core samples and well logs, the geology, source rock potential, and oil-source correlation of the Nisku formation from three main areas (Bashaw, West Pembina, Hays-Enchant) were examined. Over 100 samples in the Bashaw to Swalwell area (East Central Alberta) alone were collected for source rock analysis. Organic geochemical results identified a widespread (Townships 29-44, Ranges 21-27W4) potential source rock in this area, located at the transition between the Upper Ireton shale and basin filling evaporites of the Upper Nisku. The unit is 1-4 m thick, and interfingers with the open-marine carbonate platform of the Lower Nisku Formation in several locations, with the overall thickness of the unit greatest at its margins. The source bed has no discernable logging signature, and was only discovered from examination of core samples. Its lithology is comprised of three lithofacies, with the most organic-rich being a fine crystalline dolostone (mudstone), with clay interbedded/interlaminated in a coarser dolostone matrix. The organic material is classified as type II, with TOC values up to 11%. The clay laminations are punctuated by another medium crystalline dolostone (mud-wackestone) facies, with evidence of bioturbation. The base of the unit is a submarine hardground, suggesting that the unit was deposited at the same time as the carbonate platform (Lower Nisku).

Three oil families were identified in east-central Alberta from a combination of gross composition, gasoline range, and biomarker data. Two families (B and C) were attributed to a Duvernay source, with differing levels of thermal maturity. A possible explanation for this was the organic facies variation within the Duvernay (shallow vs. deep water). The oils were recovered from Nisku and Leduc reservoirs, and mixing between the two pools was suggested. The third family (A) was confined to Nisku

reservoirs, with high saturate/aromatic and low Pr/Ph, diasterane/sterane, Ts/Tm ratios. One reservoir sample (Mikwan) showed biomarker characteristics suggesting a mixture of type A and B oils.

In the West Pembina region (West-Central Alberta), the main goal of the study was to re-evaluate the source rock potential of the Cynthia Shale, previously described by the Chevron Exploration Staff (1979). Its lithology in this area is a dark gray, calcareous, silty, shale, with rare plant fragments and brachiopods. Carbonate content increases as one moves upsection. The basal part of the member (lowest 2 m - shale dominated) is considered the main source interval, with TOC values up to 2% (avg. 0.8%). As stated earlier, the DPS group now attributes oils found in this region to a Duvernay source based on stable isotope data, in contrast to the Cynthia source proposed by Chevron Exploration Staff (1979). This is reinforced by low TOC data reported, as it would be unlikely for the Cynthia member to be able to produce large quantities of hydrocarbons. However, the underlying Bigoray member shows much higher TOC values (up to 4%). Taking this into account along with the high thermal maturity data recorded for this member (late mature to overmature), the original TOC content could have been significantly higher. The DPS group propose that the Bigoray could be a contributor for oils and condensates in this area, but a high component of terrestrial organic matter in its kerogen and biomarker data still point to the Duvernay as the main source.

In a previous report, the DPS group identified two primary, mappable, potential source rocks within the Nisku formation in Southern Alberta. In the current report, they have now delineated a third interval, extending between townships 1-15 and ranges

1-25W4. Two of the three source units are located at the base and top of the Camrose Member, with the third unit situated in the middle of the Nisku formation overlying a large nodular-mosaic anhydrite unit.

The geology of the potential source rocks was cataloged in great detail. The first unit at the base of the Camrose (directly overlying the Ireton) is 0.5 to 3.0 m thick, and covers a large portion of southern Alberta. Its lithology is dominated by two lithofacies, one organic-rich, the other organic-lean. The organic-rich facies (constituting up to 50% of the overall interval) is a dark shale/fine dolostone (mudstone). Interbedded within this facies are laminations of light, organic-lean, coarse dolostone (wackestone) facies, with little evidence of bioturbation. Deposition of this interval was postulated to have occurred in an open-marine setting, possibly a large carbonate platform.

The second source rock at the top of the Camrose forms a sharp contact with underlying strata, varying in thickness from 1.0 to 2.3 m. Its distribution is restricted to that of a laminated anhydrite unit present below it, indicating restricted depositional conditions (possibly a tidal flat). It is easily identified in well logs, and is composed of lithofacies similar to the first source unit, with a minor clay component forming wavy laminae within it. Some evidence of bioturbation was observed. Geochemical analysis of samples from source units 1 and 2 show TOC contents up to 10%, comprised of mostly Type I organic matter (marine, oil prone). However, the DPS group stated that based on present data, these Nisku intervals were not mature enough to have generated any substantial quantities of hydrocarbons in Southern Alberta.

The recently identified third unit is restricted to the south-eastern corner of the province, with a thickness of up to 4.0 m comprising a large portion of the Nisku in this

area. It is also situated above a large anhydrite unit, making it easily identifiable in well logs. It has similar lithology to the previous two source rocks, and was thought to have been deposited under conditions similar to the second unit.

Oils from the Hays-Enchant area of Southern Alberta showed similar characteristics to each other, suggesting a common source. They differed substantially from oils of East-Central Alberta, but showed evidence of migration over large distances. This was confirmed by biomarker data on hydrocarbon stains taken from Nisku core samples in wells unrelated to hydrocarbon production. The DPS group would not say unequivocally that a separate Nisku source exists for oils in Southern Alberta, due to lack of core samples examined between the southern and central Alberta (well logs do exist).

PARTIAL COPYRIGHT LICENSE

I hereby grant the right to lend my thesis (or dissertation) to users of the University of Victoria Library, and to make single copies only for such users or in response to a request from the Library of any other university, or similar institution, on its behalf or for one of its users. I further agree that permission for extensive copying of this thesis for scholarly purposes may be granted by me or a member of the University designated by me. It is understood that copying or publication of this thesis for financial gain shall not be allowed without my written permission.

Title of Thesis/Dissertation: Compound Specific Isotope Correlation (CSIC)
Using Gasoline Range Hydrocarbons: A Novel
Approach for Petroleum Exploration.

Author



Scott A. Harris

April 20, 1999

VITA

Surname: Harris

Given Names: Scott Allan

Place of Birth: Winnipeg, Manitoba

Date of Birth: Oct. 14, 1974

Educational Institutions Attended:

University of Victoria

1996-1999

McGill University

1993-1996

Degrees Awarded:

B.Sc. (First Class Honours) McGill University

1996

Honours and Awards:

Franc Joubin Bursary for Environmental Studies

1996

Bourse Hydro Quebec

1995

Publications:

Harris, S.A., Whitar, M.J. and Eek, M.K. 1999. Molecular and Isotopic
Analysis of Oils by SPME of Gasoline Range Hydrocarbons. Special
Volume of Organic Geochemistry (in press)